Haptic feedback control designs in teleoperation systems for minimal invasive surgery

Haptic feedback control designs in teleoperation systems for minimal invasive surgery

I. Font Balaguer PDEng

DCT Report No. 2004.117

Eindhoven, November, 2004

Coaching:
Prof.Dr.Ir. M. Steinbuch
Dr.S. Weiland

Exam Committee:
Prof.Dr.Ir. M. Steinbuch
Dr.S. Weiland
Dr.Ir.M.J.G.v.d.Molengraft
Ir.P.C.Mulders

Technische Universiteit Eindhoven
Department of Mechanical Engineering
Stan Ackermans Institute

ISBN 90-444-0460-1

CIP-DATA STAN ACKERMANS INSTITUUT

Font Balaguer, I.

Haptic feedback control designs in teleoperation systems for minimal invasive surgery / by I. Font Balaguer. - Eindhoven : Stan Ackermans Instituut, 2004. - Eindverslagen Stan Ackermans Instituut ; 2004/112 -
ISBN 90-444-0460-1
NUR 954
Keywords: Haptic feedback / Teleoperation / Master-slave systems

No esperem el blat
sense haver sembrat,
no esperem que l'arbre doni fruits sense podar-lo;
l'hem de treballar,
l'hem d'anar a regar,
encara que l'ossada ens faci mal.

Enterrem la nit,
enterrem la por.
Apartem els núvols que ens amaguen la claror.
Hem de veure-hi clar,
el camí és llarg
i ja no tenim temps d'equivocar-nos.

Cal anar endavant
sense perdre el pas.
Cal regar la terra amb la suor del dur treball.
Cal que neixin flors a cada instant.

Lluis Llach

Preface

This report is written as my final design project for the Mechatronics Design Program at the Stan Ackermans Institute (SAI). This project is done within the Medical Robotics Group at the Eindhoven University of Technology (Departments of Mechanical Engineering & Biomedical Engineering).

Abstract

The state-of-the-art in Robotic telesurgery as being available for minimal invasive surgery (MIS) is to provide haptic feedback to the hand of the surgeon. That is, the surgeon that remotely controls the instruments wants to have the ability to distinguish between different tissues and organs during operation. However, the current master-slave teleoperator systems do not provide force information to the surgeon, so surgeon needs to carry out much training before being able to perform delicate medical tasks. In order to provide haptic information sensors have to be added to the slave and actuators to the master. A control system should process the data and make a coupling between slave and master.

Furthermore, one of the major current problems when designing a control system for master-slave systems, is the enormous changes in the environment characteristics. When operating a patient, the surgeon palpates soft tissues and organs like the intestine or the fallopian tubes, as well as stiff tissues and organs like ovaries and bones in order to conclude a valid diagnostic. This means, that the controlled master-slave system has to provide robust performance and stability against such different environments.

In order to get a better insight into master-slave systems, in this project we investigate the haptic control design of one degree-of-freedom master-slave set-up available in our laboratory. To this end, we focus primarily on model-based control design within the framework of H_∞ optimization. Three different control designs have been studied. First a plain H_∞ design, robust for unstructured uncertainties, and based on performance requirements which are straightforward: matching of position and force of the slave and the master device. Second, a Linear Parametrically Varying (LPV) controller, which improves performance and it is adaptable for changes in tissue characteristics. The tissue is modeled as a second order linear mass-spring-damper system with the stiffness and damping parameters being uncertain. Finally, a passive controller is designed based on the formalism of passivity as a performance measure, which we believe is a sufficient condition to guarantee haptic feedback.

Simulation experiments have been carried out for each of the designed controllers considering linear time-invariant and time-variant parameter uncertainties in the environmental system. The three designs results to be robust against a defined range of uncertain tissue parameters.

Acknowledgments

The completion of this TWAIO wouldn't have been possible without the support and friendship from several people who have contributed to my learning process in the broadest point of view.

First, I would like to thank my supervisor, Maarten Steinbuch, for his guidance, support, and encouragement, during these two years. Bedankt dat de deur altijd open staat. I also extend my gratitude to Siep Weiland, for his enthusiasm, his valuable suggestions and discussions on my research topic. To the coordinator of Mechatronic Design, Piet Mulders, for being comprehensive and teaching me that everything outside the norms is possible. Also I would like to thank Lettie Werkman for being such a nice person and being always willing to help the others.

Specially thanks to Uri, without whos help I would not have been possible to start this experience. Thanks for all the effort you have made for me, no ho oblidare' mai! Thanks also to Talia and Paola, for sharing this long trip with me and with whom I shared unforgettable moments. Thanks also to Jan, for his help, for being my tandem english-spanish and with whom I spent nice time in the (bar) sport centrum. I would like also to thanks "the family": Eva, Talia, Paola, Apostolos, Athon, and Emmanuelle which I shared really nice moments. Especially thanks to Eva for being a good friend and with whom I spend nice times and had so great talks.

Thanks also to my officemates: Wouter and Dennis for their help and patience especially with my Latex problems. My sincere gratitude to Wouter, for all the time he spend helping me and for being always willing to answer my questions. I really appreciate all his effort. Thank's to Dennis for be the creator of LAFIX, its definitely gooood! Also Martijn, for helping me with the set-up. I really enjoyed the time we spent together playing futbolin!

My gratitude to Loy, who transmitted his knowledge and experience about master-slave teleoperator systems to me.

I would like also to thank my friends from Catalunya: Marta, Laura, Carla, Laurita, Alfons,

Miquel, Secret, Yago, Suely, and the rest, for their words when I most needed them. Especially thanks to Marta, with whom it has been proved that, definitely, the distance can not cool down our intense friendship. Also thanks to the representative of my family in the Netherlands, Sonsoles and Erik, from whom I received support and affect, and which made me feel at home.

Last, but not in any measure, the least, I would like to thank Claudi, for his moral support and understanding which gave me strength to do this TWAIO. I thank him for being patient especially during the last few months, and for being with me throughout. Gracies *amore* per deixarme volar! Also, I would like to thank my family for their support and motivation. In particular I want to thank MaAngeles, for being always willing to bring together part of my family every time I go home. Unas comidas inolvidables! Specially thanks to my brother, Salva, and his wife, Carol, for their words of support especially during my last effort.
Finally, I would like to dedicate this project to my parents for bringing me up to what I am now and for providing me the best education possible through their hard work and sacrifices.

Contents

List of Tables

List of Figures

Chapter 1

Introduction

During the last quarter of the 20th century, and especially during the last decade, many surgery procedures have experienced a turnover on the way they are performed. These surgical procedures are focussed on less or minimal invasiveness, which offers many benefits to patients compared to traditional (open) surgery. The so-called Minimal Invasive Surgery (MIS) allows surgeons to perform operations with minimal injury to the body. This results in more rapid recovery and a faster return to normal living for the patients. Unfortunately, these techniques have some disadvantages compared to traditional techniques: the reduced access at the surgical scene or the decreased capability of the surgeon to feel what he is touching inside the patient, are some examples.

Some of the disadvantages of using conventional minimal invasive surgery can be overcome by using Robotic Telesurgery, a new trend of MIS techniques where a master-slave robot can replace the conventional minimal invasive instruments. These master-slave robots are systems where the direct contact between the surgeon and the patient is uncoupled. This is done using a remote system that transmits the motion of the surgeon's hand to the instruments placed in the patient's body. The present generation of teleoperated master-slave systems solves part of the current problems of the conventional MIS but not all of them. Its major limitation is the lack of haptic feedback, i.e., the surgeon that remotely controls the instruments losses the ability to discriminate between different tissues and organs during operation.

This chapter aims to introduce the above mentioned concepts in more detail. The first and second section gives the reader a more extended introduction about Minimal Invasive Surgery and Robotic Telesurgery. The haptic concept is defined in the third section and finally the problem statement is given in the fourth section. This project is a continuation of the master thesis of Rovers [39], [40], who designed a one degree-of-freedom (DOF) master-slave setup. Extended information about MIS, Medical Robotics, Haptic Feedback can be found in the

afore-cited references.

1.1 Minimal Invasive Surgery (MIS)

Minimally invasive surgery (MIS) is a surgical technique which is becoming a method of choice over traditional (open) surgery and it covers a wide range of surgical procedures. It is minimally invasive in the sense that the surgeons operate through tiny incisions. Tubes (trocars) are inserted into the incisions and tiny instruments, such as video cameras and cutting tools, are slipped through them. Also known as endoscopic surgery, MIS refers to a growing number of surgical procedures that achieve the same surgical results as traditional operations, but are performed with much smaller incisions and little or no cutting of healthy tissue[1].

Conventional MIS instruments offer many benefits to patients in comparison to traditional surgery. The main advantage of this technique is the reduced damage to healthy tissue, which is the major reason for post-operational pain and long hospital stay of the patient in traditional surgery. Furthermore, minimally invasive procedures result in less blood loss, less pain, minimal scarring and a significant shortened recovery period for patients. It has been noted that this technique can also result in fewer post-operative infections, fewer complications and better long-term results [43],[44].

Some of the more common minimal invasive operations are: laparoscopy (abdominal cavity), thoracoscopy (chest cavity), arthroscopy (joints), pelviscopy (pelvis), and angioscopy (blood vessels). Figure 1.1 shows the location of the trocar, the instrument and the visual camera for laparoscopic surgery.

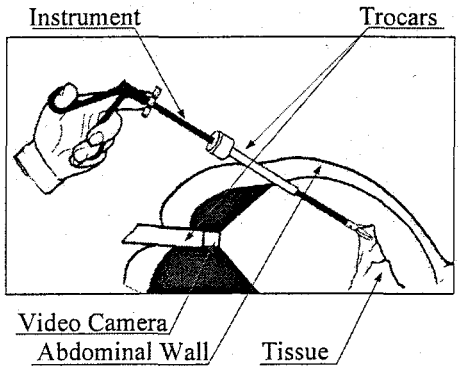

Figure 1.1: Laparoscopic Surgery

[1]The damage done to the skin, muscle, connective tissue, and bone to reach the region of interest.

The other side of MIS, unfortunately, is the surgeon's point of view: the surgeon has no direct view on the surgical scene and his accessibility is being reduced due to the tiny incisions. As a result of the reduced access, dexterity is significantly reduced because of the loss of DOF's compared to traditional instruments. Besides the reduced dexterity, there is fulcrum effect at the entry point of the instrument, i.e., the motion of the tip of the instrument, which is placed inside the patient, and the external part of the instrument, which is handled by the surgeon, are reversed. This results in more difficult instrument handling and requires specific and extensive surgical training of the surgeon [10], [38], [44]. Figure 1.2 clarifies the concepts of dexterity and the fulcrum effect.
Furthermore, the transmission mechanism of these elongated MIS instruments exhibits friction and backlash. Hence, the information received by palpation during open surgery, such as locating arteries and tumors hidden in tissue, is significantly reduced. Moreover, as the instruments get longer, the surgeon's natural tremor is augmented.

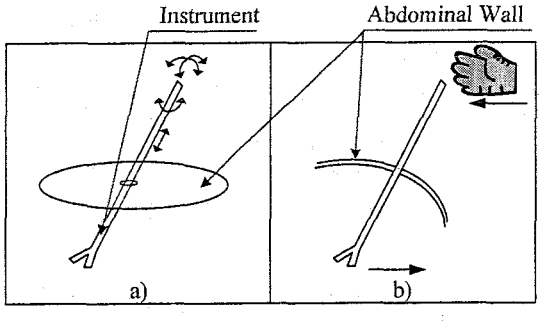

Figure 1.2: a) Dexterity of the MIS instrument. b) Fulcrum effect.

The next section explains how Robotic Telesurgery solves many of the problems of using conventional MIS, while providing more sophisticated advantages. The importance of palpation during surgery and its relation with haptics is explained in section 1.3.

1.2 Medical Robotics

The development of robotics in medical applications has been increased over the last decade. Despite the existence of many medical areas where robotics is currently being applied, our interest in robotics is centered on surgical procedures. Focused on MIS procedures, the next section introduces Robotic Telesurgery, a new trend to perform minimal invasive operations.

1.2.1 Robotic Telesurgery: Master-Slave Teleoperator Systems

Minimal invasive surgery itself is teleoperation since the surgeon is physically separated from the workspace. In Robotic Telesurgery, the conventional MIS instruments can be replaced by robotic slave manipulators controlled remotely by the surgeon through a master manipulator. Master-slave robots are systems where the direct contact between the surgeon and the patient is uncoupled using a remote system that tracks the motion of the surgeon, i.e., the surgeon operates a master control (joystick) that causes a slave robotic arm to respond. Figure 1.3 shows a master-slave system.

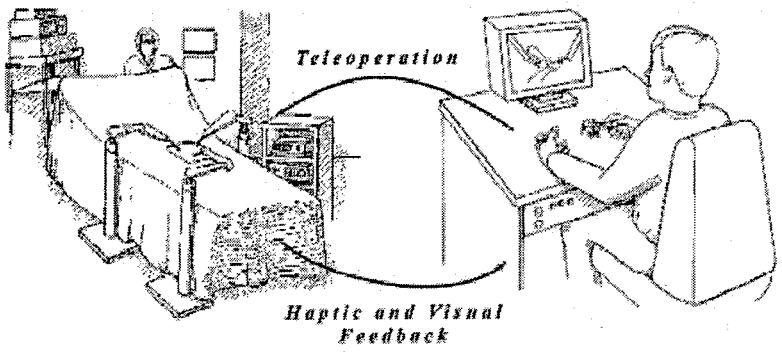

Figure 1.3: Concept of a master-slave for surgery, from [11]

The master part consists of a monitor, which shows the surgical scene, and two manipulators (joysticks) that control the instruments placed on the slave part. The slave part consists of three arms controlled by the master: two arms holding the surgical instruments and a third arm holding a special (endoscope) camera which reproduces the surgical scene.

The advantages of these systems are large because many of the obstacles of conventional MIS surgery are overcome. Dexterity is improved, the fulcrum effect is eliminated and the ergonomic position of the surgeon is enhanced. In addition, it is currently possible to make surgeries that were technically difficult or previously unfeasible. These robotic systems enhance dexterity in several ways. Instruments with increased degrees of freedom greatly enhance the surgeon's ability to manipulate instruments and thus the tissues. These systems are designed so that the surgeons' tremor can be compensated on the end-effector motion of the instrument through appropriate hardware and software filters. In addition, teleoperated systems can scale movements so that large movements of the surgeon's hand can be transformed into micromotions inside the patient. Furthermore, they eliminate the fulcrum effect, making instrument manipulation more intuitive. With the surgeon sitting at a remote, er-

gonomically designed workstation, current systems also eliminate the need to twist and turn in awkward positions to move the instruments and visualize the monitor. Thus, the proper hand-eye coordination is restored [10], [30], [44].

Nevertheless, these systems still have some disadvantages. First of all, robotic telesurgery is a new technology and its utility and efficiency have not been well established yet. To date, almost no long-term follow-up studies have been performed. Another disadvantage of these systems is their cost, which it is nearly prohibitive, and their operation, for which the surgeons need to have special training before being able to operate the robots correctly [30]. In addition, telesurgical procedures increase the problem of loss of feeling found in conventional MIS techniques so that the surgeon does not feel anything while touching the different tissues.

At the moment two master-slave systems, based on conventional MIS techniques, are commercially available: `DaVinci` [20] and `Zeus` [50]. Force feedback is not available on these systems so valuable haptic information for the surgeon is lost. The haptic concept is introduced in the next section.

1.3 Haptic Feedback

Palpation is a widely used and effective tool in many medical procedures. The palpation of human (soft) tissues and organs can only be properly examined and identified by assessing its softness, viscosity and elasticity properties. Indeed, surgeons use palpation to quickly localize hidden tumors in tissue during open surgery. The use of conventional MIS instruments (see section 1.1), makes the surgeon to lose his/her ability to discriminate between different tissues and organs during the operation. Using Robotic Telesurgery, this ability completely disappears. In both cases, the diagnostic that palpation gives to the surgeon is not useful anymore and may seriously limit the efficiency and safety of the operation [22], [32], [36], [38]. Haptic techniques can overcome this problem .

Haptic comes from the Greek term, *haptesthai*, meaning 'to touch', and its perception is one of the five human senses. In contrast to the visual sense and the senses of hearing, taste and smell, the haptic perception has no defined sensory organ (eyes, ears, tongue, nose), but its receptors (i.e., sensors of the human body) are distributed all over the body. In addition, touching an item always involves a bi-directional flow of mechanical energy from the human to the item, as well as the other way around, whereas for the other senses energy is transferred only from the environment to the human [19].

The two constituents of the human haptic perception are tactile and kinesthetic sensing. Tactile sensing is provided via different kind of receptors located in the skin. They are responsible for sensing surface characteristics such as smoothness, and detect contacts of the human body

with his/her environment. Kinesthetic sensing is provided via different receptors located in the muscles, tendons and joints. They provide information about positions, locations, orientation, movements and forces. Kinesthetic sensing encompasses larger scale details, such as basic object shape and mechanical properties, for example, compliance. By combining both tactile and kinesthetic information signals in the brain, the final feeling of touch is created.

In terms of devices, a haptic device is a robotic manipulator configured to convey tactile and/or kinesthetic feedback to the human operator. Tactile feedback deals with the devices that interact with the nerve endings in the skin, which indicate heat, pressure and texture. These devices are typically used to indicate whether or not the user is in contact with the environment. Force or kinesthetic feedback deals with the devices that interact with the muscles and tendons to give the human a sensation of a force being applied [42], [46]. These devices can be classified into two categories: impedances displays and admittances displays. Impedances displays generate forces back to the user in response to measured displacements, while admittance displays generate displacements in response to measured forces.

A master-slave teleoperated system attempts to be a haptic device. That is, in an ideal master-slave setup including haptic feedback, the surgeon experiences the same forces and textures as if he were physically present at the remote site, i.e., touching the remote environment (tissue) directly.

1.4 Problem Definition

Master-Slave teleoperated systems are becoming a popular technique for certain procedures since the benefits of MIS techniques have become general knowledge. However, one of the major shortcomings of the present generation of teleoperated master-slave systems is the lack of haptic feedback. That is, the surgeon is not able to feel what he/she is touching while performing surgery to a patient.

In order to re-establish this sense of feeling considering only kinesthetic sensing, different performance criteria were developed by different authors during the last fifteen years. The previous project done by Rovers [39] used a criterion based on the idea of perfect tracking of forces and positions. However, it would be motivating to study other control goals trying to fulfill, in a better way, the haptic requirement. Therefore, as a recommendation of his work, different performance formulations have been studied in more detail.

One of the major current problems when designing a controller for master-slave systems, is the enormous change in the environmental properties. During a typical operation in the body, the slave part comes in touch both with (relatively) stiff materials (when grasping a needle or touching a bone) and soft tissues, sometimes even with nothing during free movement in

the air. This means that the master-slave controller should be robust against changes in the remote environmental system.

The aim of this project is to design a controlled system, for the available master-slave setup, which restores the lack of haptic (kinesthetic) feedback. The master-slave setup is a simple one degree-of-freedom device, consisting of a master manipulator and a slave manipulator both actuated by an ordinary DC motor. In order to identify the control goals, different problem formulations are studied in more detail. Model-based robust control design methodology (H_∞) is used to optimize the chosen formulations.

Three different approaches are presented in this report. First, a plain H_∞ design, robust for tissue properties, and based on performance requirements which are straightforward: matching of the position and force of the slave and the master device. In order to improve performance, a gain scheduled controller (Linear Parametrically Varying) is designed, which is able to adapt to changes in the environment characteristics. Finally, a third controller based on passivity formalism is designed within the framework of H_∞ optimization.

Chapter 2 gives an overview of existing control design problem formulations as used in haptics literature in terms of stability and performance. The passivity based performance criterion is introduced. In Chapter 3 the new optimization problems are solved using model-based robust control design methodology (H_∞). Simulation results are shown in Chapter 4. Finally, conclusions and recommendations for future work are given in Chapter 5.

Chapter 2

Bilateral Control Design Problem Formulation for Haptic Devices

The aim of this chapter is to present an overview of the control goals for the master-slave teleoperator systems. The first section introduces the general teleoperation system and the importance of haptics in teleoperation. The second section gives an overview of stability and performance requirements found in literature in order to restore kinesthetic sensing. Within this section, the so-called two-port network models are explained in order to understand the notation present in literature and in the report at hand. Finally, an overview of the available master-slave control architectures for haptic feedback are introduced.

2.1 Introduction to Teleoperation

A master-slave teleoperator system consists of three subsystems: the master manipulator, the slave manipulator and the controller which also embeds the communication channel. The teleoperator interacts with two other subsystems, the human operator and the remote environment[1]. The human operator moves the master manipulator, and the master manipulator sends the required information to the slave via the controller. The slave manipulator is controlled to track the motion imposed by the human operator, while performing a task on the remote environment. Thus, the (motion) information is flowing in one direction, from the operator to the remote environment[2]. However, the design goal of any teleoperator system is to achieve the so-called telepresence, i.e., the operator feels like he/she is touching the remote

[1]In literature, the human operator and the environment are sometimes described as being part of the teleoperator system.

[2]This explanation holds for control architectures where the motion signal is fed back to the controllers

environment directly without being physically there. Thus, telepresence requires feedback information from the environment to the operator, in order to assure good performance of the surgeon, while he is operating the remote site. By means of the controller, exchange of information between the master and the slave devices is possible. Accordingly, teleoperation systems are said to be controlled bilaterally. Figure 2.2 shows the master-slave teleoperated system with the operator and the environment systems.

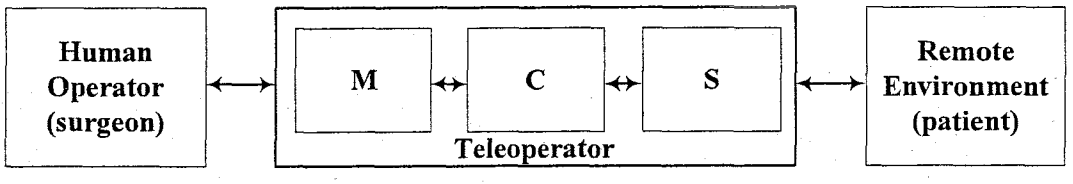

Figure 2.1: Master-Slave teleoperated system. M, S and C represents the Master, the Slave and the Controller respectively.

The information which is fed back from the environment to the operator can be provided in different forms. For instance, visual displays can be used such that the surgeon directly sees into the target operating site. However, it is not sufficient to guarantee haptic feedback. As mentioned in section 1.3, performing palpation tasks, requires both kinesthetic and cutaneous information to assure a valid diagnostic to the surgeon. Despite the importance of both requirements for the medical diagnosis, only kinesthetic information is going to be taken into account in this project. That is, force information needs to be fed back to guarantee kinesthetic sensing for the surgeon.

2.2 Teleoperator control problem formulation

In any bilateral teleoperation system design, the essential desire is to provide a good transmission of signals (positions, velocities, forces) between the master and slave to couple the surgeon as closely as possible to the remote task. The goal of designing a bilateral teleoperation, and in general for any design which involves a system to be controlled, is to make the system stable and achieve desired performance in the possible presence of time delays, plant disturbances, measurement noise and modeling errors.

In order to analyze stability and performance issues in teleoperation, and to be able to understand the terminology used in literature, the two-port model representation for bilateral systems is going to be explained in the next subsection. After that, an overview of stability and performance is introduced.

2.2.1 Formulation using the Two-Port Representation

There exist different basic ways to describe linear systems. In mechanical systems, it is common to describe a system by its transfer function or by its state space representation. Transfer functions relate one output signal with one input signal, whereas in state space representations the relationship between input and output is defined via a finite dimensional state vector. In electrical systems, besides the utilization of transfer functions, another way to describe a system is using two-port models.

Two-port or multi-port models are widely used in circuit analysis to characterize the behavior of a network with two accessible terminals for each ports. A general multi-port system is a "black box" which captures the relationships between currents and voltages at each port. Multi-port forms can also be used in the analysis of mechanical systems by substituting velocities or positions for currents (flows) and forces for voltages (efforts). At each port, the product of forces and velocities defines the power that the port delivers to the system [3]. Thus, a multi-port system provides relations between the power delivered to the system at each port. One-port and two-port networks are depicted in Figure 2.2.

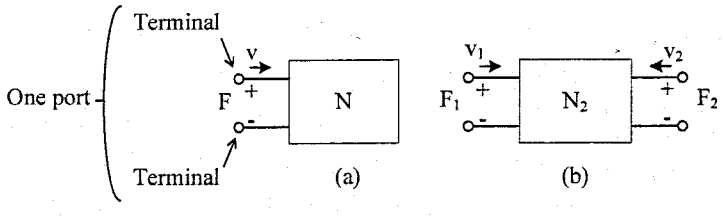

Figure 2.2: (a) One-port and (b) Two-port network using mechanical notation

Bilateral teleoperation can be viewed as a cascade interconnection of two-port and one-port blocks. The teleoperator system can be described as a two port network coupled together with two one-port blocks representing the human operator and the environment. The general configuration of a controlled bilateral teleoperation system using a network representation is depicted in Figure 2.3.

Here, M, S and C denote the components that are generally referred to as the *master*, the *slave* and the *controller* of the system. The master is a mechanical device that interacts with its environment (i.e., human operator) through the force F_{op} and the velocity v_{op} (or position x_{op}). Similarly, the slave interacts with its environment (i.e., patients' tissue) through the force F_{env} and the velocity v_{env} (or position x_{env}). In the project at hand, the M and S are given, while the controller C needs to be designed such that the two-port system that results

[3]The usual sign convention is that the power is positive if work is done on the system, negative if work is done by the system.

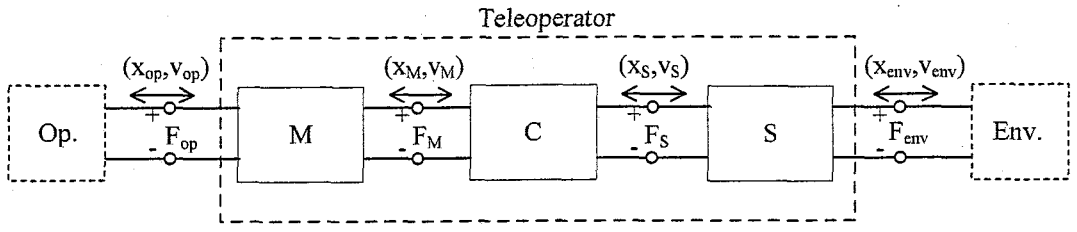

Figure 2.3: General bilateral teleoperation system using a network representation

from the interconnection has a desired behavior. The behavior that a teleoperator system has to fulfill is presented in subsections 2.2.2 and 2.2.3.

When modeling with two-port networks, it is necessary to describe the relation between efforts and flows (or vice versa) of the teleoperator system as well as of the operator and the environment in terms of an input/output relation. Depending on how these relations are described, different kinematics arise. For the two-port teleoperator system, the general way to describe the relationship between input and output signals is using the following linear matrix representation:

$$\begin{bmatrix} y_1 \\ y_2 \end{bmatrix} = \begin{bmatrix} S_{11} & S_{12} \\ S_{21} & S_{22} \end{bmatrix} \begin{bmatrix} u_1 \\ u_2 \end{bmatrix} \tag{2.1}$$

The above equations represent an input/output structure for a 2-port network, where the inputs are denoted as $u = [u_1 \quad u_2]^T$, the outputs as $y = [y_1 \quad y_2]^T$ and S_{ij}, $i,j \in 1,2$, denotes the two-port parameters. The choice of the input/output (I/O) relation is not unique. That is, a two-port network can be described using three main representations: Immitance, Transmission or Hybrid representation as shown in table 2.1. Each representation leads to two different configurations. For instance, the impedance representation (first column in table 2.1) can be described in terms of impedance parameters, mapping from flows to efforts, or in terms of admittance parameters, mapping from efforts to flows. The transmission representation (second column in table 2.1) can be described in terms of A-parameters, mapping the effort and flow of port 2 to the effort and flow of port 1, or in terms of B-parameters, mapping the effort and flows of port 1 to the effort and flows of port 2 [4]. The hybrid representation (third column in table 2.1) maps a combination of the effort and flow of different ports to their respective flow and effort.

The one-port networks, i.e., the operator and the environment, can be modeled only as impedances or as admittances. The impedance and the admittance are defined by the rela-

[4]Transmission representation is not commonly used when modeling Teleoperation systems for MIS surgery

Immitance Representation	Transmission Representation	Hybrid Representation
Impedance-parameters:	**A-parameters:**	**Hybrid-parameters (H):**
Input/output: $u^T = [u_1 \quad u_2] = [v_1 \quad v_2]$ $y^T = [y_1 \quad y_2] = [F_1 \quad F_2]$ *Matrix Representation (2.1):* $\begin{bmatrix} F_1 \\ F_2 \end{bmatrix} = \begin{bmatrix} Z_{11} & Z_{12} \\ Z_{21} & Z_{22} \end{bmatrix} \begin{bmatrix} v_1 \\ v_2 \end{bmatrix}$	*Input/output:* $u^T = [u_1 \quad u_2] = [F_2 \quad v_2]$ $y^T = [y_1 \quad y_2] = [F_1 \quad v_1]$ *Matrix Representation:* $\begin{bmatrix} F_1 \\ v_1 \end{bmatrix} = \begin{bmatrix} A_{11} & A_{12} \\ A_{21} & A_{22} \end{bmatrix} \begin{bmatrix} F_2 \\ v_2 \end{bmatrix}$	*Input/output:* $x^T = [u_1 \quad u_2] = [v_1 \quad F_2]$ $y^T = [y_1 \quad y_2] = [F_1 \quad v_2]$ *Matrix Representation:* $\begin{bmatrix} F_1 \\ v_2 \end{bmatrix} = \begin{bmatrix} H_{11} & H_{12} \\ H_{21} & H_{22} \end{bmatrix} \begin{bmatrix} v_1 \\ F_2 \end{bmatrix}$
Admittance-parameters:	**B-parameters:**	**Hybrid-parameters (G):**
Input/output: $u^T = [u_1 \quad u_2] = [F_1 \quad F_2]$ $y^T = [y_1 \quad y_2] = [v_1 \quad v_2]$ *Matrix Representation:* $\begin{bmatrix} v_1 \\ v_2 \end{bmatrix} = \begin{bmatrix} Y_{11} & Y_{12} \\ Y_{21} & Y_{22} \end{bmatrix} \begin{bmatrix} F_1 \\ F_2 \end{bmatrix}$	*Input/output:* $u^T = [u_1 \quad u_2] = [F_1 \quad v_1]$ $y^T = [y_1 \quad y_2] = [F_2 \quad v_2]$ *Matrix Representation:* $\begin{bmatrix} F_2 \\ v_2 \end{bmatrix} = \begin{bmatrix} B_{11} & B_{12} \\ B_{21} & B_{22} \end{bmatrix} \begin{bmatrix} F_1 \\ v_1 \end{bmatrix}$	*Input/output:* $u^T = [u_1 \quad u_2] = [F_1 \quad v_2]$ $y^T = [y_1 \quad y_2] = [v_1 \quad F_2]$ *Matrix Representation:* $\begin{bmatrix} v_1 \\ F_2 \end{bmatrix} = \begin{bmatrix} G_{11} & G_{12} \\ G_{21} & G_{22} \end{bmatrix} \begin{bmatrix} F_1 \\ v_2 \end{bmatrix}$

Table 2.1: Classification of two-port parameters

tions:

$$Impedance: \quad F_i = Z(v_i) \quad or \quad F_i = Z(x_i) \tag{2.2}$$

$$Admittance: \quad v_i = Y(F_i) \quad or \quad x_i = Y(F_i), \tag{2.3}$$

where for linear systems, in steady-state the impedance could be seen as the stiffness of the environment, and the admittance as the compliance (inverse of the stiffness) of the environment.

Anderson and Spong [5], Hannaford [23], Colgate [16], Lawrence [31], Yasuyoshi and Yokokohij [48], and many others (see Table 2.4 which is provided at the end of this chapter) have incorporated two-port network representations for the analysis of telemanipulator stability and performance. Hannaford introduced a framework for the design of teleopeartors based on the two-port hybrid matrix. Anderson and Spong used two-port network theory to guarantee stability for bilateral teleoperation with time delay.

2.2.2 Stability

Several researchers have focussed on stability analysis for teleoperator systems. Stability of a teleoperator depends on the stability of the teleoperator itself, but also the human and the environment play an important role on the stability of the overall system. This is due

to the dynamics of the operator and the environment, which can be considered as integral parts of the teleoperator closed loop. Unfortunately, the human and the environment are quite unpredictable which makes the teleoperator system face arbitrary dynamical systems. Although the environment and the operator can be characterized as highly nonlinear dynamic processes, for simplicity, some researchers model them by linear time invariant (LTI) differential equations to enable the usage of well known linear theory both for analysis and synthesis purposes [21], [9]. Some authors describe them as passive dynamic systems.
Others do not consider to model the dynamics of the operator, and consider the force of the human as an external disturbance to the system [17], [48].

Since classical control techniques are not well adapted to the "unpredictable" problem, alternative approaches like Robust Control Theory or Network Theory, have to be explored in order to guarantee stability (and performance) of a haptic teleoperated system. In the literature review, we found that stability analysis can be broadly classified in two main fields: network theory and control theory. Within network theory, passive theory, scattering theory and wave theory are included, whereas control theory includes classical control theory, modern control theory and robust control theory.

Network theory

A number of researchers have investigated network models to characterize stability and performance in teleoperation. The stability of two-port models depends on its terminal one-port elements (operator and environment). Most of the authors base stability arguments upon the assumption that the human operator and virtual environment are passive one-port elements, i.e., they do not supply energy to the teleoperation system [5],[16], [48], [31], [1] and [25] among others (see table 2.4). Strictly speaking, it is not realistic to assume that an operator is passive, because an operator's muscle force could be changed arbitrarily according to the intention [45]. However, from the perspective that the operator can manipulate a passive environment in a stable way, the above assumption can be taken.

Ensuring passivity of the operator and the environment, the controller design only needs to guarantee passivity of the teleoperator system. A physical interpretation of passivity is that the system cannot generate energy, and thus, from a control point of view, a passive system can never become unstable [5]. Analogously, an element is passive if it cannot produce energy. Examples are masses, inertias, springs, and dampers in mechanical systems. A system containing only passive elements is called a passive system. An element which can deliver external energy into the system is called an active element. External forces and torques are some examples of active elements in mechanical systems.

Colgate states in [16] that a necessary and sufficient condition to guarantee stability of a LTI

two-port coupled to an arbitrary passive network is that the LTI two-port itself is passive. Colgate and Hogan [17] mentioned that even if the system has an active term, the system stability is guaranteed unless the active term is in some way state-dependent. Here it comes the assumption of the role for the human operator, where his/her force can be assumed as a disturbance in the system. Yokokohji and Yoshikawa [48] assume that the operator input (F_{op}) acts as a disturbance of master-slave system to analyze stability via passivity.

Control Theory

A stability analysis based on the characteristics of a closed loop transfer function of the teleoperator including models of the environment and the human operator can be found in [21], [48]. Stability of the closed loop can be determined from the pole locations of this transfer function.

Hannaford and Rayu [21], Yokokohji and Yoshikawa [48] use the closed loop characteristic polynomial to analyse stability of teleoperator systems including the operator and the environmental dynamics. However, any teleoperation system must maintain stability under operator and environment variations. Çavuşoğlu, Sherman and Tendick [9], use a robust stability criterion for unstructed uncertainties as given in Zhou, Doyle and Glover [49]. They defined an upperbound for the operator and for the environmental impedance and then they checked for robust stability. Other authors like [27] or [25] use H_∞ control theory to guarantee stability and performance for teleoperator systems.

Time Delay

In bilateral teleoperation, the master and the slave manipulators are coupled via a communication network and time delay can be incurred in transmission of data between the master and the slave side. Systems which are stable in the case when no time delay is present, can turn into unstable systems when a delay occurs. Anderson and Spong [5] introduced the well-known scattering formalism which preserves passivity (stability) of the communication channel for constant transmission delay. The scattering transformation approach in [5] or the equivalent wave variable transformation proposed by Niemeyer and Slotine in [35], guarantees passivity of the network block for constant delay in the communication channel. Lozano, Chopra and Spong demonstrate in [34] how passivity is lost in case of time-varying transmission delay and they show that a suitable time varying gain inserted in the transmission path can recover passivity, provided a bound on the rate of change of the delay is known .

2.2.3 Performance measures

Ideally, teleoperation has simultaneously perfect position and force tracking of the master and the slave manipulators. Physically this corresponds to a massless, infinitely stiff rod connecting the master and the slave. However, this requires infinite bandwidth and zero time delay, which is not possible in practice.

Besides the fundamental requirement of *stability*, in the ideal master-slave setup including force feedback, the surgeon experiences the same forces as if he/she is touching the remote environment directly. In order to re-establish this sense of feeling, different criteria were developed during the last decade. Next, three criteria are explained in more detail: the transparency, fidelity, and passivity criterion.

Transparency Criterion

Transparency is the main form of performance measures used in teleoperation literature. Yokokohji and Yoshikawa defined transparency in terms of perfect tracking of both forces and positions [48]. Raju describes this goal in terms of impedances [37]. On either side of the two-port, the *impedance* and the *admittance* is defined by the relations

$$F_{\text{op}} = Z_{\text{op}}(v_{\text{op}}), \qquad F_{\text{env}} = Z_{\text{env}}(v_{\text{env}}) \tag{2.4}$$

$$v_{\text{op}} = G_{\text{op}}(F_{\text{op}}), \qquad v_{\text{env}} = G_{\text{env}}(F_{\text{env}}) \tag{2.5}$$

In robotic telesurgery applications, a basic requirement is good tracking in free space while the slave is in contact with a tissue. As a performance measure, [37] suggests that the impedance transmitted to the operator, Z_{op}, is the same as the environmental impedance Z_{env}. However his definition is quite general and can not be achieved for all frequencies. Assuming the mapping (2.4) and (2.5) to be linear (or linearized), Lawrence [31] defines transparency as the ratio between the transmitted and the environmental impedance, $T(j\omega) = \frac{Z_{\text{op}}(j\omega)}{Z_{\text{env}}(j\omega)}$, which needs to be kept close to one over a maximum bandwidth.

Fidelity Criterion

However, in telesurgery it is often more important to be able to detect variations in impedance[5], rather than perceive the exact impedance of the environment. Changes in impedance provide valuable information in two ways. First, the interaction between instruments and tissue can be sensed, one can feel when a needle punctures or leaves a tissue. Second, structures hidden

[5]Impedance and admittances are equivalent in that explanation.

in the tissue, like blood vessels or tumors, can be detected by palpating the tissue. An attempt to formalize this is given in Çavuşoğlu, Sherman and Tendick [9], [10], where a *fidelity criterion* is defined as

$$S_{\text{fid}} = \left\| W \frac{dZ_{\text{op}}}{dZ_{\text{env}}}|_{Z_{\text{env}}=\hat{Z}_{\text{env}}} \right\|_2 \tag{2.6}$$

Here, W is a frequency dependent weighting filter, $\hat{Z}_{\text{env}}$ is the nominal environment impedance, $\|\cdot\|_2$ denotes the H_2 norm, and differentiation is understood in the sense that the impedance Z_{op} is viewed as a function of the environmental impedance Z_{env}. The criterion therefore reflects variations in impedance. For kinesthetic feedback, a low-pass filter with a cut-off frequency of about 40 Hz is used as the weighting filter W by [9], [18], and [41].

Transparency is one specific choice of fidelity measure which quantifies how close the transmitted impedance is to the environment impedance [9], [10].

Passivity Criterion

A drawback of the previous performance criteria is that they impose an input-output structure in the teleoperation system that does not necessarily correspond to the physical reality. Indeed, the human operator and the environment need to be modeled either by means of impedances or admittances in order to apply the previous criteria. That can be reflected in the two-port of Figure 2.3, which has no 'natural' input and output structure.

The project at hand proposes a performance criterion based on passivity. Some concepts need to be clarified before explaining this criterion.

Consider the system

$$\Sigma : \begin{cases} \dot{x} = Ax + Bu \\ y = Cx + Du \end{cases} \tag{2.7a}$$

where $u(t) = \text{col}(F_{\text{op}}(t), -F_{\text{env}}(t))$, and $y(t) = \text{col}(v_{\text{op}}(t), v_{\text{env}}(t))$.

Suppose $u(t) \in \mathcal{U}$ and $y(t) \in \mathcal{Y}$ where $\mathcal{U} = \mathcal{Y} = \mathbb{R}^m$ have the same dimensions.
Let $S : \mathcal{U} \times \mathcal{Y} \to \mathbb{R}$ be a function defined as $S(u, y) = u^T y$. We call S the supply function and consider its time dependence $S(u(t), y(t))$ which we refer to as the power supplied on either side of the two-port of the teleoperator at time t, $p(t)$[6].

The two port of Figure 2.3 represented by Σ is said to be *dissipative* with respect to the supply $S = u(t)^T y(t)$, if there exists a nonnegative function $V(x)$ representing the internal energy of the system, such that

$$V(x(t_0)) + \int_{t_0}^{t_1} (p_{\text{op}}(t) - p_{\text{env}}(t))\, dt \geq V(x(t_1)) \geq 0 \tag{2.8}$$

[6]The sign convention is that power is positive if energy is delivered to the system.

for all $t_0 \leq t_1$ and for all trajectories (F_M, F_S, v_M, v_S). Here,

$$\begin{aligned} & p_{\text{op}}(t) = F_{\text{op}}(t) v_{\text{op}}(t) \\ & p_{\text{env}}(t) = F_{\text{env}}(t) v_{\text{env}}(t) \\ \text{and} \quad & p(t) = S(u(t), y(t)) = p_{\text{op}}(t) + p_{\text{env}}(t) \end{aligned} \tag{2.9}$$

Expression (2.8) states that the total energy input to the system over an arbitrary time interval $[t_0, t_1]$ is greater or equal to the net change in energy of the system. The difference between the total energy input and the net change is the energy dissipated by the system. That is why the systems which satisfy (2.8) are called dissipative systems. A dissipative system is (Lyapunov) stable as it is proofed in Appendix A.

Analogously, a system is called *conservative* if the first equality of equation 2.8 holds for all $t_0 \leq t_1$ and for all trajectories. That is,

$$V(x(t_0)) + \int_{t_0}^{t_1} (p_{\text{op}}(t) - p_{\text{env}}(t))\, dt = V(x(t_1)) \geq 0 \tag{2.10}$$

This expresses the existence of a *conservation law* where V, the internal energy, is preserved at all time and for all possible behavior of the system. Hence, passivity requires that the work done on the system, i.e., the energy that the operator supplies to the teleoperator system in any time interval, will be equal to the energy the teleoperator system supplies to its environment. Taking into account that we are dealing with a bilateral teleoperator, also passivity requires that the energy that the environment supplies to the system at any time interval will be equal to the energy that the system supplies to the operator.

A system is called *cyclo dissipative* if

$$\int_{t_0}^{t_0+T} (p_{\text{op}}(t) - p_{\text{env}}(t))\, dt \geq 0 \tag{2.11}$$

for all *T-periodic* trajectories $(F_{\text{M}}, F_{\text{S}}, v_{\text{M}}, v_{\text{S}})$.

Analogously, a system is called *cyclo conservative* if

$$\int_{t_0}^{t_0+T} (p_{\text{op}}(t) - p_{\text{env}}(t))\, dt = 0 \tag{2.12}$$

for all *T-periodic* trajectories $(F_{\text{M}}, F_{\text{S}}, v_{\text{M}}, v_{\text{S}})$.

Assuming now that for the initial time t_0 the internal energy $V(x(t_0))$ is zero, i.e., the system is at rest, and for the time t_1, $x(t_1)$=0 (this condition do not imply periodicity of the signals). Then, we will call the system *passive* if

$$\int_{-\infty}^{t_1} (p_{\text{op}}(t) - p_{\text{env}}(t))\, dt = 0 \tag{2.13}$$

for all *T-periodic* trajectories (F_M, F_S, v_M, v_S) and for all t_1.

Thus, passivity as a performance measure is seen in terms of energy. That is, the energy supplied from the operator to the environment has to be equal as the energy supplied from the environment to the operator. Note that, if the time intervals are chosen really small, this concept is more restrictive and better performance can be achieved in terms of energy.

2.3 Control Algorithms

The general teleoperation system of Figure 2.3 may lead to many different control schemes. In the literature a number of different control schemes have been proposed for telemanipulation systems, based on different criteria. In each scheme, stability and performance issues are the major concerns. Arcara and Melchiorri [6] provides an overview of the several bilateral control schemes proposed in literature. Lawrence [31] presents a general multivariable system architecture which includes four types of data transmission between master and slave: force and velocities in both directions. He shows that a proper use of all four channels is necessary to achieve high performance telepresence in the sense of an accurate transmission environment impedance to the operator. He compare different common architectures in terms of stability and transparency and he showed that exists trade-off between stability and transparency. Figure 2.4 shows the position control architecture

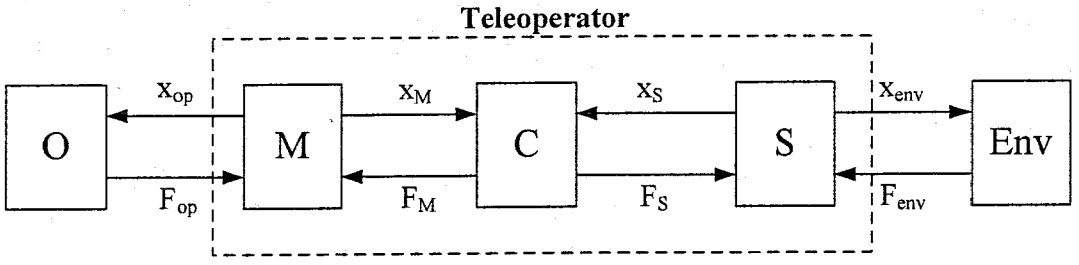

Figure 2.4: Position control architecture

where the controller C,

$$\mathrm{C}: \begin{pmatrix} x_M \\ x_S \end{pmatrix} \mapsto \begin{pmatrix} F_M \\ F_S \end{pmatrix}$$

In this project we consider a special case of the above mentioned architecture: the position error (PERR) control architecture depicted in Figure 2.5. The PERR architecture is the same as the open loop impedance control in [18], the symmetric servo system in [29] and the force reflection in [7].

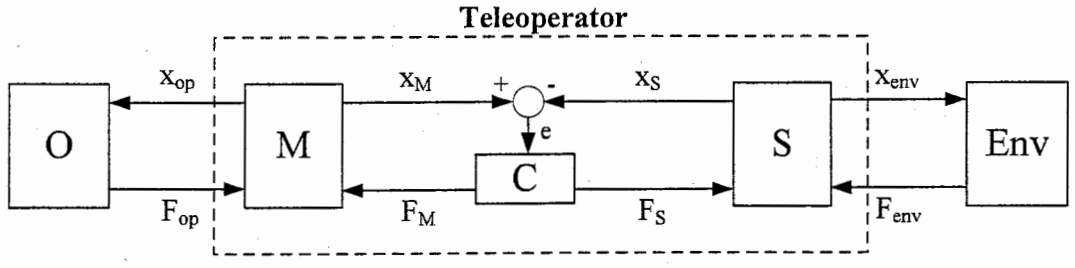

Figure 2.5: Position Error control architecture

where the controller C,

$$\mathrm{C} : \begin{pmatrix} x_M - x_S \end{pmatrix} \mapsto \begin{pmatrix} F_M \\ F_S \end{pmatrix}$$

where the forces F_M and F_S are generated by the controller C, that is fed by the position error $e = x_M - x_S$ between the master and the slave. Position and force tracking can only be obtained by using high controller gains, which are only possible at low bandwidths in order to prevent instabilities. Because the master and slave are coupled by a (stiff) controller, the human operator perceives inertia and damping of both the master and slave device on top of the environment impedance.

An extensive description of the different control architectures for telesurgery is provided by Rovers [39].

Author/year	Title Paper	Formulation	Stability	Performance	Observations
Hannaford 1989 [24]	**Stability and Performances tradeoffs in bilateral telemanipulation**	**✓2-Port Network:** *Hybrid Matrix* **✓Transfer Functions:** *= f(hybrid parameters)*	**✓Assumption: Linear model Op./Env.** Roots(Char.Pol.)∈RHP	**✓Transparency:** v's and F's	Time Delay
Hannaford 1989 [23]	**A design framework for teleoperation with kinesthetic feedback**	**✓2-Port Network:** *Hybrid Matrix* **✓Transfer Functions:** *= f(impedances)*	**✓Assumption: Linear model Op./Env.** Roots(Char.Pol.)∈ RHP	**✓Transparency:** v's and F's	Time Delay
Anderson and Spong 1989[4]	**Asymptotic Stability for force reflecting teleoperation with time delay**	**✓Hilbert Network** *Impedance matrix*	Passivity	**✓Transparency:** v's and F's	Time Delay
Raju, Verghese and Sheridan 1989 [37]	**Design Issues in 2-Port Network Models of bilateral remote telemanipulator**	**✓2-Port Network:** *Impedance Matrix*	**✓Assumption: Passive Op./Env.** Passivity	**✓Transparency:** Z_{op}=Z_{env}	
Anderson and Spong 1989[5]	**Bilateral control of teleoperators with time delay**	**✓2-port Network:** *Hybrid Matrix* *Scattering Matrix*	Passivity	**✓Transparency:** v's and F's	Time delay
Colgate 1991[16]	**Power and Impedance scaling in bilateral manipulation**	**✓2-port Network:** *Scattering Matrix*	**✓Assumption: Passive and Linear Op./Env.** Passivity⇒Stability Robust stability		Power Scaling
Lawrence 1993 [31]	**Stability and Transparency in Bilateral Teleoperation**	**✓2-Port Network:** *Hybrid Matrix* *Scattering Matrix* **✓Transfer Functions:** *= f(Impedances)*	Passivity	**✓Transparency:** $T = \frac{Z_{op}}{Z_{env}} = 1$	Time Delay
Yasuyoshi and Yokokohji 1994[48]	**Bilateral Control of MSM for ideal kinesthetic coupling**	**✓2-Port Network:** *Impedance Matrix* Scattering Matrix **✓Transfer Functions:** *= f(Impedances)*	**✓Assumption: Passive Env. Disturbance Op.** Passivity ⇒ Stability **✓Assumption: Linear model Op./Env** Roots(Char.Pol.)∈RHP	**✓Transparency:** x's and F's	

Table 2.2: Author's Review.1

Author/year	Title Paper	Formulation	Stability	Performance	Observations
Kazeroni, Tsay and Hollerbach 1993 [27]	A controller Design framework for telerobotic systems	✓Transfer Functions: = *f(Impedances)*	Small Gain Theorem	✓Transparency: x's and F's	H_∞ Control Theory
Hu, Salcudean and Loewen 1995 [25]	Robust controller Design for teleoperation systems	✓2-port Network: *Impedance Matrix*	✓Assumption: Passive Op./Env. Small Gain Theorem (Robust Stability)	✓Transparency: x's and F's	H_∞ control theory Time delay
Hu, Salcudean and Loewen 1996 [26]	Optimization-Based Teleoperation Controller Design	✓2-port Network: *Admittance Matrix*	✓Assumption: Passive Op./Env. Small Gain Theorem (Robust Stability)	✓Transparency: v's and F's	H_∞ control Theory Motion Scaling
Adams, Moreyra and Hannaford 1998 [2]	Stability and Performance of Haptic displays: Theory and Experiments	✓2-port Network: *Immitance Matrix*	✓Assumption: Passive Op./Env. Passivity⇒Stability	✓Transparency: v's and F's	
Adams and Hannaford 1998 [3]	A two-port framework for the design of unconditionally stable Haptic Interfaces	✓2-port Network: *Hybrid Matrix*	✓Assumption: Passive Op./Env. Passivity⇒Stability	✓Transparency: v's and F's	
Adams and Hannaford 1999 [1]	Stable Haptic Interaction with Virtual Environments	✓2-port Network: *Hybrid Matrix*	✓Assumption: Passive Op./Env. Passivity⇒Stability	✓Transparency: v's and F's	
Sherman, Çavuşoğlu and Tendick 2000 [41]	Comparison of Teleoperation control architectures for palpation tasks	✓2-Port Network: *Hybrid Matrix* ✓Transfer Functions: = *f(Impedances)*	✓Assumption: Linear Op./Env. Robust Stability Criterion	Optimization: Fidelity Position tracking	Uncertainty in Op./Env. impedances
Sherman, Çavuşoğlu and Tendick 2001 [9]	Bilateral controller design for telemanipulation in soft environment	✓2-Port Network: *Hybrid Matrix* ✓Transfer Functions: = *f(Impedances)*	✓Assumption: Linear Op./Env. Robust Stability Criterion	Optimization: Fidelity Position tracking	Uncertainty in Op./Env. impedances
Sherman, Çavuşoğlu and Tendick 2002 [12]	Desgin of bilateral teleoperated controllers for haptics. Exploration and telemanipulation of soft environments	✓2-Port Network: *Hybrid Matrix* ✓Transfer Functions: = *f(Impedances)*	✓Assumption: Linear Op./Env. Robust Stability Criterion	Optimization: Fidelity Position tracking	Uncertainty in Op./Env. impedances

Table 2.3: Author's Review.2

Author/year	Title Paper	Formulation	Stability	Performance	Observations
Lozano, Chopra and Spong 2002 [34]	**Passivation of force reflecting bilateral teleoperators with time varying delay**	**✓Differential Equations ✓Scattering Transformation**	Passivity	**✓Transparency:** v's and F's	Time-varying delay Internet communication medium
Leeraphan, Maneewarn and Laowattana 2002 [33]	**Stable Adaptive bilateral Control of Transparent Teleoperation through time-varying delay**	**✓Differential Equations**	Passivity	**✓Transparency:**	Constant Time delay Time-varying delay
Chopra, Spong, Hirche and Buss 2003 [13]	**Bilateral Teleoperation over the Internet : the Time varying delay problem**	**✓Differential Equations ✓Scattering Transformation**	Passivity	**✓Transparency:** v's and F's	Time-varying delay
Chopra, Spong and Barabanov 2004 [14]	**On position tracking in bilateral teleoperation**	**✓Differential Equations ✓Scattering transformation**	Passivity	**✓Transparency:** v's and F's	Time delay

Table 2.4: Author's Review.3

Chapter 3

Model-Based Control Design

Focused on model-based control design within the framework of H_∞ optimization, two criteria are going to be studied in more detail using H_∞ approach: the transparency criterion and the passivity approach explained in Chapter 2. First, the dynamic model of the available system is described. Then, the general H_∞ control problem is introduced. Next, we synthesize three different controllers using the PERR architecture.

3.1 Experimental setup

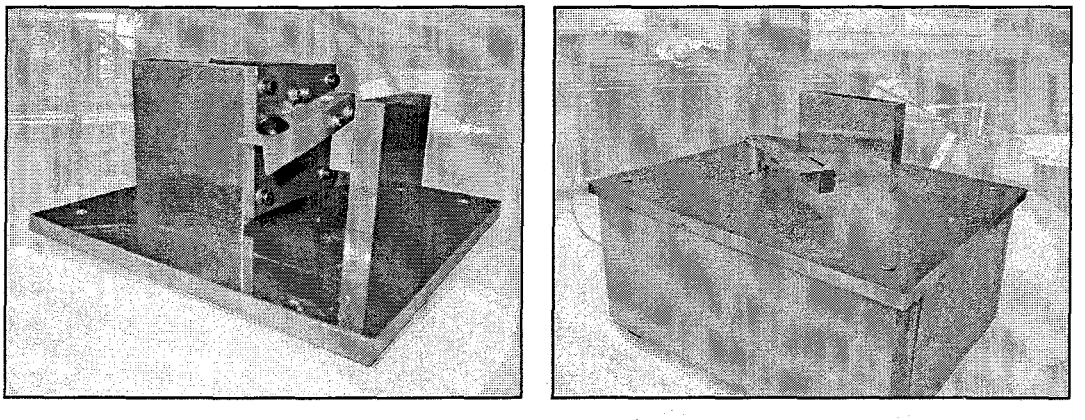

Figure 3.1: Master (left) and Slave (right)

For the experimental setup it was chosen that both master and slave devices must be able to perform rotational motion. To satisfy the specifications, a special DC motor was chosen as actuator of both master and slave. The signals that currently can be measured in the setup are positions of both master and the slave, and the force that is acting on the environment. For the position measurement, and encoder with 1000 counts per turn is used. For the force

measurement a load cell is used. Figure 3.1 shows the resulting master and the slave devices. Both systems have been build as a modular platform. This means that the tools connected to the motor can be replaced, e.g., the push-button interface for palpation that is connected to the master can be replaced by forceps handle.

For further details about the design and selection of the components that constitute the available setup referred to Rovers [39].

From now on, the explanations will be based on linear motion despite that the set-up provides rotational motion. Thus, forces and linear velocities stands for torques and angular velocities respectively.

3.1.1 Dynamic Model Description

System identification of the available master-slave device was done by Rovers [39]. He shows that both, master and slave systems are very stiff and resonances only occur at frequencies far above the region of interest. He concluded that, up to certain frequencies, both master and slave systems can be modeled as a simple mass depicted by m_M and m_S respectively.

Master and Slave System

With reference to the PERR control structure of Figure 2.5, the *master* consists of a mass m_M that is subject to the external forces F_{op} and F_M, where F_{op} represents the force that is applied by the human operator, and F_M represents the resulting force of the (master) controller. Similarly, the *slave* consists of a mass m_S that is subject to external forces F_{env} and F_S, where F_{env} represents the force that the environment apply to the slave device, and F_S represents the resulting force of the (slave) controller. Both the master and the slave are represented by Newton's second law

$$m_M \ddot{x}_M = F_{\text{op}} - F_M \tag{3.1a}$$

$$m_S \ddot{x}_M = F_S - F_{\text{env}} \tag{3.1b}$$

where x_M and x_S denote the displacement of the master and the slave, respectively.

Human Operator System

As was mentioned in section 2.2.2, the human operator can be modeled using a dynamic expression or can be considered as an external disturbance. A disturbance consideration offers to the operator an active role when manipulating the master device, which corresponds

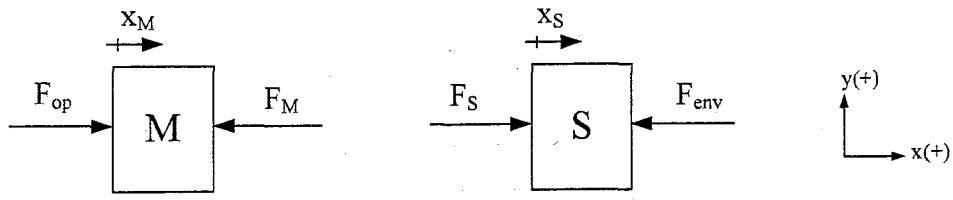

Figure 3.2: Master and Slave system representation

with the reality. A disturbance is defined as a signal which does not have any relation with the states of the system on which it is present. Thus, it seems that no relation between the position of the master manipulator and the force of the human operator is possible. However, the human's finger can not be considered as a rigid body. It has some stiffness, which implies a relation between the position of the master manipulator, x_M, and the force of the human, F_{op}. This relation can be highly non-linear but for simplicity, several authors described this relation using linear passive dynamical systems. Hence, both definitions do not completely correspond to reality. Indeed, the human is a non-rigid active element.

In this project, the dynamics of the human operator are not considered, and it is assumed that the force applied by the operator, F_{op}, acts as a disturbance.

Uncertain Environmental System

The environment system is modeled as a linear second order mass-spring damper system. Taking into account that the tissue properties are highly unpredictable, we consider it necessary to treat them as uncertainties. That is, the tissue can be viewed as an uncertain dynamical system represented by the equation

$$F_{\text{env}} = m_T\ddot{x}_T + b_T\dot{x}_T + k_T x_T, \quad v_{\text{env}} = \dot{x}_T \tag{3.2}$$

where x_T is the tissue displacement, and m_T, k_T and b_T represent the mass, the stiffness and the damping coefficient of the tissue.

Two different modes of operation can be distinguished in surgical operations: a 'free mode' in which the tissue is not connected to the slave (tip of the instrument), and a 'contact mode' in which the slave touches the tissue. When in contact, the slave displacement x_S and the tissue displacement x_T coincide, i.e.,

$$x_T = x_S. \tag{3.3}$$

Considering exclusively the contact mode, the master and slave system are linear time-

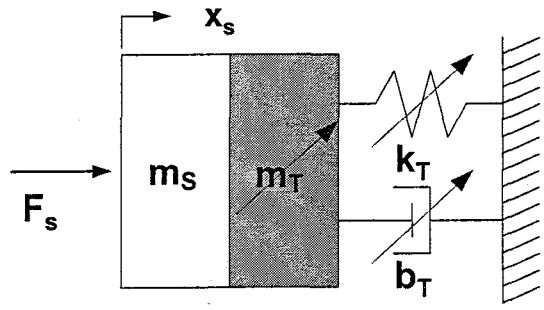

Figure 3.3: Coupled slave and environment system with parameter uncertainty

invariant (LTI) with transfer functions

$$M(s) = \frac{1}{m_M s^2}, \qquad S(s) = \frac{1}{(m_S + m_T)s^2 + b_T s + k_T} \tag{3.4}$$

where $M(s)$ and $S(s)$ results from the equations 3.1, 3.2 and 3.3 mapping $\{F_{\text{op}} - F_M\} \mapsto \{x_M\}$ and $\{F_S - F_{\text{env}}\} \mapsto \{x_S\}$ respectively. The slave and the environment system can be represented like in Figure 3.3, where the inertia, the damping and the stiffness represent the uncertain parameters of the tissue. These parameters can vary along time, while palpating a tissue, and also along different tissues.

Two different ways to deal with the uncertainty are presented in this project. First, a frequency dependent uncertainty, where the nominal plant $(M_{nom}(s), S_{nom}(s))$ is bounded by some frequency dependent band. That is,

$$M(s) = M_{\text{nom}}(s) + \Delta_M(s)$$
$$S(s) = S_{\text{nom}}(s) + \Delta_S(s)$$

with $|\Delta_M(j\omega)| < \delta_M(j\omega)$ and $|\Delta_S(j\omega)| < \delta_S(j\omega)$.
Second, a parametric uncertainty, where the parameters k_T and b_T are varying inside a predescribed box,

$$(k_T, b_T) \in \mathcal{P}_{\text{BOX}} \subset \mathbb{R}$$

Hence, two different controllers are going to be designed, one called the nominal H_∞ controller design which deals with the first mentioned type of uncertainty, explained in section 3.3. The other one is called LPV controller design, which treats the uncertainty as a parametric uncertainty and it is explained in section 3.5.

The physical parameters are given in Table 3.1,

m_M [kgm]	m_S [kgm]	m_T [kgm]	
2×10^{-4}	8.5×10^{-4}	1×10^{-3}	

k_T^- [Nm/rad]	k_T^+ [Nm/rad]	b_T^- [Nms/rad]	b_T^+ [Nms/rad]
0.1	0.9	0.003	0.1

Table 3.1: Physical parameters.

where k_T^+, k_T^-, b_T^+ and b_T^- define the parameter box $\mathcal{P} = [k_T^-, k_T^+] \times [b_T^-, b_T^+]$. $\mathcal{P}$ is represented in Figure 3.4.

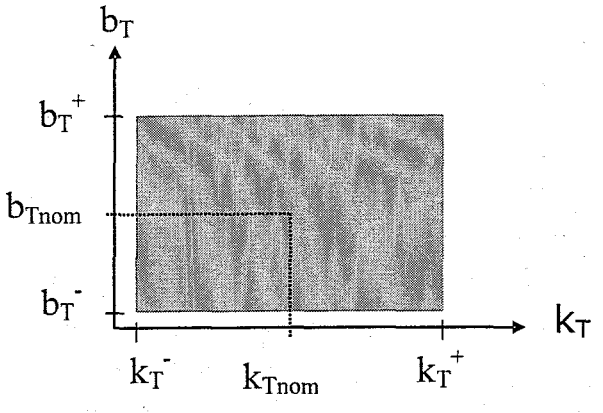

Figure 3.4: Parameter box $\mathcal{P}$

where the *nominal values* of k_T and b_T are taken to be the averages

$$k_T^{\text{nom}} := \frac{k_T^+ + k_T^-}{2}, \qquad b_T^{\text{nom}} := \frac{b_T^+ + b_T^-}{2}$$

Note that the physical parameters have rotational units due to the rotational motion that the set-up provides.

3.1.2 Control Specifications

Considering the requirement of providing kinesthetic sensing to the human operator, some remarks need to be emphasize:

• A single finger can stand a force up to 7 N without experiencing discomfort or fatigue. For that reason, the force applied by the human operator is assumed to satisfy $|F_{\text{op}}(t)| < 10\text{N}$. This specification is translated in terms of torques due to the rotational motion that both,

master and slave devices, perform. Assuming a distance of 60mm between the rotation point of the actuator and the force applied to the master probe, a maximum torque of 0.6Nm is required

- The human operator can perform movements up to 10 Hz. The tremor signal is present between 8 and 12 Hz.
- Kinesthetic sensing detects frequencies up to 10 Hz. Thus, the bandwidth is required to be at least 10 Hz.

Furthermore, the position error $e = x_M - x_S$ is required to be at most 0.01 rad when the maximal force is applied by the operator.

For further details on the properties of the human operator see Rovers [39].

3.2 Robust Control technique: H_∞ control

Classical control theory has allowed people to control and automate their environment for decades. Classical control is characterized by the use of Root Locus, Bode plots, Nichols charts and Nyquist plots for design and analysis. The resulting controller design attempts to make the closed-loop system perform as required. On the other hand, modern control techniques have allowed engineers to optimize the control system they build for cost and performance. However, optimization control algorithms are not always tolerant with the unmodeled dynamics of the system to be controlled. Robust control refers to the control of uncertain plants with subject to unknown (but bounded) disturbances.

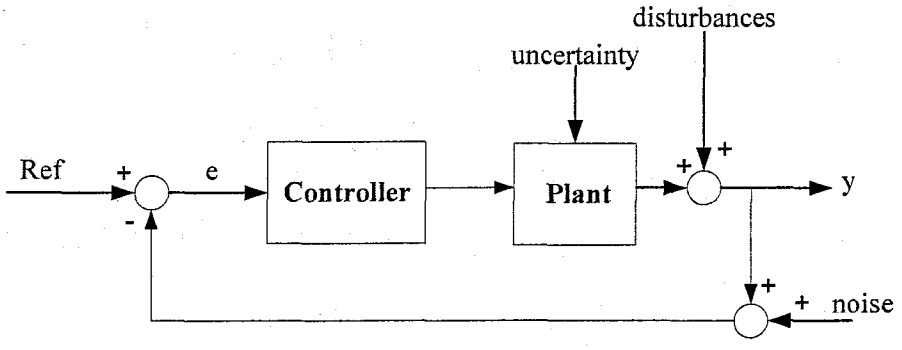

Figure 3.5: Plant control loop with uncertainty

Figure 3.5 shows an expanded view of the simple control loop that one can find in classical control theory. Uncertainty is shown entering the system in three different places: there is uncertainty in the model of the plant, there are disturbances that occur in the plant system, and there is noise which is read in the sensor inputs.

Modern control used to deal with uncertainty using stochastic control, that is, uncertainties in the system are modeled as probability distributions. Robust control methods seek to bound the uncertainty rather than express it in the form of a distribution. Given a bound on the uncertainty, the control can deliver results that meet the control system requirements in all cases. It must be recognized that some performance may be sacrificed in order to guarantee that the system meets certain requirements.

There are a variety of techniques that have been developed for robust control. This section attempts to briefly describe the basic concept of the so-called H_∞ control.

3.2.1 Standard H_∞ Control Problem

In this section we introduce what is known as H_∞-optimization as a design tool for linear multivariable control systems. In order to be able to perform an H_∞-optimization, an augmented plant has to be constructed. Figure 3.6 shows the general control configuration. The system block $H_{\text{aug}}(s)$ denotes the generalized plant and typically includes the model of the plant $T(s)$, i.e., the models of the master and the slave devices (see equation 3.1), together with all shaping filters that are needed for characterizing the exogenous inputs w, and weighing filters to penalize the exogenous outputs z.
The block C(s) denotes the controller which has as inputs the measured outputs signals y, and as outputs gives the inputs signals u to control the plant.

Every such admissible controller C(s) gives rise to a closed loop system which maps disturbance inputs w to the to-be controlled output variables z. The Δ block models the uncertainty of the (controlled) system.

By solving the H_∞ optimal control problem, a controller C(s) is obtained which minimizes the H_∞ norm of the closed loop transfer function mapping w to z, i.e.,

$$\mathrm{C}(s) = \arg \inf_{\mathrm{C}} \sup_{\mathrm{w}} \frac{\|\mathrm{z}\|_2}{\|\mathrm{w}\|_2} \tag{3.5}$$

where

$$\|z\|^2 := \{\int_0^\infty \left(z(t)^T z(t)\right) dt\}^{1/2}$$

is the usual L_2 norm of a signal, and $\mathrm{C} \in \mathcal{C}$ where $\mathcal{C}$ is the class of linear time invariant (finite dimensional) systems that internally stabilize H_{aug}. For any $\mathrm{C} \in \mathcal{C}$, the output z in (3.5) can be represented (in closed loop) as

$$\dot{\xi} = A_{\text{cl}}\xi + B_{\text{cl}}\mathrm{w}$$
$$\mathrm{z} = C_{\text{cl}}\xi + D_{\text{cl}}\mathrm{w}$$

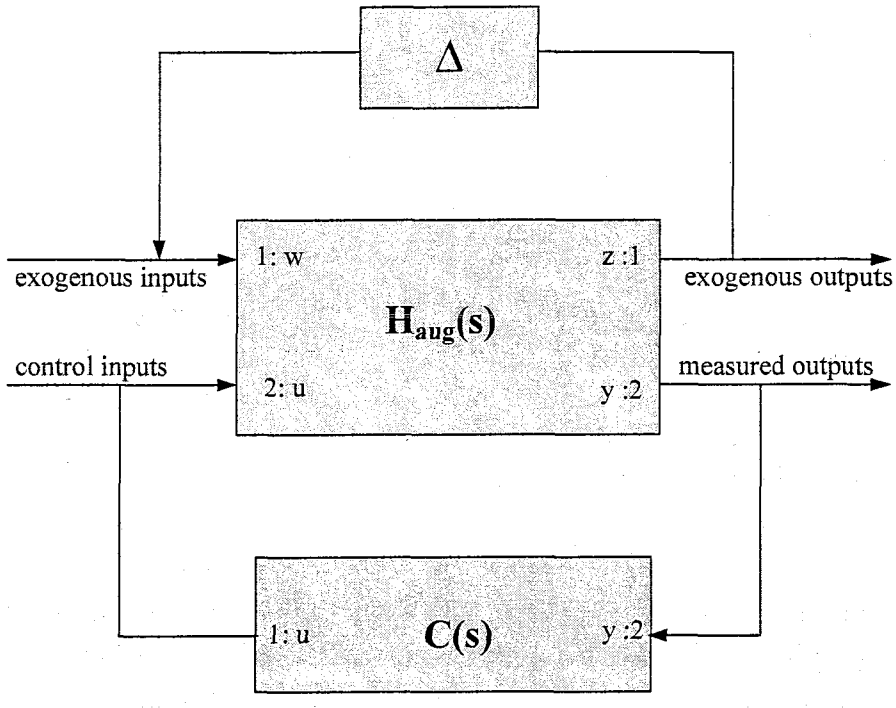

Figure 3.6: Schematic view of the augmented plant

Let $T_{\mathrm{cl}} = C_{\mathrm{cl}}(Is - A_{\mathrm{cl}})^{-1}B_{\mathrm{cl}} + D_{\mathrm{cl}}$ denote the closed loop transfer function, then

$$\sup_{\mathrm{w}} \frac{\|\mathrm{z}\|_2}{\|\mathrm{w}\|_2} = \sup_{\omega} \sigma_{\max}(T_{\mathrm{cl}}(j\omega)) = \|T_{\mathrm{cl}}\|_{H_\infty} \tag{3.6}$$

where $\sigma_{\max}$ denotes the maximal singular value and $\|\mathrm{w}\|_2$ denotes the usual two-norm $\|\mathrm{w}\|_2^2 = \int_0^\infty |\mathrm{w}(t)|^2 dt$. The norm $\|\cdot\|_{H_\infty}$ defines the H_∞ norm of the system.

Several mathematical techniques have been developed to compute H_∞-optimal controllers, i.e., feedback controllers which stabilize a closed loop system and at the same time minimize the H_∞ norm of a closed loop transfer function from $\mathrm{w} \mapsto \mathrm{z}$. The solution presented in this report admits a relatively straightforward implementation in Matlab.

3.3 H_∞ optimal design for transparency

The term transparency was presented in section 2.2.3, where it was defined in different ways by different authors. Considering Lawrence definition [31]:

$$T(j\omega) = \frac{Z_{op}(j\omega)}{Z_{env}(j\omega)} = 1; \quad |\omega| \leq \text{Max.BW}, \tag{3.7}$$

where Z_{op} and Z_{env} are the linear transfer functions of the transmitted impedance to the operator and the environment impedance. The criterion to keep the transparency close to

one for a specified bandwidth can be expressed in terms of the H_∞ norm. This amounts to find a stabilizing controller C that minimizes the H_∞ norm

$$\min_{C}\|(Z_{\text{op}} - Z_{\text{env}})\|_{H_\infty} \quad \text{or} \quad \min_{C}\|(G_{\text{op}} - G_{\text{env}})\|_{H_\infty} \tag{3.8}$$

with $C \in \mathcal{C}$, and G denotes admittance. Considering the PERR control structure, C is a MIMO system with one input being the position error, $e = x_M - x_S$, and two outputs being the control efforts F_M and F_S.

In that project, we assume that F_{op} is equal to F_{env}. Thus, equation (3.8) can be rewritten as

$$\min_{C}\|\frac{x_M - x_S}{F_{op}}\|_{H_\infty} \quad \text{or} \quad \min_{C}\|\frac{F_{op}}{x_M - x_S}\|_{H_\infty} \tag{3.9}$$

3.4 Nominal H_∞ Design

The first design using the modified transparency criterion explained in the foregoing section is the nominal H_∞ design. Here, the controller C is calculated for a nominal plant with nominal values of k_T and b_T. The PERR structure from Figure 2.5 is equivalent to the following scheme:

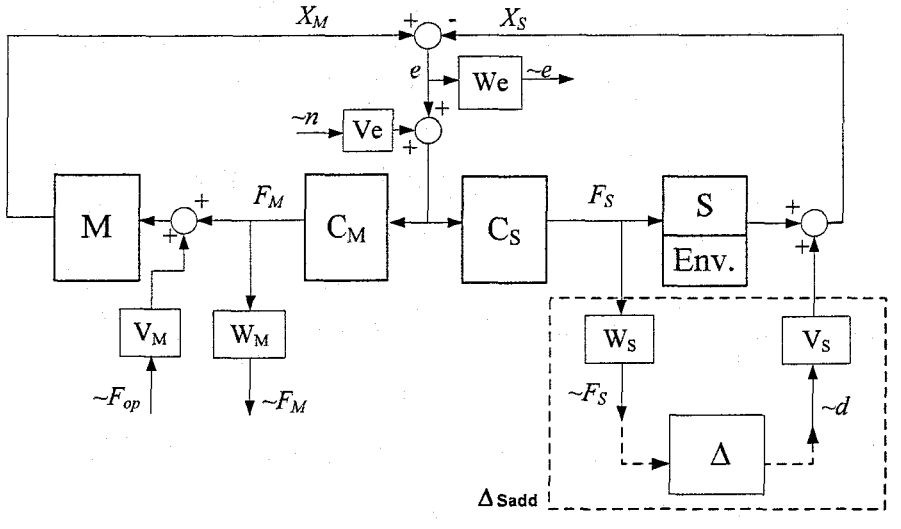

Figure 3.7: PERR structure for a disturbance operator and the coupled environment

where in that case, the operator is seen as a disturbance, and the environment is coupled with the slave. V_M, V_e, V_S are shaping filters and W_M, W_e, and W_S are weighting functions that are designed on the basis of human specifications, limitations of the real setup,and the

desired frequency response of the controlled system. The appropriate choices for these filters is discussed in the next chapter. The closed-loop transfer function maps w = col(F_{op}, d, n) to z = col(e, F_M, F_S) . The H_∞ control problem amounts to characterizing

$$\gamma^* := \inf_{C} \sup_{w} \frac{\|z\|_2}{\|w\|_2} \tag{3.10}$$

Let C_{nom} be a nominal controller which achieves γ^* (or $\gamma^* + 10^{-10}$ if no optimal controller exists).

For the nominal design, Linear Fractional representation of uncertainty is used. Considering an additive uncertainty, the nominal plant $S_{\text{nom}}(s)$ is bounded by some frequency dependent band expressed by Δ_{Sadd}. That is, Δ_{Sadd} defines a bounded band around the nominal plant $S_{\text{nom}}(s)$ such that the real plant $S(s)$ lies within the bound. This idea is depicted in Figure 3.8.

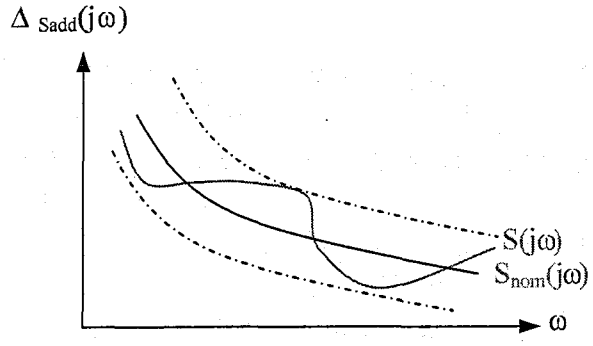

Figure 3.8: Additive Representation of uncertainty

Once a stabilizing controller C which accomplish 3.8 is obtained, robustness can be checked by considering:

$$\begin{aligned} &S(j\omega) = S_{\text{nom}}(j\omega) + \Delta_{\text{Sadd}}(j\omega) \rightarrow S(j\omega) - S_{\text{nom}}(j\omega) = \Delta_{\text{Sadd}}(j\omega) \\ &\Delta_{\text{Sadd}}(j\omega) = W_S \Delta V_S, \quad \|\Delta\|_{H_\infty} \leq \frac{1}{\gamma^*} \end{aligned} \tag{3.11}$$

where γ^* is given and represents the maximum gain of all transfer functions from all exogenous inputs w to all exogenous outputs z.

Notice that these uncertainties are bounded in gain but not in phase. This means that the system can be stable even when, for $\omega = \omega_0$, $|S(j\omega_0)| > |S_{\text{nom}}(j\omega_0)| + |\Delta_{\text{Sadd}}(j\omega_0)|$ if the phase of $S(j\omega_0)$ does not correspond with the critical line for the frequency ω_0. This idea is depicted in Figure 3.4.

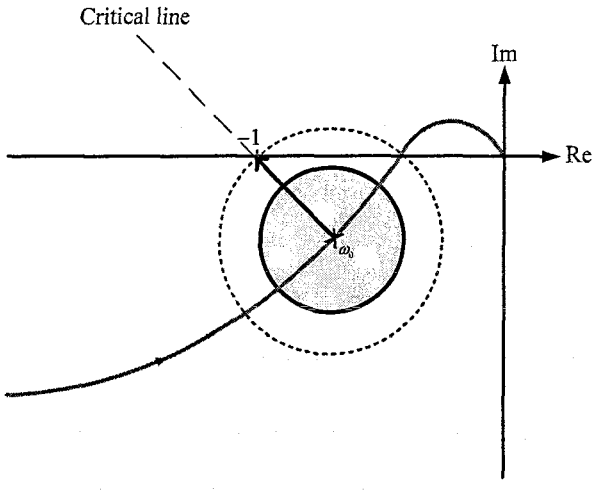

Figure 3.9: Additive uncertainty $\Delta_{\text{Sadd}}(j\omega)$ at frequency $\omega = \omega_0$ (colored area).

3.5 Linear Parameter Varying (LPV) Design

A second design based on the transparency criterion is the linear parameter varying (LPV) design. A linear parameter dependent plant is defined as in equation 3.12, where $A(.)$, $B(.)$, $C(.)$ and $D(.)$ are known functions of some parameter vector $p = (p_1, p_2, ..., p_n)$.

$$\begin{aligned} \dot{x} &= A(p)x + B(p)u \\ y &= C(p)x + D(p)u \end{aligned} \tag{3.12}$$

An affine parameter dependent system is defined as:

$$\begin{aligned} A(p) &= A_0 + p_1A_1 + p_2A_2 + ... + p_nA_n; \\ B(p) &= B_0 + p_1B_1 + p_2B_2 + ... + p_nB_n; \\ C(p) &= C_0 + p_1C_1 + p_2C_2 + ... + P_nC_n; \\ D(p) &= D_0 + p_1D_1 + p_2D_2 + ... + p_nD_n; \end{aligned} \tag{3.13}$$

where each uncertainty or time-varying parameter lies within some predefined limits $p_i \in [p_{i_{min}}, p_{i_{max}}]$.

Define

$$\mathcal{P}_{\text{BOX}} = [p_{1_{\min}}, p_{1_{\max}}] \times ... \times [p_{n_{\min}}, p_{n_{\max}}]$$

and the corner points of $\mathcal{P}_{\text{BOX}}$ as

$$\mathcal{P}_{\text{BOX}}^{\text{cp}} = \{p_{1_{\min}}, p_{1_{\max}}, ..., p_{n_{\min}}, p_{n_{\max}}\}.$$

Then, $\mathcal{P}_{\text{BOX}}$ is the convex hull of $\mathcal{P}_{\text{BOX}}^{\text{cp}}$ and it is important to observe that $\mathcal{P}_{\text{BOX}}^{\text{cp}}$ in a finite set.

The *stability* is checked using Lyapunov. That is, giving a parameter dependent closed loop system defined as

$$\begin{aligned} \dot{x} &= A_{cl}(p)x + B_{cl}(p)w \\ z &= C_{cl}(p)x + D_{cl}(p)w, \end{aligned} \tag{3.14}$$

for $p \in \mathcal{P}_{\text{BOX}}$, the closed loop system is stable if and only if

$$\exists \quad P > 0 : \quad A_{cl}(p)^T P + P A_{cl}(p) < 0 \ \forall p \in \mathcal{P}_{\text{BOX}} \tag{3.15}$$

In that case $V(x) := x^T P x$ is a Lyapunov Function for the uncertain system (3.15). Unfortunately, (3.15) requires an infinite number of verifications.

However, if A_{cl} is affine (3.13) in p, with $p = [p_1, p_2, ..., p_n]$, then it suffices to verify,

$$\exists \quad P > 0 : \quad A_{cl}(p)^T P + P A_{cl}(p) < 0 \ \forall p \in \mathcal{P}_{\text{BOX}}^{\text{cp}} \tag{3.16}$$

which it is a finite test.

The parameter vector $p := \text{col}(k_T, b_T)$ is assumed to be an uncertain element in a polytopic subset $\mathcal{P}$ of $\mathbb{R}^2_+$. We will take this to be a box in that

$$p = \begin{pmatrix} k_T \\ b_T \end{pmatrix} \in \mathcal{P} := [k_T^-, k_T^+] \times [b_T^-, b_T^+] \tag{3.17}$$

where $k_T^- < k_T^+$ and $b_T^- < b_T^+$ are defined in section 3.1.1. The parameter box $\mathcal{P}$ is depicted in Figure 3.10. It is easy to see that (3.2), (3.3), (3.17) admits a representation as an affine parameter dependent system (3.13). In this way, the teleoperation system is a *parameter varying* system. Consider the transparency criterion adapted to the parameter varying system

$$\gamma^*_{\text{LPV}}(\mathcal{P}) := \sup_{p \in \mathcal{P}} \quad \inf_{\text{C}} \sup_{\|\text{w}\|_2 < \infty} \frac{\|\text{z}\|_2}{\|\text{w}\|_2} \tag{3.18}$$

where w and z are the exogenous input and to-be-controlled output, respectively, and the infimum is taken over all LTI controllers C that stabilize the system for all $p \in \mathcal{P}$. Obviously, $\mathcal{P}' \subseteq \mathcal{P}''$ implies that $\gamma^*_{\text{LPV}}(\mathcal{P}') \leq \gamma^*_{\text{LPV}}(\mathcal{P}'')$. It is important to observe that this formulation implies that the resulting controller may depend on the parameter p. This problem can be solved explicitly using optimization techniques based on linear matrix inequalities (LMI's) [8] provided that the parameter p enters a state space representation of the to-be-controlled system in an *affine* way. In that case, the parameter p may, in principle, be time varying as long as it assumes values in the polytope $\mathcal{P}$. As observed, (3.2), (3.3), (3.17) satisfies this requirement.

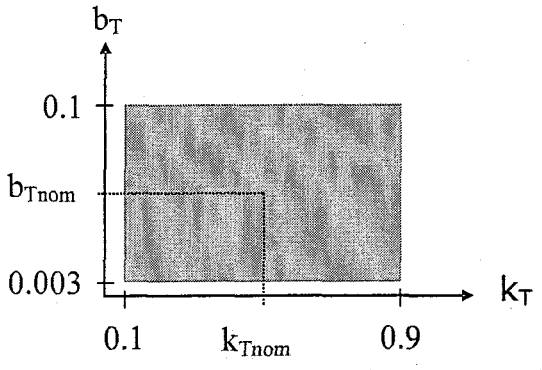

Figure 3.10: Predescribed parameter box $\mathcal{P}$

3.6 Passive Design using H_∞ Formulation

A third design is based on the passivity criterion defined in 2.2.3. Its definition was presented in equation 2.13. Setting $F = \text{col}(F_{\text{op}}, F_{\text{env}})$ and $v = \text{col}(v_{\text{op}}, v_{\text{env}})$ then equation 2.13 can rewrite as,

$$\int_{-\infty}^{t1} F^T \cdot v \, dt = 0. \tag{3.19}$$

However, the above criterion is non-linear and thus, it can not be directly used as an H_∞-optimization problem. Using a suitable change of variables, the non-linear problem can become linear, and hence, suitable for H_∞. If we introduce a change of variables:

$$\mathrm{w}_1 = \frac{F_{\text{op}} + v_{\text{op}}}{2}, \qquad \mathrm{w}_2 = \frac{-F_{\text{env}} + v_{\text{env}}}{2} \tag{3.20a}$$

$$\mathrm{z}_1 = \frac{F_{\text{op}} - v_{\text{op}}}{2}, \qquad \mathrm{z}_2 = \frac{-F_{\text{env}} - v_{\text{env}}}{2} \tag{3.20b}$$

and set $\mathrm{w} = \text{col}(\mathrm{w}_1, \mathrm{w}_2)$ and $\mathrm{z} = \text{col}(\mathrm{z}_1, \mathrm{z}_2)$ then, the passivity criterion (2.13) is equivalent to saying that,

$$\begin{aligned} &\|\mathrm{w}\|_{L2}^2 - \|\mathrm{z}\|_{L2}^2 = \\ &= \int_{-\infty}^{t_1} \left(\mathrm{w}(t)^T \mathrm{w}(t) - \mathrm{z}(t)^T \mathrm{z}(t)\right) dt = \\ &= \int_{-\infty}^{t_1} \left(F_{\text{op}}(t) v_{\text{op}}(t) - F_{\text{env}}(t) v_{\text{env}}(t)\right) dt = \\ &= \int_{-\infty}^{t_1} \left(F(t)^T \cdot v(t)\right) dt = 0 \end{aligned} \tag{3.21}$$

for all time t and all possible (w, z) that satisfy the system equations. This means that the system will be passive if and only if the newly defined port variables w and z satisfy $\|\mathrm{w}\|_2 = \|\mathrm{z}\|_2$ for all possible square integrable trajectories $F(t)^T \cdot v(t)$. The mathematical deduction can be found in the appendix A. In the newly defined variables, w is taken as input

and z as output so that the teleoperation system defines a hybrid representation $\mathrm{z} = T_{\mathrm{cl}}\mathrm{w}$ in the frequency domain. Using Parseval, the system is then passive if and only if the singular values of the closed loop defined by

$$\sigma(T_{\mathrm{cl}}(j\omega)) = 1 \tag{3.22}$$

for all frequencies $\omega \in \mathbb{R}$. To achieve this, we synthesized an H_∞ optimal controller C_{passive} for the augmented plant

$$H_{\mathrm{aug}} : \begin{pmatrix} \mathrm{w} \\ u \end{pmatrix} \mapsto \begin{pmatrix} \mathrm{z}' \\ y \end{pmatrix} \tag{3.23}$$

where the control $u = \mathrm{col}(F_M, F_S)$ and the measurement $y = e = x_M - x_S$ are as in the previous subsections and $\mathrm{z}' = \mathrm{col}(z, \tilde{e}, F_M, F_S)$ with $\tilde{e} = W_e e$ the weighted tracking error. The input-output relations in H_{aug} are defined by (3.1). Unlike the previous designs, the environment defined in (3.2) is now *not* part of the plant model.

Chapter 4

Control Design and Results

In this chapter we synthesize and compare three different controllers using the PERR control scheme. The first design is an H_∞ optimal controller that is designed for nominal values of k_T and b_T in (3.2) and that is required to be robustly stable against perturbations of the environment in the range of the parameter box (3.17). The second design is a linear parameter varying design in which the controller explicitly depends on the parameters (k_T, b_T) that may or may not depend on time. Finally, we synthesize a controller based on the passivity criterion (2.13).

4.1 An H_∞ optimal design

The H_∞ control design is based on an extension of the PERR configuration as was shown in Figure 3.7. To synthesize the controller, the configuration of Figure 3.7 is converted to the configuration of Figure 4.1 which coincides with the general control configuration of an H_∞ robust control design of Figure 3.6. The bode plot of the plant, T, denoted in Figure 4.1 as the mapping from $\{F_{\text{op}}, F_M, F_S\}$ to $\{e = x_M - x_S\}$, is depicted in Figure 4.2. The augmented plant involves an LTI partitioned plant

$$H_{\text{aug}} : \begin{pmatrix} \text{w} \\ u \end{pmatrix} \mapsto \begin{pmatrix} \text{z} \\ y \end{pmatrix}$$

where the measurement $y = e = x_M - x_S$ and the control $u = \text{col}(F_M, F_S)$ are input and output of the controller C, respectively.

As shown in Figure 4.1, the augmented plant H_{aug} has the exogenous input $\text{w} = \text{col}(\tilde{d}, \tilde{F}_{\text{op}}, \tilde{n}_e)$ and the exogenous output $\text{z} = \text{col}(\tilde{\text{e}}, \tilde{F}_M, \tilde{F}_S)$. Disturbances are represented by $d = V_S \tilde{d}$ which expresses the position disturbances around the slave plant due to the uncertain environment.

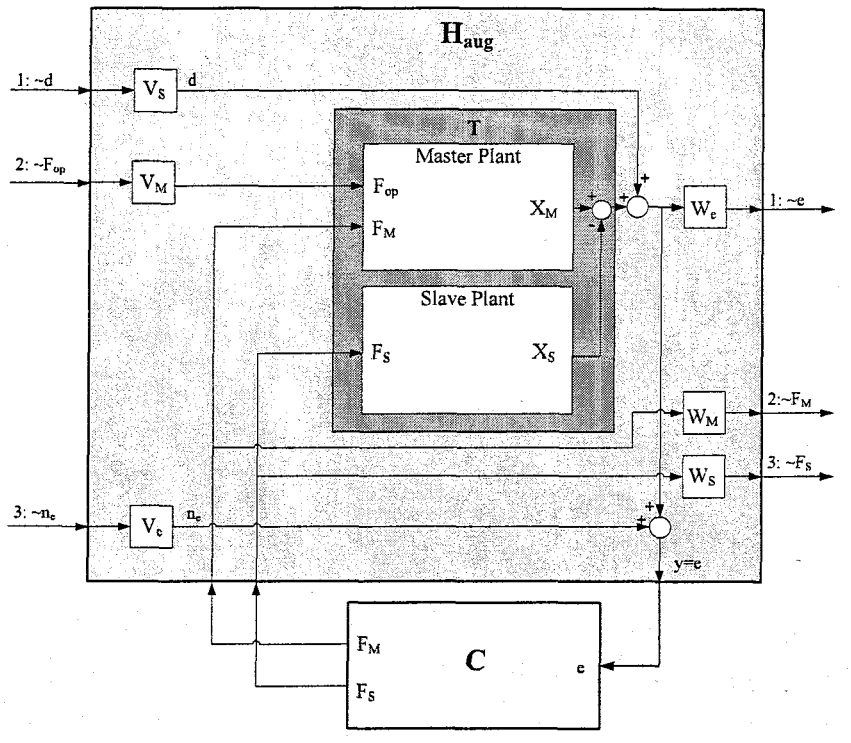

Figure 4.1: Augmented plant based on Transparency Criterion

The uncertainty is modeled as a feedback transformation $\tilde{d} = \Delta \tilde{F}_S$ where Δ is an arbitrary stable transfer function satisfying $\|\Delta\|_{H_\infty} \leq 1/\gamma^*$ (explained in section 3.4). $F_{\text{op}} = V_M \tilde{F}_{\text{op}}$ is the frequency weighted force applied to the master device by the human operator where $\tilde{F}_{\text{op}}$ is modeled as an external disturbance. Measurement noise from the position error encoders has been modeled as $n_e = V_e \tilde{n}_e$ where $\tilde{n}_e$ is an exogenous input. The desired behaviour of the exogenous outputs z is modeled by the weighting functions W_e, W_M, and W_S.

All the above mentioned filters are designed on the basis of human specifications, limitations of the real setup, and the desired response of the controlled system. The singular value plots of filters are depicted in Figure 4.4.

Appropriate choices for the input shaping filters are as follows:

- V_M (Figure 4.4.(a)) represents the torque applied by the human operator. Because the motions of the human operator are limited to 10Hz and the maximal force is assumed to be less than $10N$ or, analogously, less than 0.6 Nm (see section 3.1.2), a low-pass filter is used as shaping filter. Its transfer function is given by

$$V_M = \frac{6.2}{s + 103}.$$

which corresponds to a dc gain of approximately 0.06.

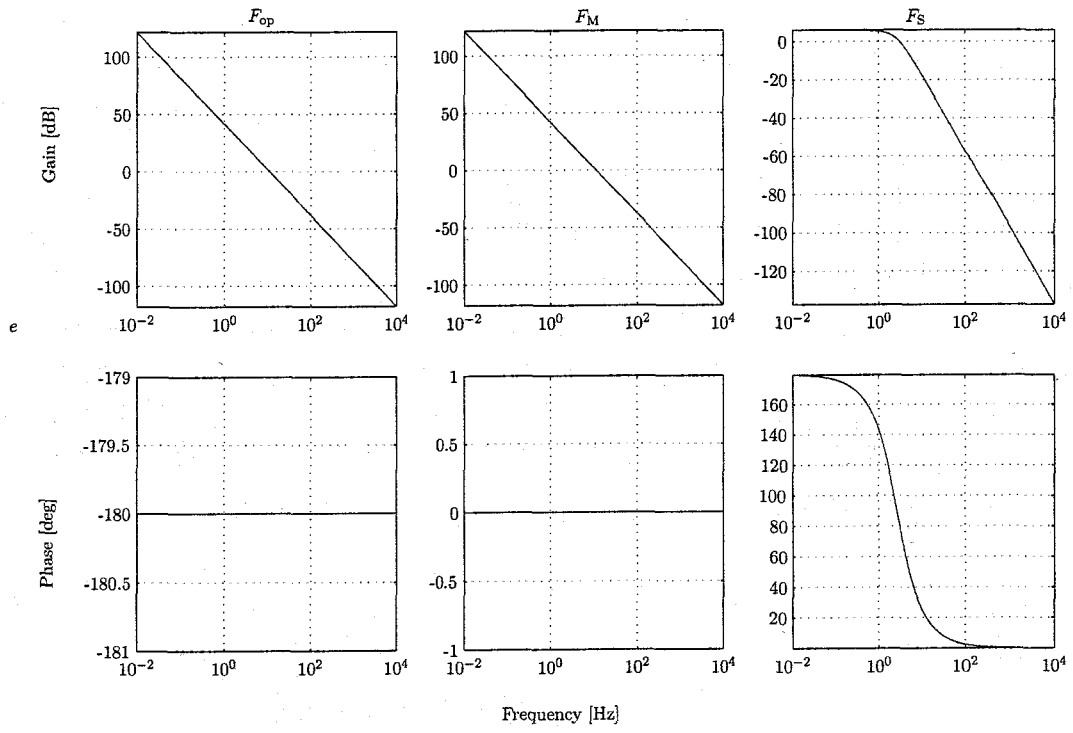

Figure 4.2: Plant using PERR structure mapping $\{F_{op}, F_M, F_S\}$ to $\{e = x_M - x_S\}$

- V_e (Figure 4.4.(b)) represents measurement noise. The discrete nature of the encoder will usually cause high-frequent noise, and therefore, V_e is a high-pass filter. We take

$$V_e = \frac{4 \cdot 10^{-3} s + 3.75}{0.75 + 1045}$$

which corresponds to a dc gain of $3.6 \cdot 10^{-3}$. This is because we assume a maximal error for the encoder of $\frac{2*pi}{2000}$ $rad.$

- V_S reflects, together with W_S, the additive uncertainty of the slave coupled to the environment according to

$$\begin{aligned} S &= S_{\text{nom}} + \Delta_{\text{Sadd}} \\ \Delta_{\text{Sadd}} &= W_S \Delta V_S \end{aligned} \tag{4.1}$$

where S_{nom} is the nominal slave transfer function of the form

$$S_{\text{nom}}(s) = \frac{1}{(m_S + m_T)s^2 + b_{T\text{nom}} s + k_{T\text{nom}}} \tag{4.2}$$

Δ_{Sadd} represents the additive uncertainty around S_{nom}, and Δ is any stable transfer function satisfying $\|\Delta\|_{H_\infty} \leq \frac{1}{\gamma^*}$ with γ^* being the maximum gain from all exogenous inputs to all exogenous outputs (see section 3.2).

In order to design V_S, we first need to plot how the uncertainties Δ_{Sadd} look like for different values of k_T and b_T within the parameter box defined by the extremal points k_T^-, k_T^+, b_T^- and b_T^+. The corresponding parameter box is showen in table 3.1 and represented in Figure 4.3(a). Apparently, the worst scenarios that the nominal plant can confront are presented in the corners of the box. Thus, the nominal value of the parameters (point A in 4.3(a)), together with the corners of the box (points B, C, D, E) and an arbitrary point F are going to be evaluated. Figure 4.3(b) displays the different plants for the points A, B, C, D, E and F of the parameter box. These plants are referred to S in (4.1) and their transfer function is described in (4.2) replacing $k_{T\text{nom}}$ and $b_{T\text{nom}}$ with the values of k_T and b_T defined by the points A, B, C, D, E and F. The nominal plant S_{nom} is represented by the dashed line (A). Note that the worst points are B and C. This result is expected since B and C are the least damped situations.

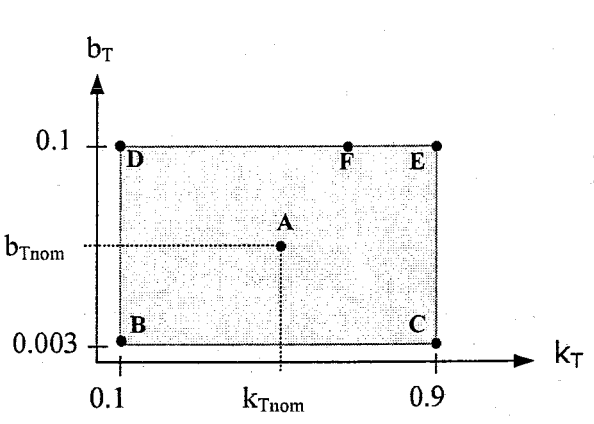

(a) Parameter Uncertainty

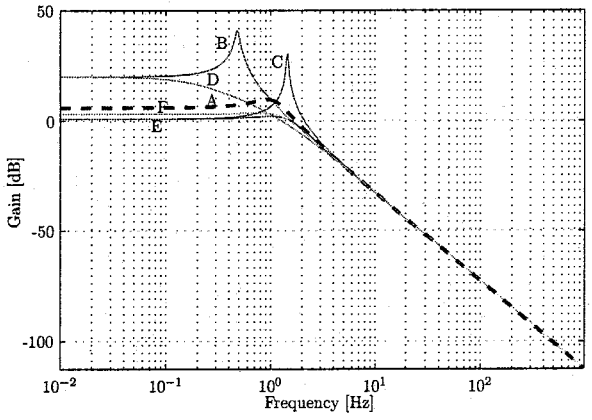

(b) Different plants S for different values of k_T and b_T. Nominal plant is represented by A S_{nom}.

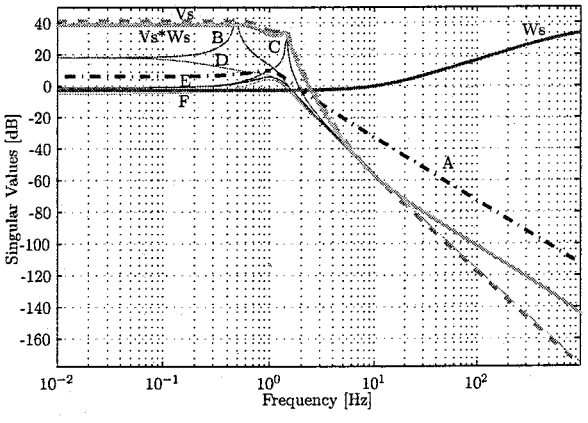

(c) Additive uncertainty around the nominal plant S_{nom}. Fifth order filter V_S (dashed line).

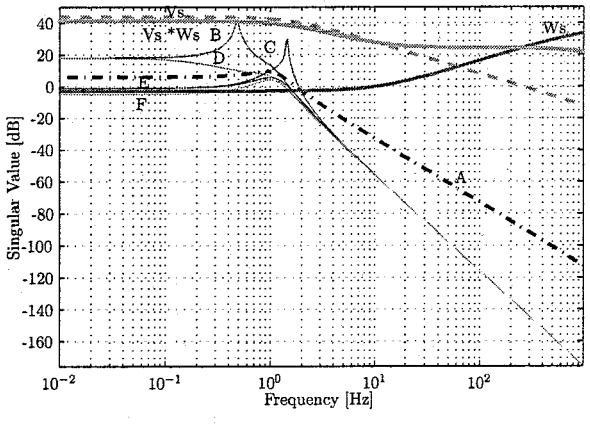

(d) Additive uncertainty around the nominal plant S_{nom}. First order filter V_S (dashed line).

Figure 4.3: Uncertainty around the slave plant

The uncertainty Δ_{Sadd} for the different points is represented in Figure 4.3(c) and (d). Note that the nominal plant S_{nom} is also depicted although it does not represent uncertainty. The purpose is to give the reader an idea about the size of the uncertainty with respect to the nominal plant.

The first idea is to design a filter as close as possible to the group of uncertainties while covering all of them along the frequencies of interest. First, a fifth order filter V_S is designed and depicted in Figure 4.3(c). It covers the uncertainty properly in the desired frequency band, and at high frequencies a good shape close to the uncertainties is achieved. However a high order filter implies a high order controller C which results in difficulties concerning the implementation. Furthermore, there is no need to model the filter as tight as possible to the uncertainties if it covers all of them at all frequencies of interest. Therefore, a first order filter V_S is considered and depicted in Figure 4.3(d). Assuming $\|\Delta\|_{H_\infty} = 1$ ($\gamma^* = 1$) with the magnitude of its transfer function being $1/\gamma^*$ in its frequency range (flat spectrum), the frequency band uncertainty Δ_{Sadd} is equal to $V_S W_S$ and depicted in Figure 4.3(c)(d) for a given W_S. Note that if the resulting γ^* is larger than 1, the frequency band uncertainty Δ_{Sadd} decreases and thus, it is not guaranteed that the system is robust against all possible uncertainties predefined in the parameter box.

Observe that V_S has to have a high gain in order to comprise all the possible uncertainties. Concretely, the gain of the disturbances are in the order of +60%-25% with respect to the nominal gain of the slave plant. Thus, the emerging question is whether it is correct to consider them as reasonable. We believe that it is not possible to design a robust controller for such a great variety of uncertainties. A solution could be to divide the current box in small boxes and design a nominal controller for each of these new boxes together with a switching mechanism. However, this solution is not implemented in this project. Alternatively, the uncertainty could be modelled less conservative by using the parametric form as explained at the end of this section. A small value of V_S (Figure 4.4.(c)) is considered , namely

$$V_S = \frac{0.0001}{s + 10}$$

The appropriate choices of the output weighting filters are as follows:

- W_e (Figure 4.4.(d)) weights the position error e. A low-pass filter is used to penalize tracking errors that occur in the frequency range that is relevant for kinesthetic feedback. In order to achieve the performance requirement of a maximum error of 0.01rad for a maximal torque of $0.6Nm$ (see section 3.1.2), a dc gain of at least 60dB is needed, and hence

$$W_e = \frac{1.95 \cdot 10^5}{s + 199}$$

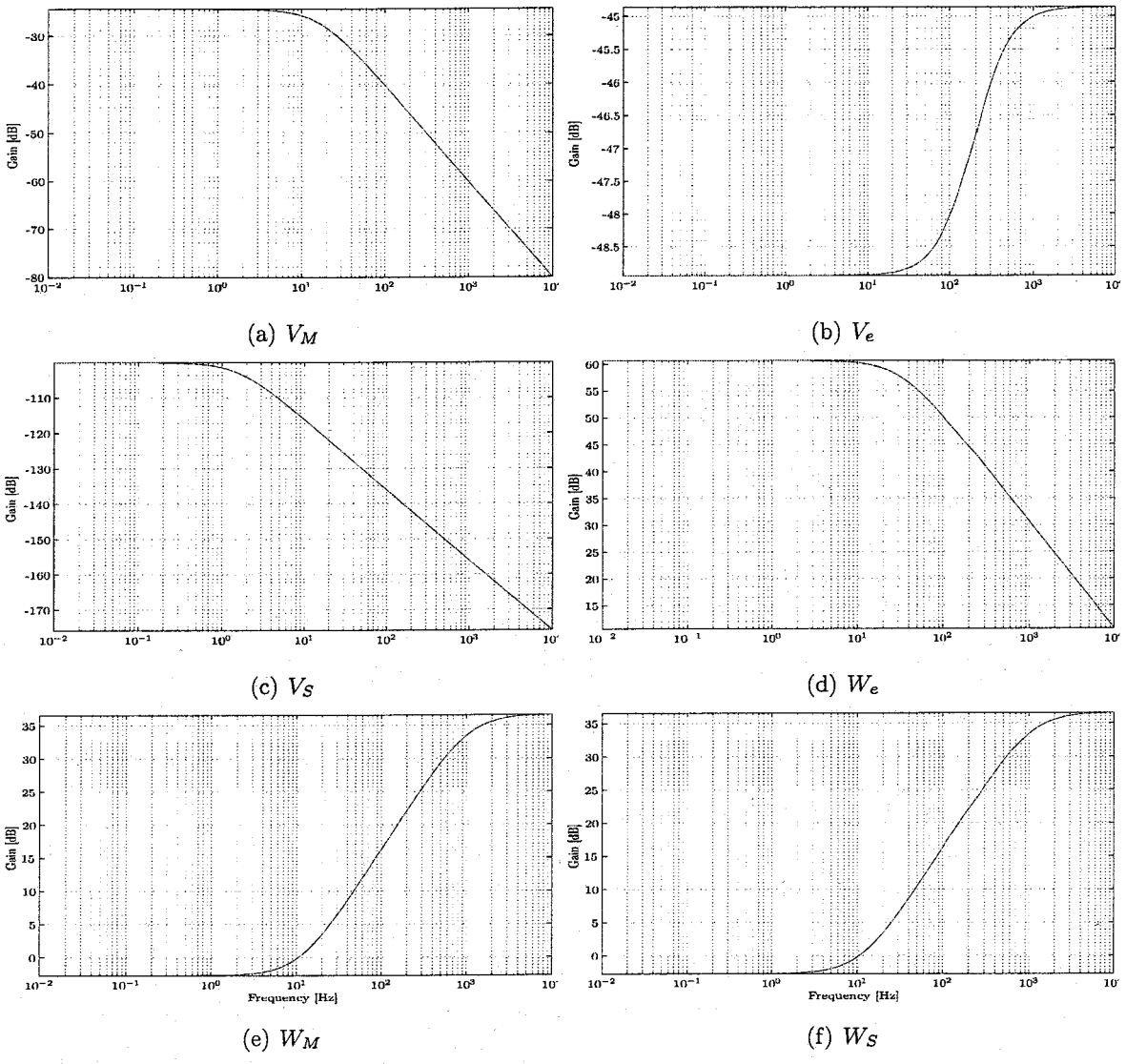

(a) V_M (b) V_e

(c) V_S (d) W_e

(e) W_M (f) W_S

Figure 4.4: Shaping filters (V) and Weighting filters (W)

- W_M and W_S (Figure 4.4.(e and f)) weight the control effort of the master and the slave. The controller only needs to provide (low frequency) haptic feedback. Therefore, a high-pass filter is used to penalize high frequency components,

$$W_M = W_S = \frac{7s + 476}{0.1s + 650}$$

Notice that V_e, V_S, W_M and W_S are scaled with respect their corresponding maximal values, whereas the filters V_M and W_e are scaled with respect to the input F_{op}. We could have scaled all the filters in the same way, however we did not do it in this project.

The controller C_{nom} is synthesized so as to achieve the performance

$$\gamma := \inf_{C} \sup_{\|w\|_2<\infty} \frac{\|z\|_2}{\|w\|_2}$$

With the mentioned choices of the weighting filters, the minimal achievable closed-loop H_∞ norm is $\gamma^* = 4.18$. Decreasing the gain of the filter W_e, a smaller γ can be achieved, and better stability robustness can be obtained. Hence, it can be seen that there exists a trade-off between robust stability and performance.

The bode plot of the nominal controller $C_{nom} = (C_{M_{nom}}, C_{S_{nom}})$ that satisfies the given γ^* is depicted in Figure 4.5. Observe that the master controller has more gain than the slave controller despite the fact that they have similar shapes. This is because the master needs to overcome the disturbance F_{op}.

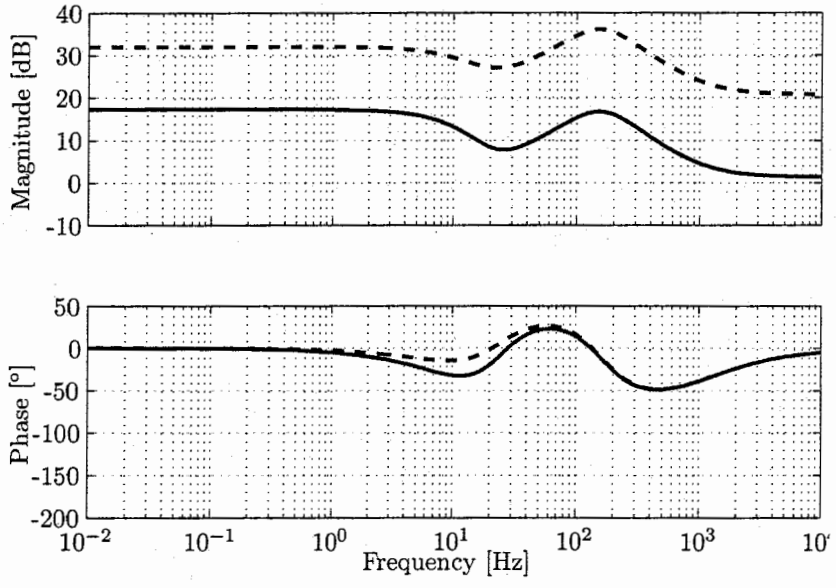

Figure 4.5: Master (dashed line) and slave (solid line) controller

The transparency criterion in the second equation of (3.9) involves the transfer function from F_{op} to e. The bode plot of the closed-loop transfer function mapping the operator force F_{op} to the position error $e = x_M - x_S$ is depicted in Figure 4.6.

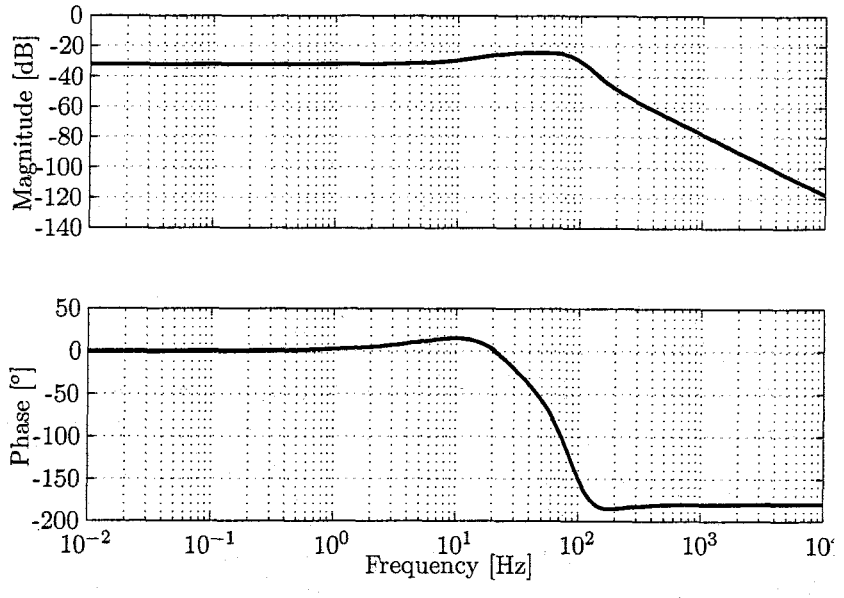

Figure 4.6: Bode plot from F_{op} to position error e

In order to understand Figure 4.6 we refer to the classical control scheme shown in Figure 3.5. Indeed, the PERR structure of Figure 3.7 can be written in the form of classical control (without considering the filters) as is shown in Figure 4.7. The transfer function that we refer to is the process sensitivity, which maps the disturbances at the input of the plant, F_{op}, to the output of the closed loop system, $y(= e)$. This explains the shape of the mentioned bode diagram.

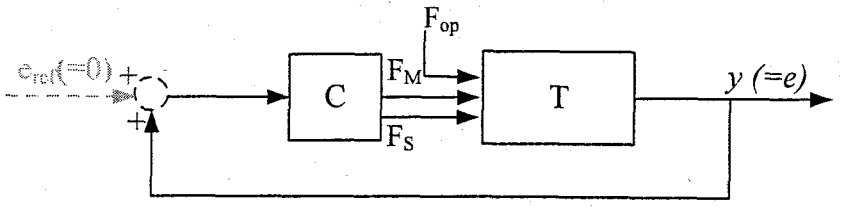

Figure 4.7: Equivalent PERR in classical control scheme

where the input e_{ref} is assumed to be zero all the time. The open loop from y to $e' = e_{ref} - y$ is given by the transfer function $T \cdot C_{nom}$, which expression is straightforward from Figure 4.7. The bode plot of the open loop system, together with the Nyquist plot, is represented in Figure 4.8.

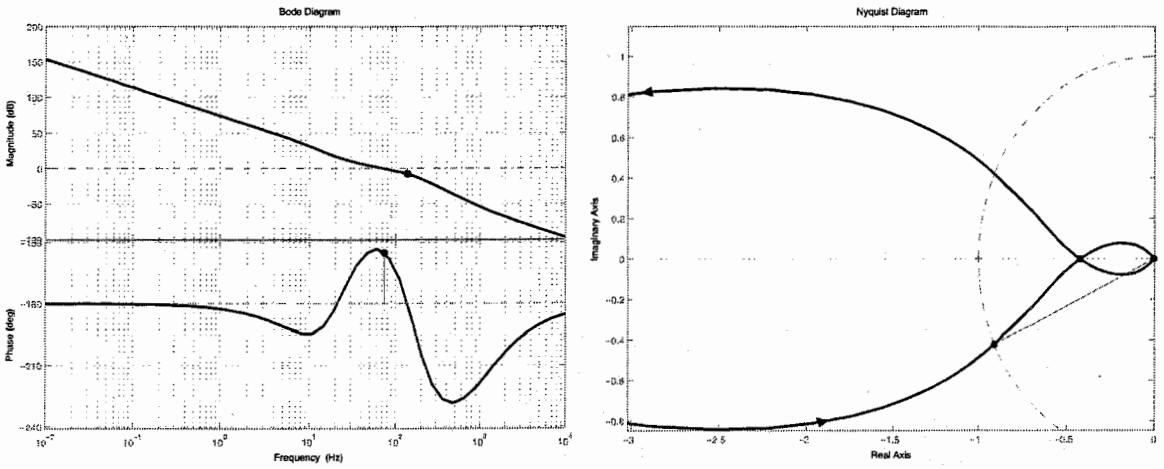

(a) (b)

Figure 4.8: (a) Bode plot and (b) Nyquist plot for the open loop.

Observe that the open loop system has positive gain and phase margin, and hence the nominal closed loop system is stable with a bandwidth of, approximately, 60Hz, which is higher than the specification for kinesthetic sensing.

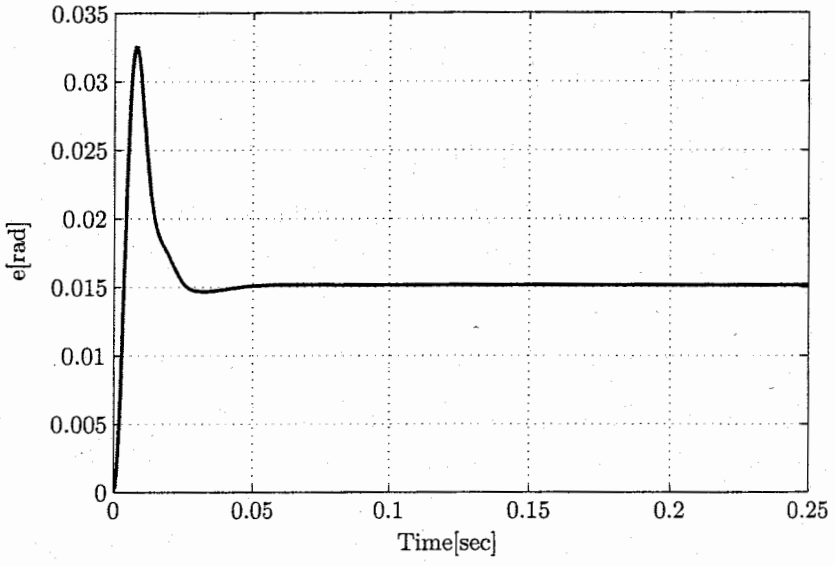

Figure 4.9: Closed-loop step response $F_{\text{op}} \mapsto e$ with controller C_{nom}

Figure 4.10.(a) shows the step response of the closed loop transfer function from F_{op} to e with a steady-state error of 0.015rad by a maximum torque of 0.6Nm. The tracking specification is not fulfilled but it gets really close to its desired value. Consider now a parabolic force

F_{op} which could be seen as a realistic input when palpating a tissue. The closed loop error response for this parabolic input is depicted in Figure 4.10.

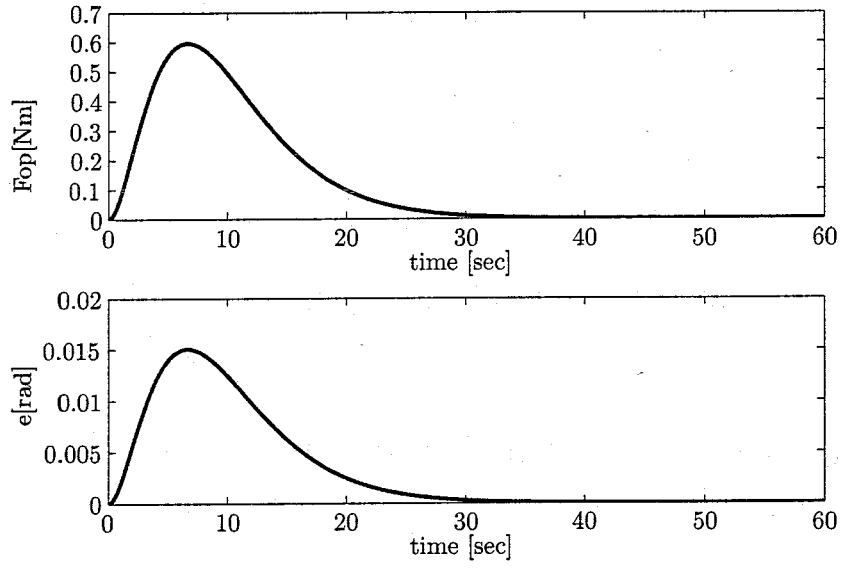

Figure 4.10: Closed loop response with a parabolic input F_{op}

Again, a maximal error of 0.015rad is achieved for a maximum torque of 0.6Nm. Thus, the specification is just not fulfilled.

The system will be robustly stable for all uncertainties (4.1) with $\|\Delta\|_{H_\infty} \leq 1/\gamma^*$, in case the uncertainties are conservatively modelled (as only gain bounded but phase can be anything). Hence, robust stability of the system is not guaranteed for the target set of uncertainties in (4.1).

Describing the plant as (affine) parameter-dependent on k_T and b_T, and k_T and b_T changing in the prescribed parameter box defined in 3.1.2, we want to analyze the robustness against parameter uncertainty of the closed loop system with the parameter-dependent plant, T, and the nominal controller C_{nom}. Using the command *quadstab* in Matlab, we can assess the quadratic (robust) stability as expressed in (3.16). The closed loop system admits a quadratic Lyapunov function if the box $\mathcal{P}$ is shrinked to 68.85% of its area around the nominal value (point A). Therefore, the controller C_{nom} achieves (robust) quadratic stability for the parameter box

$$\mathcal{P}' = p_{\text{nom}} + \frac{68.85}{100}(\mathcal{P} - p_{\text{nom}}), \text{ with } p_{\text{nom}} = \text{col}(k_T^{\text{nom}}, b_T^{\text{nom}})$$

that lies inside $\mathcal{P}$. $\mathcal{P}'$ is represented in Figure 4.11 by a shaded box.

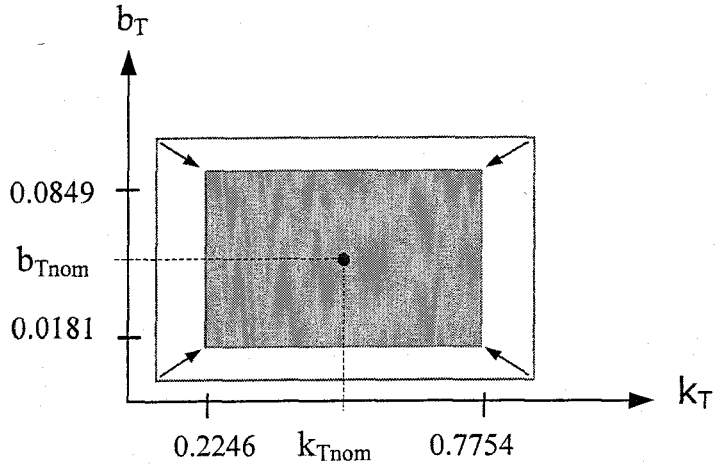

Figure 4.11: Shrinked Parameter box $\mathcal{P}$

The step response of the master-slave system using C_{nom} for *time-varying* tissue parameters $p(t)$ that vary in a spiral pattern in the prescribed parameter box $\mathcal{P}'$ is shown in Figure 4.12.

To prevent conservatism with respect to uncertainties, we could use H_∞-μ design to synthesize our system. However, if we assume that the parameters of the environment can be measured, then linear parameter varying synthesis can be used to obtain a less conservative design. The design and the resulting controller is explained in the next section.

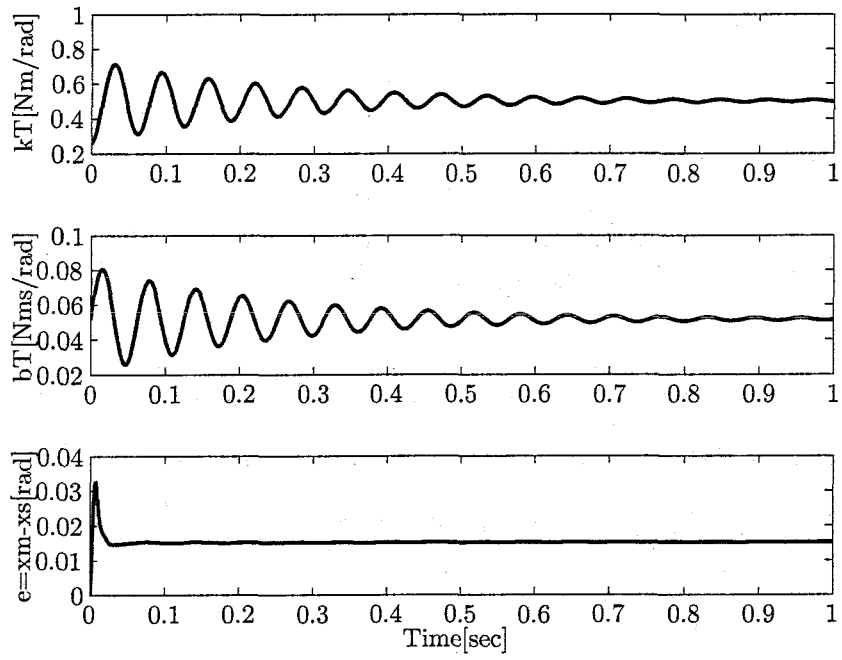

Figure 4.12: Step response of the closed loop with C_{nom} system when k_T and b_T a vary in time along a spiral

4.2 A linear parameter varying (LPV) design

We consider the same system as in the previous section, but with the uncertainty (4.1) replaced by the more explicit parametric uncertainty described by (3.17) where the extremal points are specified in Table 3.1. The augmented plant $P_{aug}(p)$ then becomes dependent of the parameter $p = col(k_T, b_T)$ and this dependence is affine in the matrices of a suitable state-space representation of the augmented system.

$$\begin{aligned} A(k_T, b_T) &= A_0 + k_T A_1 + b_T A_2 \\ B = B_0,\ C &= C_0,\ D = D_0 \end{aligned} \tag{4.3}$$

This is necessary to synthesize a parameter dependent controller to determine

$$\gamma^*_{LPV,\mathcal{P}} := \sup_{p\in\mathcal{P}} \inf_{C} \sup_{\|w\|_2<\infty} \frac{\|z\|_2}{\|w\|_2}$$

with $C \in \mathcal{C}_{stab.}$ and w and z as defined before. The resulting controller $C_{LPV}(p)$ may explicitly depend on p and will be implemented in the PERR structure of Figure 2.5.
Note that,

$$\mathcal{P}'_{BOX} \subset \mathcal{P}_{BOX} \implies \gamma^*_{LPV,\mathcal{P}'} \leq \gamma^*_{LPV,\mathcal{P}} \tag{4.4}$$

In order to assess the robust stability of the affine parameter-dependent system we use the command *pdlstab* in Matlab. It differs from *quadstab* in that *pdlstab* uses parameter-dependent Lyapunov functions, $V(x) := x^T P(p)x$, to establish the stability of uncertain state-space models over some parameter range ($\mathcal{P}$ in our case). That is, the referred P in (3.16) is, using *pdlstab*, $p-$dependent in an affine way

$$P(p) = P_0 + k_T P_1 + b_T P_2.$$

Pdlstab is a useful tool to analyze systems with time-invariant or slowly varying parameters. Hence, the resulting robust stability test is less conservative than using the common quadratic stability test.

Considering time-invariant parameters p, the achieved performance measures are

$$\gamma^*_{\mathrm{LPV},\mathcal{P}} = 14.89, \qquad \gamma^*_{\mathrm{LPV},\mathcal{P}'} = 4.20 \tag{4.5}$$

where $\mathcal{P}$ and the shrinked box $\mathcal{P}'$ are represented in Figure 4.11. Hence, the performance is substantially better for the uncertainty box $\mathcal{P}'$ when compared with $\mathcal{P}$, and hence, the robust stability for the new prescribed parameter box $\mathcal{P}'$ is increased. Figure 4.13 shows the step response when the parameters k_T and b_T are chosen randomly within the new prescribed parameter box $\mathcal{P}'$. Note that for a range of parameters in $\mathcal{P}'$, the specified maximal error is

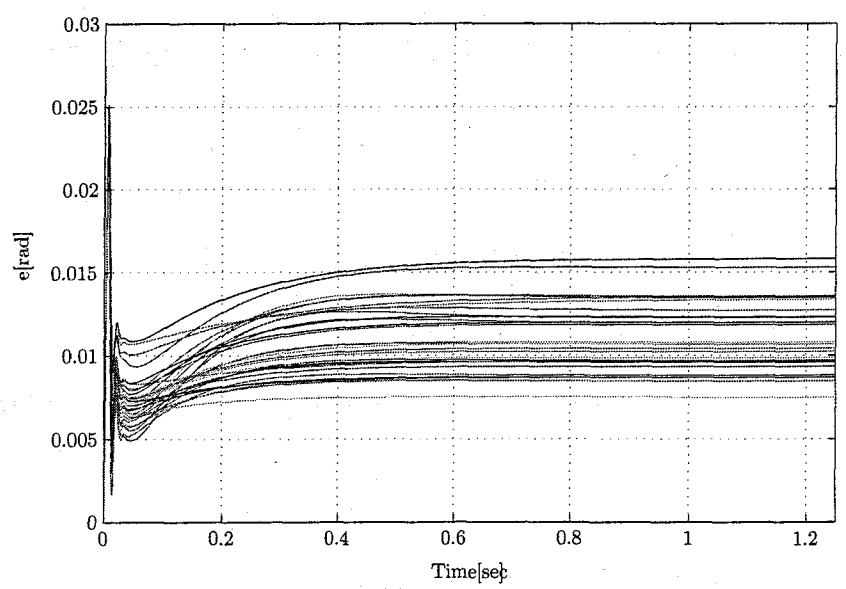

Figure 4.13: Step response of the master-slave system with $\mathrm{C_{LPV}}$ when k_T and b_T are chosen randomly

fulfilled.

Assume now a slowly time-varying parameters $p(t) = col(k_T(t), b_T(t))$ with a rate of variation dp_i/dt, $i = 1, 2$ bounded by 0.01 $p(t)$ in $\mathcal{P}'$. The closed loop system remains stable in the face of such slow variations. Figure 4.14 shows the step response when the parameters k_T and b_T vary in time along a spiral within $\mathcal{P}'$ with a steady-state value of 0.0107rad which satisfy the specification.

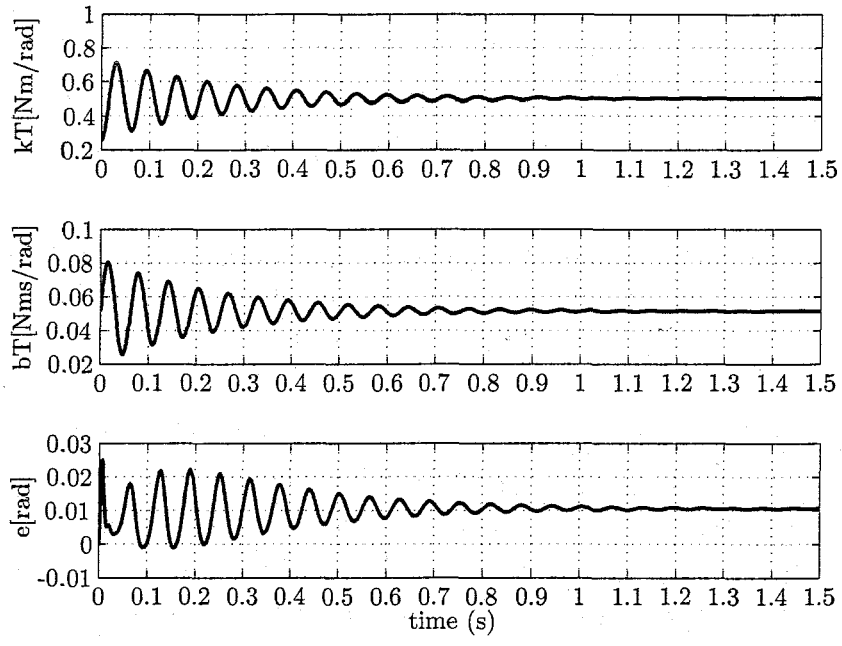

Figure 4.14: Step response of the master-slave system with C_{LPV} when k_T and b_T vary along a spiral

4.3 A passive design

A third controller design is based on the passivity condition introduced in (3.19). To achieve passivity, we synthesized an H_∞ optimal controller $C_{passive}$ for the augmented plant

$$H'_{aug} : \begin{pmatrix} w \\ u \end{pmatrix} \mapsto \begin{pmatrix} z' \\ y \end{pmatrix}$$

where the control $u = \text{col}(F_M, F_S)$ and the measurement $y = e = x_M - x_S$ are as in the previous sections. The exogenous inputs are defined by the vector w and the exogenous outputs by $z' = \text{col}(z, \tilde{e}, F_M, F_S)$ with w and z representing the change of variables presented in (3.20) and $\tilde{e} = W_e e$ being the weighted tracking error. Unlike the previous designs, the environment defined in (3.2) is now not part of the plant model. The new augmented plant is depicted in Figure 4.15, where T' defines the mapping

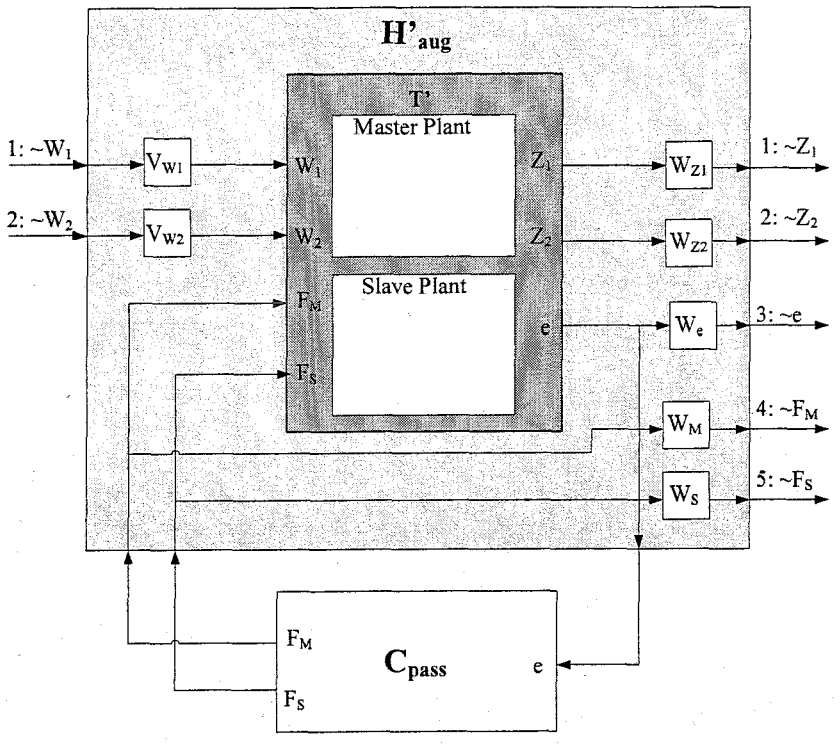

Figure 4.15: Augmented plant based on passivity criterion

$$\mathrm{T}' : \{\mathrm{w}_1, \mathrm{w}_2, F_M, F_S\} \mapsto \{\mathrm{z}_1, \mathrm{z}_2, e\},$$

The controller $\mathrm{C}_{\mathrm{pass}}$ is synthesized so as to achieve the performance

$$\gamma_{\mathrm{pass}} := \inf_{\mathrm{C}} \sup_{\|\mathrm{w}\|_2 < \infty} \frac{\|\mathrm{z}'\|_2}{\|\mathrm{w}\|_2}$$

Again, we need to design the filters represented by V_{W1}, V_{W2}, W_{Z1}, W_{Z2}, W_e, W_M and W_S. However, the inputs w and outputs z are abstract signals representing linear combination of torques plus velocities. Thus, we do not consider to scale them and hence, filters V_{W1}, V_{W2}, W_{Z1} and W_{Z2} are going to be chosen constant with a value of 1. The other filters will be explained later on.

First, consider the exogenous inputs to be w and the exogenous outputs to be $\mathrm{z}' = \mathrm{z}$, i.e., the filters W_e, W_M and W_S are set to 0. The passivity condition (3.22) is verified by inspecting the closed loop singular values $\sigma(T_{\mathrm{cl}}(j\omega))$ with T_{cl} being the closed loop transfer function from w to z. The closed loop singular values $\sigma(T_{\mathrm{cl}}(j\omega))$ are 1.00001 and 0.766 for all frequencies $0 \leq \omega \leq 20$ Hz which shows that the system is 'approximately passive' for all trajectories in the relevant bandwitdh. The optimal value γ_{pass} in this case is 1.01.

Considering now the design of the filter W_e. Changing its value, different singular values can be obtained as it is shown in Figure 4.16.(b). Notice that, in all cases, the value of the

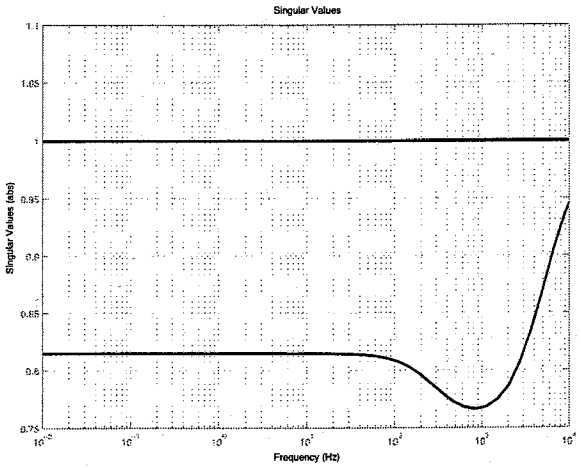

(a) Singular Values considering only the inputs w and outputs z

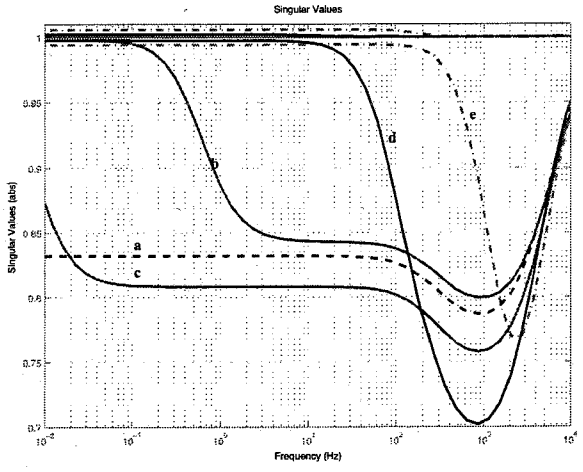

(b) Singular values considering the inputs w and the outputs z,$\tilde{e}$, changing the filter W_e:a. $W_e = 0$;b. $W_e = 1$; c. $W_e = 0.01$; d. $W_e = 100$; e. $W_e = \frac{1.95 \cdot 10^5}{s+199}$

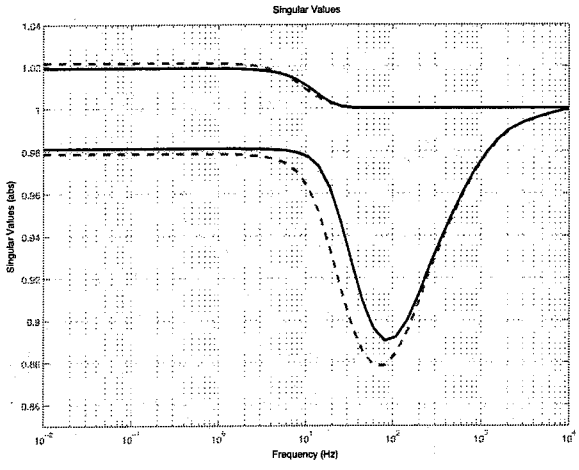

(c) Singular values considering the inputs w and the outputs z,$\tilde{e}, \tilde{F_M}, \tilde{F_S}$, with $W_M = W_S = \frac{0.7(0.1s+6.8)}{0.0010s+6.5}$ and $W_e = 100$ (dashed line) and $W_e = \frac{1.95 \cdot 10^5}{s+199}$

Figure 4.16: Singular Values of te closed loop transfer function with with C_{pass} from w to z.

maximum singular value can not be decreased with respect to the maximum singular value represented in Figure 4.16.(a). Hence, we can not achieve the passive condition defined in (3.22), where the maximum singular values of T_{cl} needs to be exactly 1. As a result, in any of the cases represented in Figure 4.16.(b) the value of γ_{pass} is decreased but it is kept to 1.01.

In Figure 4.16.(c), the filters W_M and W_S are taken into account. They improve the minimal singular value, which gets closer to 1, but does not improve the maximal singular value. Furthermore, more outputs are considered and thus more closed loop transfer functions are present which may increase the value of γ_{pass}. However, notice that the value of the γ_{pass} does not play an important role in this design. That is, γ_{pass} represents the maximal singular value of the closed loop from all exogenous inputs w to all exogenous outputs z'. Thus, if we define more outputs than only z, γ_{pass} will be the maximal singular value from w to $z'(\neq z)$ which does not give any information of passivity.

Hence, apparently the only way to reduce the singular values of T_{cl} is by reducing the filters $V_{U's}$and/or $W_{Z's}$. However we are no able to reduce their values because we do not know the meaning behind of the related signals w and z.

Consider the Bode diagrams of the $C_{\text{pass}} = (C_{\text{pass.M}}, C_{\text{pass.S}})$ depicted in Figure 4.17 obtained by choosing W_e=100. The next step is to prove that the closed loop ,T_{cl}", defined by the system T"

$$\text{T}'' : \{F_{\text{op}}, F_{\text{env}}, F_M, F_S\} \mapsto \{v_M, v_S, e\},$$

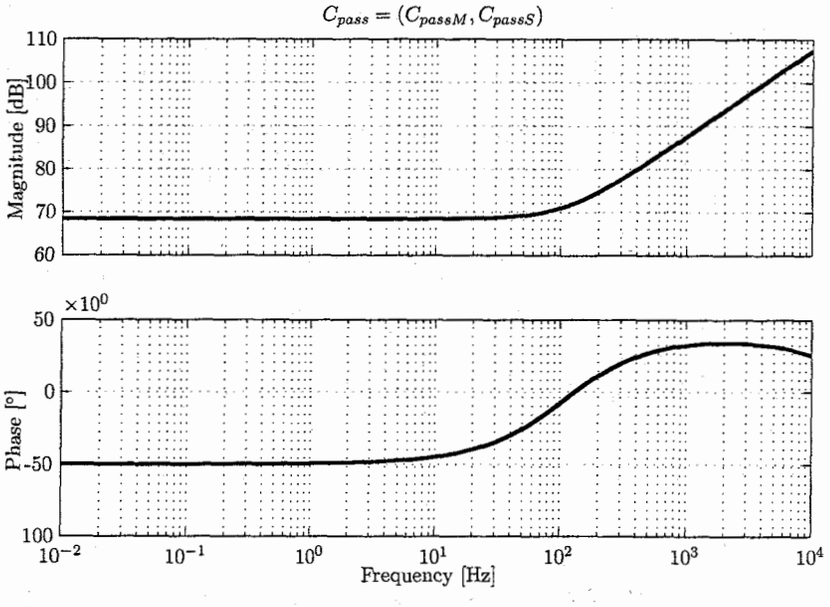

Figure 4.17: Passive controller $C_{\text{pass}}(C_{\text{pass.M}} \cong C_{\text{pass.S}})$

and the passive controller C_{pass} is also passive and stable. However, if the singular values of T_{cl} are not smaller or equal than one, then the passivity of T_{cl}" from F to v is not guaranteed.

Calculating the T_{cl}" results in a non-minimal realization of the system. Doing its minimal realization, the system is stable. The performance is evaluated in terms of energy, i.e., the energy supplied in any interval of time by the operator has to be equal to the energy supplied by the environment as it is explained in section 2.2.3. Modeling F_{op} and F_{env} as sinusoids of amplitude 0.6 and frequency 1rad/s, the relation between the power supplied by the operator, p_{op}, and the power supplied by the environment, p_{env}, is depicted in Figure 4.18.

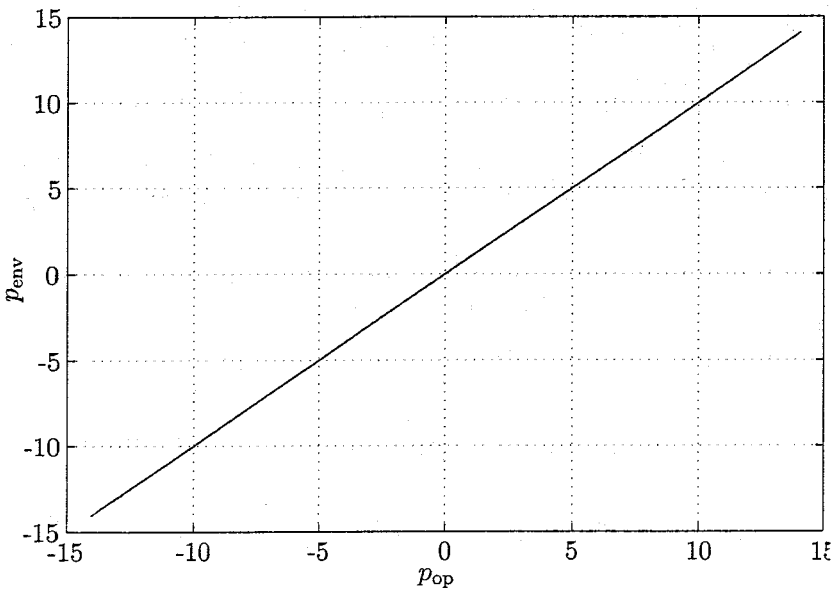

Figure 4.18: Power signals

where it can be seen that the slope between both powers is 45deg, and thus, equal. The passivity condition in terms of energy is achieved as it can be seen in Figure 4.19. Note that is not a straight line at zero due to some drift in the inputs signals.

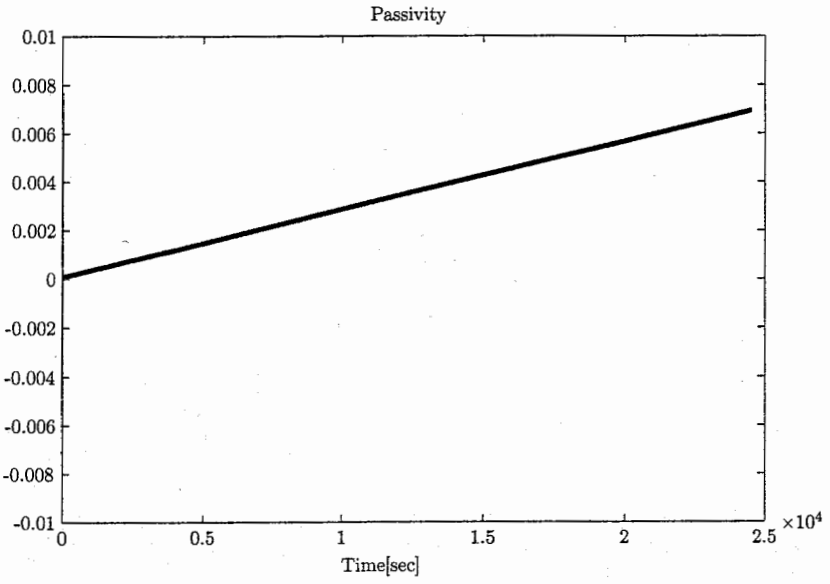

Figure 4.19: Energy supplied to the system

The closed loop transfer from $F_{\text{op}} \mapsto e$ and $F_{\text{env}} \mapsto e$ are depicted in Figure 4.20.(a) and (b) respectively.

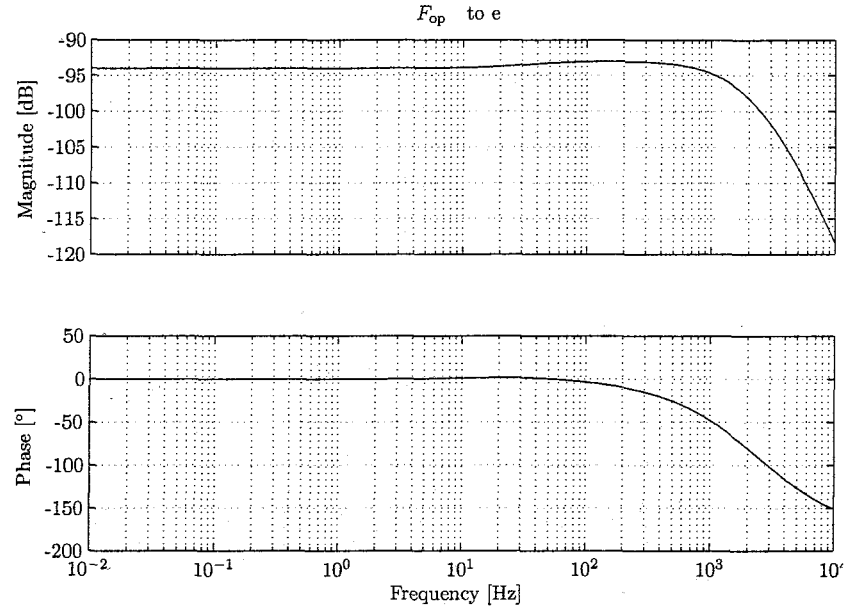

(a) Closed loop bode plot mapping from F_{op} to e

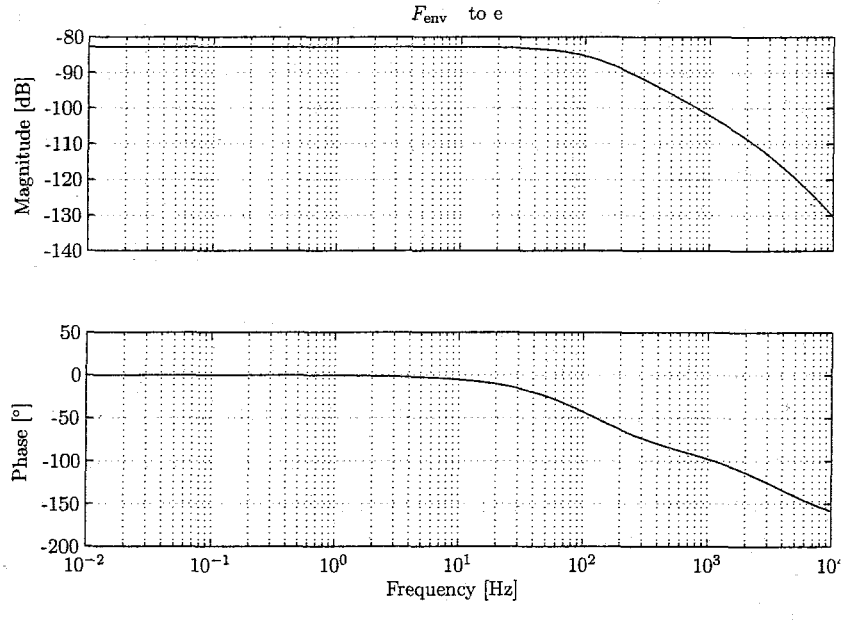

(b) Closed loop bode plot mapping from F_{env} to e

Figure 4.20: Closed loop Bode plots with C_{pass} mapping (a) $F_{op} \mapsto e$ (b) $F_{env} \mapsto e$.

It can be seen that a smaller position error compared with the other controllers can be achieved in the frequency range of interest.

Consider now to describe the plant as (affine) parameter-dependent plant with k_T and b_T changing in the predescribed parameter box defined in 3.1.2. We want to analyze the robust-

ness of the closed loop system with the parameter-dependent plant and the controller C_{pass} against parameter uncertainty. The closed loop system guarantees a quadratic Lyapunov function if the box $\mathcal{P}$ is shrinked to 0.2% of its area around the nominal value. However, the step response for random choice of parameters within $\mathcal{P}'$ is stable as it is shown in Figure 4.3.

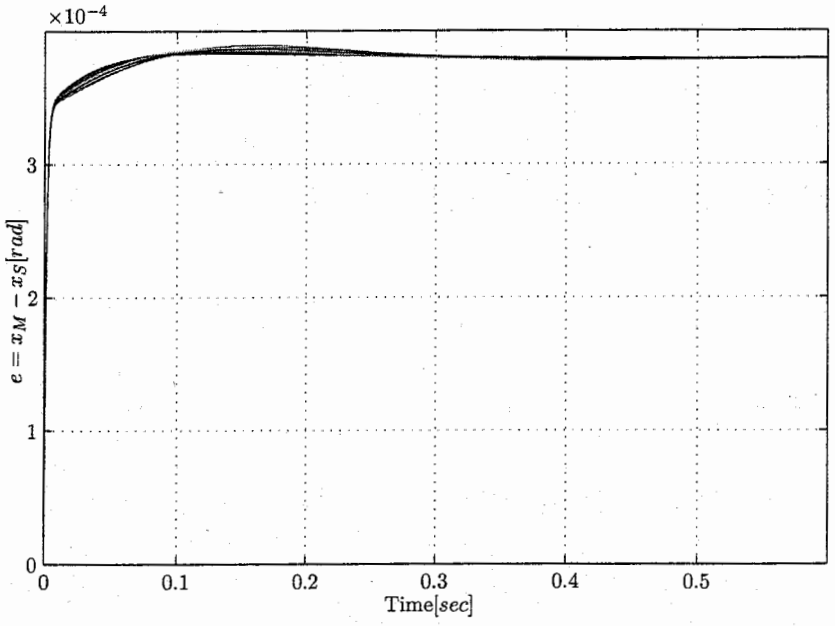

Figure 4.21: Step response for the passive design for random parameters within $\mathcal{P}'$

The steady-state error is about $3.8 \cdot 10^{-4}$rad which satisfy by far the specification. Figure 4.22 shows the step response when the parameters k_T and b_T vary in time along a spiral within $\mathcal{P}'$ with the same steady-state value as in the previous figure.

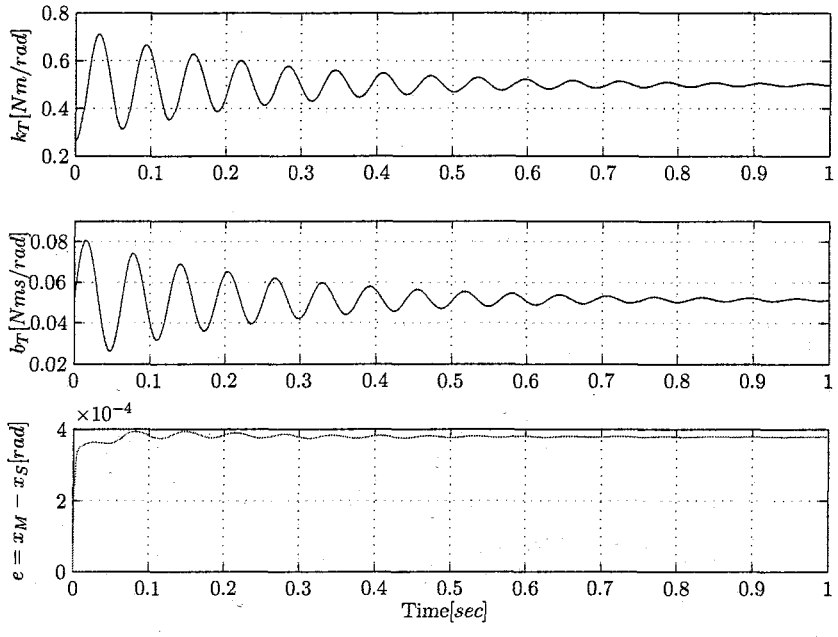

Figure 4.22: Step response for the passive design when the parameters vary in time along a spiral in $\mathcal{P}'$

4.4 Discussion

Figure 4.23 shows the step disturbance responses with time varying k_T and b_T for the three controllers C_{nom}, C_{LPV} and C_{pass}. It can be seen that the controller C_{nom} provides faster response to time varying changes of k_T and b_T than C_{LPV} and C_{pass}. However, the steady-state error response of the system controlled by C_{LPV} is better than when controlled by C_{nom}. The passive controller C_{pass} shows faster and damped error response to time varying parameter changes with respect to C_{LPV} but it is slower than the nominal controller C_{nom}. The position error provide by the passive controlled system is about a factor 10^2 smaller when compared to C_{nom}, C_{LPV}.

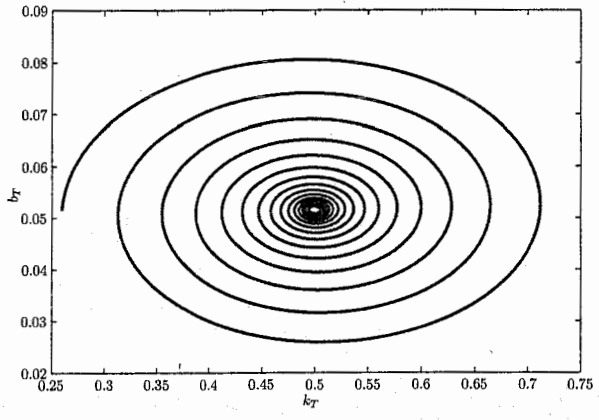

(a) Spiral pattern

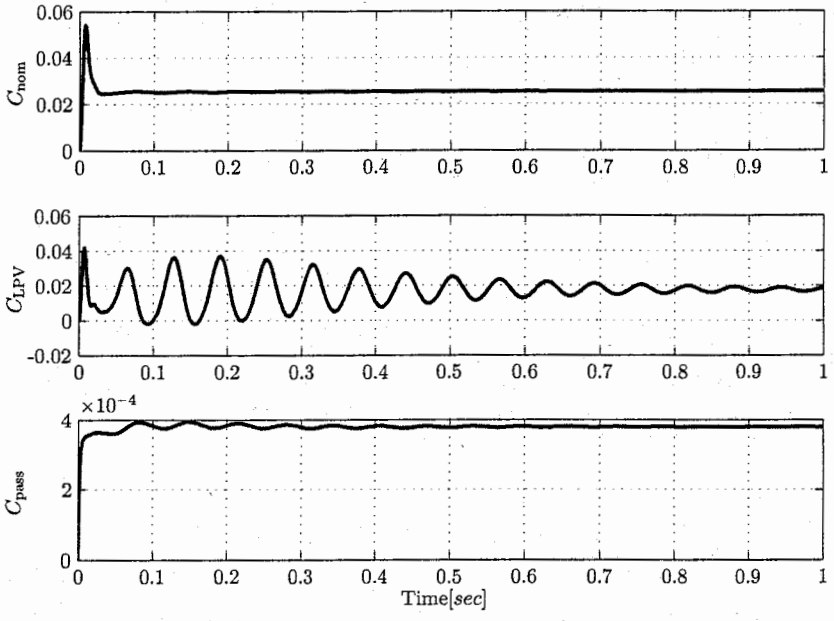

(b) Step disturbance responses with time varying k_T and b_T

Figure 4.23: Comparison of the step disturbance responses for three controllers with time varying k_T and b_T in a spiral.

Chapter 5

Conclusions and Recommendations

In this project, three different haptic controllers of a Master-Slave systems for minimal invasive surgery have been designed and implemented in the Matlab/Simulink environment. The following conclusions and recommendations for future research can be made.

5.1 Conclusions

The objective of this project was the design of a controlled system that restores the lack of haptic (kinesthetic) feedback taking into account that master-slave systems deals with uncertainty in the environmental properties. Thus, we consider necessary the use of Robust Control techniques in order to analyze and design these systems. Concretely, H_∞ robust control has been used to design three different controllers based on two different performance criteria.

A first performance criterion is based on the so-called transparency where the aim is to track forces and positions. For that purpose it has been designed a nominal H_∞ controller, C_{nom}, which minimizes the position tracking error for a given (bounded) input force. This design is robust against linear fractional uncertainties around the slave system. However, it would be enquiring to explore the robustness of the nominal controller, C_{nom}, versus parametric uncertainty defined within some parameter box. Accordingly, the plant has been modelled as affine parameter dependent on (k_T, b_T) defined in a parameter box $\mathcal{P}$. Varying the parameters within the predescribed box $\mathcal{P}$ the nominal controller C_{nom} is quadratically (robust) stable for a new parameter box $\mathcal{P}'$ which is the 68.85% of $\mathcal{P}$.
A second design based on the same performance criterion is the linear parameter varying (LPV) design, where the plant is defined as an affine parameter dependent plant and the resulting controller, C_{LPV}, may depend also on the parameters. Considering linear time-

invariant or slowly-varying parameters, robust stability is guaranteed for the predescribed parameter box $\mathcal{P}$. Hence, better robustness is achieved on the basis of the LPV design.

The second performance criterion is the passivity based performance where it aims to "track" the energy supplied by the operator and the energy supplied by the environment. In order to design the passive controller, C_{pass}, a change of variables has been carried out in order to be able to implement the passivity condition using H_∞ optimization. It has been shown that the passive performance condition is guaranteed. The next step is to determine if this condition guarantees kinesthetic sensing but that can only be done by implementing the controller in the real set-up.

Simulations show that in case of time-invariant parameters, the passive design provides with less steady state error within the specification with a factor 10^2 smaller when compared to C_{nom} and C_{LPV}. The LPV design achieves this specification for some parameters (k_T, b_T) in $\mathcal{P}'$, whereas the nominal controller does not achieve the specification. The LPV controller is less conservative than C_{nom} and C_{pass}. However, C_{nom} provides with faster response than with C_{LPV} and C_{pass}.

Finally, some simulations have been executed for slow time-varying parameters when varying in a spiral pattern. The nominal controller C_{nom} provides with faster response compared with the C_{LPV} and C_{pass} but its steady-state error it is outside the specification. The LPV controller C_{LPV} provides a better steady-state error than C_{nom}, despite its slower and oscillating response. However, the passive design gives a steady-state error with a factor 10^2 smaller when compared to C_{nom} and C_{LPV}. This means that the three designs can be used to control time-invariant and slow time-varying parameters guaranteeing certain robustness stability and performance.

5.2 Recommendations

Concerning the goal of this project, it would be worthwhile to implement the three controllers in the real set-up, which are design to provide haptic feedback. For that purpose, it is suggested to get more insight on the design of the shaping and weighting filters should be perform. Concretely, the weighting filters that characterize the control efforts should have more realistic values. In this case, we guarantee less gain in the controllers that makes the controller implementation feasible.

Using the passive design, only one simulation has been carried out in order to extract the supplied power. More simulations should be done using different kind of periodical and non-periodical signals. Then, prove if the passivity condition is still satisfied.

Furthermore, the linear parameter varying design invites to investigate the environment parameters identification and to look for different models of the environment.

Another recommendation is to model the friction of the master-slave system and include time-delay in the analysis of the stability and performance of the three designed systems.

Finally, implementation of the passive design in the real set-up is suggested in order to gain a better inside, whether the passivity performance condition guarantees kinesthetic sensing or not. This implementation does not required to modify the current set-up because the amount of kinesthetic sensing that is perceived by the human operator is quite ambiguous.

Bibliography

[1] R.J. Adams and B. Hannaford, "Stable haptic interaction with virtual environments," *IEEE Transactions on Robotics and Automation,* Vol. 15, NO. 3, pp. 465-474, June 1999.

[2] R.J. Adams, M.R. Moreyra, and B. Hannaford, "Stability and performance of haptic displays: Theory and Experiments," in *Proc. ASME International Mechanical Engineering Congress and Exhibition,* pp. 227-34, Anaheim, CA, 1998.

[3] R.J. Adams, and B. Hannaford, "A Two-Port Framework for the Design of Unconditionally Stable Haptic Interfaces," in *Proc. IEEE/RSJ International Conference on Intelligent Robots and Systems,* pp. 1254-9, Victoria, B.C., 1998.

[4] R.J. Anderson, M.W. Spong, "Asymptotic Stability for Force Reflecting Teleoperators with Time Delay," *Int. Journal of Robotics Research,*vol. 9, no. 2, 1992, pp. 135-49.

[5] R.J. Anderson, M.W. Spong, "Bilateral control of teleoperators with time delay," *IEEE Transactions on Automatic Control,*vol. 34, no. 5, May 1989,p. 494-501.

[6] P. Arcara, "Control of haptic and robotic telemanipulation systems," *Ph.D. Thesis, Universita degli Studi di Bologna - Facolta di Ingegneria -DEIS, 2002.*

[7] P. Arcara, C. Melchiorri, "Control scemes for teleoperation with time delay: a comparitive study," *Robotics and Autonomous Systems, Vol.38, No.1, Jan. 2002, p.49-64.*

[8] S. Boyd, L. El Ghaoui, E. Feron, and V. Balakrishnan, "Linear Matrix Inequalities in System and Control Theory," SIAM, 1994.

[9] M.C. Çavuşoğlu, A. Sherman, F. Tendick, "Bilateral controller design for telemanipulation in soft environments," in *Proceedings of the IEEE International Conference on Robotics and Automation (ICRA 2001),* Seoul, Korea, May 21-26, 2001.

[10] M.C. Çavuşoğlu, S. Shankar, F. Tendick and M. Cohn, "Laparoscopic Telesurgical Workstation," *In Proceedings of the SPIE International Symposium on Biological optics (BIOS'98),* San Jose, CA, January 24-30, 1998.

[11] M.C. Çavuşoğlu, "Telesurgery and Surgical Simulation: Design, and Evaluation of Haptic Interfaces to Real and Virtual Surgical Environments," *University of California at Berkley, PhD Thesis, 2000.*

[12] M.C. Çavuşoğlu, A. Sherman and F. Tendick, "Design of Bilateral Teleoperation Controllers for haptic Exploration and Telemanipulation of Soft Environments," *in IEEE Transactions on Robotics and Automation*, VOL.XX, NO. Y, August 2002.

[13] N. Chopra, M.W. Spong, S. Hirche and M. Buss, "Bilateral Teleoperation over the Internet: the Time Varying Delay Problem," *Proc. of the American Control Conference*, Denver, US, 2003.

[14] N. Chopra, M.W. Spong, R. Ortega and N.E. Barabanov, "On Position Tracking in Bilateral Teleoperation," *Proc. of the 2004 American Control Conference*, Boston, Massachusetts, June 30-July 2, 2004.

[15] S. Cools, "Design of a master slave system with force feedback," *Eindhoven University of Technology, DCT Report nr. 2003.53, June 2003.*

[16] J.E. Colgate, "Power and impedance scaling in bilateral manipulation," *Proc. IEEE International Conference on Robotics and Automation*, Sacramento, California, April 1991.

[17] J.E. Colgate and N. Hogan,"Robust control of dynamically interacting systems," *(*Int. J. Control.) Vol. 48, NO 1, pp.65-88, 1988.

[18] R.C. Craig, R.C. Kevin, "Closed-loop force control for haptic simulation of virtual environments," *Haptics-e*, Vol. 1, No. 2, February 2000, (http://www.haptics-e.org).

[19] C. Doerrer, T. Kern, T. Weber and R. Werthschuetzky "Actuator-Sensor-System for a Haptic Display to operate machines," *8th Mechatronics Forum International Conference (Mechatronics 2002)*, Twente, July 2002.

[20] Intuitive Surgery Inc. "DaVinci Homepage", *DaVinci homepage (http://www.intuitivesurgical.com).*

[21] B. Hannaford, J.H. Ryu, "Time domain passivity control of haptic interfaces," *Proc. IEEE Conference on Robotics and Automation*, Seoul, p. 863-869, 2001.

[22] B. Hannaford, J. Trujillo, M. Sinanan, M. Moreyra, J. Rosen, J. Rosen, J. Brown, R. Leuschke and M. MacFarlane, "Computerized Endoscopic Surgical Grasper," *Proc. Medicine Meets Virtual Reality*, San Diego, C.A. Janurary 1998.

[23] B. Hannaford, "A Design Framework for Teleoperators with Kinesthetic feedback," *IEEE Trans. Robotics and Automation*, vol.5, no 4, 1989, pp.426-434.

[24] B. Hannaford, "Stability and performance tradeoffs in bi-lateral telemanipulation" *Robotics and Automation*, 1989.

[25] Z. Hu, S.E. Salcudean, and P.D. Loewen, "Robust controller design for teleoperation systems," in *Proceedings of the IEEE International Conference on Systems, Man and Cybernetics,* 1995, Vol.3, pp. 2127-2132.

[26] Z. Hu, S.E. Salcudean, and P.D. Loewen, "Optimization-Based Teleoperation Controller Desgin," to be presented at *13th World Congress of IFAC,* San Francisco, CA, USA, June 30- July 5, 1996.

[27] H. Kazeroni, T. Tsay and K. Hollerbach, "A controller design framework for Telerobotic Systems," *IEEE Transactions on Control Systems Technology,* Vol. 1, NO. 1, March 1993.

[28] W.S. Kim, B. Hannaford, A.K. Bejczy, "Force-reflection and shared compliant control in operation telemanipulators with time delay," *IEEE Transactions on Robotics and Automation*, Vol. 8, No. 2, April 1992.

[29] S. Kudomi, H. Yamada, T. Muto. "Development of a hydraulic master-slave system for telerobotics," *Proc. of the 1st FPNI-PhD Symp.*, Hamburg 2000, p. 467-474.

[30] A.R. Lanfranco, A.E. Castellanos, J.P. Desai, and W.C. Meyers, "Robotic Surgery: A Current Perspective", *Annals of Surgery, 2004*, January 2004;239(1):14-21.

[31] D.A. Lawrence, "Stability and transparency in Bilateral teleoperation," *IEEE Transactions on Robotics and Automation,* p. 624-637, October 1993.

[32] M.H. Lee, H.R. Nicholls, "Tactile sensing for mechatronics-a state of the art survey," *Mechatronics, 9*, Jan 1999, pp1-31.

[33] S. Leeraphan, T. Maneewarn and D. Laowattana "Stable Adaptive Bilateral Control of Transparent Teleoperation through Time-Varying Delay," *IROS 2002, IEEE/RSJ International Conference on Intelligent Robots and Systems*, EPFL, Switzerland, September 30-October 4, 2002.

[34] R. Lozano, N. Chopra and M.W. Spong,"Passivation of force reflecting bilateral teleoperators with time varying delay," *Mechatronics'02,* Enschede, Netherlands, June 24-26, 2002.

[35] G. Niemeyer and J.E. Slotine, "Stable Adaptive Teleoperation," *IEEE Journal of Oceanic Engineering,* Vol. 16, NO. 1, January 1991.

[36] W.J. Peine, R.D. Howe, "Do human sense finger deformation odr distributed pressure to detect lumps in soft tissue?".

[37] G. Raju, G. Verghese, and T. Sheridan, "Design issues in 2-port network models of bilateral remote manipulation," in *Proceedings of the IEEE International Conference on Robotics and Automation*, p. 1316-1321, 1989.

[38] J. Rosen, B. Hannaford, "Force Controlled and Teleoperated Endoscopic Grasper for Minimally Invasive Surgery-Experimental Performance Evaluation," *IEEE Transactions on Biomedical Engineering*,Vol. 46, NO. 10, October 1999.

[39] A.F. Rovers, "Design of a robust master-slave controller for surgery applications with haptic feedback," Eindhoven University of Technology, DCT Report nr. 2003.54, June 2003.

[40] A.F. Rovers, *"A literature study on the present-day use of haptic feedback in medical robotics,"* Eindhoven University of technology, DCT Report nr. 2002.57, September 2002.

[41] A. Sherman, M.C. Çavuşoğlu, F. Tendick, "Comparison of teleoperator control architectures for palpation task," in *Proceedings on IMECE'00, Symp. on Haptic Interfaces for Virtual Environments and Tele-operator Systems*, November 5-10, 2000, Orlando, Florida, U.S.A.

[42] C.M. Smith, "Human Factors in Haptic Inter-faces," *ACM Crossroads Student Magazine, January 24, 2001* (www.acm.org/crossroads/xrds3-3/haptic.html).

[43] Tavakoli, patel, Moallem. "A Force Reflective Master-Slave System for Minimally Invasive Surgery," *Proceedings of the IEEE International Conference on Intelligent Robots and Systems, Las Vegas, Nevada, October 2003.*

[44] F. Tendick, M.C. Cavusoglu, "Human-Machine Interfaces for Minimaly Invasive Surgery," *In Proceedings of the 19th Annual International Conference of the IEEE in Medicine and Biology Society*, Chicago, IL, October 30-November 2, 1997, pp.2771-6.

[45] J. Ueda and T. Yoshikawa, "Force-Reflecting Bilateral Teleoperation with Time Delay by Signal Filtering," *IEEE Transactions on Robotics and Automation,* Vol. 20, NO. 3, June 2004.

[46] S.A. Wall, W. Harwin, "A high bandwith interface for haptic human computer interaction," Mechatronics 11 (2001) 371-387.

[47] J.C. Willems, "Dissipative Dynamical Systems, Part I: General Theory", Journal Arch. Rat. Mech. Anal., Vol. 45, p. 321-351, 1972.

[48] Y. Yokokohji and T. Yoshikawa, "Bilateral control of master-slave manipulators for ideal kinesthetic coupling-formulation and experiment," *IEEE Transactions on Robotics and Automation,* p. 605-620, October 1994.

[49] K. Zhou, J.C. Doyle and K. Glover, *Robust and Optimal Control.* Prentice Hall, 1996. Department of Computing Science, University of Glasgow.

[50] Computer Motion Inc. "Zeus Homepage", *Zeus homepage (http://www.computermotion.com).*

Appendix A

Dissipative, Conservative and Passive Systems

Dissipative and Conservative

Consider a continuous, linear, time-invariant dynamical system Σ described by its state-space representation

$$\Sigma : \begin{cases} \dot{x} = Ax + Bu \\ y = Cx + Du \end{cases} \tag{A.1}$$

and a quadratic supply function $S(u, y)$,

$$S(u,y) = \begin{bmatrix} u \\ y \end{bmatrix}^T \begin{bmatrix} S_u & S_{uy} \\ S_{yu} & S_y \end{bmatrix} \begin{bmatrix} u \\ y \end{bmatrix} \tag{A.2}$$

Definition The system Σ with a quadratic supply function $S(u, y)$ is said to be *dissipative* if there exists a positive storage function $V : \mathbb{R}^n \rightarrow \mathbb{R}(V(x) \geq 0)$ such that

$$\int_{t_0}^{t_1} S(u,y)\ dt \geq V(x(t_1)) - V(x(t_0)) \geq 0 \tag{A.3}$$

for all $t_0 \leq t_1$ and for all u in L_2. The pair $(\Sigma,\ S)$ is said to be *conservative* if the first equality holds in (A.3) for all $t_0 \leq t_1$ and for all u.

Theorem A.0.1 *Suppose $\Sigma(A, B, C, D)$ is minimal. Then, Σ is* dissipative *with respect to the supply function $S(u, y)$ being*

$$S(u,y) = u^T y = \begin{bmatrix} u \\ y \end{bmatrix}^T \begin{bmatrix} 0 & \frac{1}{2} \\ \frac{1}{2} & 0 \end{bmatrix} \begin{bmatrix} u \\ y \end{bmatrix} \tag{A.4}$$

if and only if $\exists K = K^T \geq 0$ *such that*

$$L(K) = \begin{bmatrix} -D - D^T & B^T K - C \\ KB - C^T & A^T K + KA \end{bmatrix} \leq 0 \tag{A.5}$$

That is, $L(K)$ *has to be semi-negative definite or, equivalently,* $L(K)$ *has to have all eigenvalues in the closed left half plane* [1]. *Moreover, for any such* K, *the function* $V(x) := x^T K x$ *is a valid storage function for the system* Σ *as it satisfies* (A.3)

Proof Considering the system Σ in (A.1) with a quadratic storage function $V = x^T K x$ being semi-positive definite, and K being symmetric and semi-positive definite, is *dissipative* with respect to a supply function S of the form

$$S(u,y) = u^T y + y^T u = \begin{bmatrix} u \\ y \end{bmatrix}^T \begin{bmatrix} 0 & 1 \\ 1 & 0 \end{bmatrix} \begin{bmatrix} u \\ y \end{bmatrix} \tag{A.6}$$

if

$$\int_{t_0}^{t_1} (u^T y + y^T u)\, dt \geq x(t_1)^T K x(t_1) - x(t_0)^T K x(t_0) \tag{A.7}$$

Giving the derivative of V

$$\begin{aligned} &\frac{d}{dt} x(t)^T K x(t) = \dot{x(t)}^T K x(t) + x(t)^T K \dot{x(t)} = \\ &(Ax + Bu)^T K x + x^T K (Ax + Bu) = \\ &u^T B^T K x + x^T A^T K x + x^T K A x + x^T K B u = \\ &\begin{bmatrix} u \\ x \end{bmatrix}^T \begin{bmatrix} 0 & B^T K \\ KB & A^T K + KA \end{bmatrix} \begin{bmatrix} u \\ x \end{bmatrix} \end{aligned} \tag{A.8}$$

and substituting this into the derivative of (A.7),

$$\begin{aligned} &-\frac{d}{dt} x(t)^T K x(t) + u^T (Cx + Du) + (Cx + Du)^T u \geq 0 \\ &\begin{bmatrix} u \\ x \end{bmatrix}^T \begin{bmatrix} 0 & -B^T K \\ -KB & -A^T K - KA \end{bmatrix} \begin{bmatrix} u \\ x \end{bmatrix} + \begin{bmatrix} u \\ x \end{bmatrix}^T \begin{bmatrix} D + D^T & C \\ C^T & 0 \end{bmatrix} \begin{bmatrix} u \\ x \end{bmatrix} \geq 0 \\ &\begin{bmatrix} u \\ x \end{bmatrix}^T \begin{bmatrix} -D - D^T & B^T K - C \\ KB - C^T & A^T K + KA \end{bmatrix} \begin{bmatrix} u \\ x \end{bmatrix} \leq 0 \end{aligned} \tag{A.9}$$

where $L(K)$ relates the inputs, u, and the states, x. Note that $L(K)$ change with the supply function $S(u,y)$. Stability in terms of Lyapunov is guaranteed as the storage functions are Lyapunov functions. Thus, a dissipative system is stable.□

The next theorem presents the frequency-domain inequality satisfied by all dissipative *LTI* systems.

[1] $L(K)$ gives an idea of the energy that the system absorbs.

Theorem A.0.2 *If a stable LTI system, Σ, with transfer function matrix, $G(s)$, is dissipative with respect to a quadratic supply function*

$$S(u,y) = \begin{bmatrix} u \\ y \end{bmatrix}^T \begin{bmatrix} S_{11} & S_{12} \\ S_{12}^T & S_{22} \end{bmatrix} \begin{bmatrix} u \\ y \end{bmatrix} \tag{A.10}$$

then

$$\Phi(j\omega) = \begin{bmatrix} I \\ G(j\omega) \end{bmatrix}^* \begin{bmatrix} S_{11} & S_{12} \\ S_{12}^T & S_{22} \end{bmatrix} \begin{bmatrix} I \\ G(j\omega) \end{bmatrix} \geq 0 \tag{A.11}$$

for all ω.

For a supply function of the form expressed in (A.4), the above mentioned theorem can be expressed as following:

Theorem A.0.3 *Consider a stable LTI system Σ, with minimal realization (A,B,C,D), and transfer function matrix, $G(s) = C(Is - A)^{-1}B + D$. The LTI system is dissipative if and only if its frequency response, $G(j\omega)$, satisfies*

$$\Phi(j\omega) = G^*(j\omega) + G(j\omega) \geq 0 \tag{A.12}$$

for all ω.

The above mentioned condition (A.5) is equivalent to say that the *LTI* system Σ is positive real (PR).

Passivity

Considering the change of variables $(\mathrm{w}, \mathrm{z}) = f(F, v)$

$$\begin{aligned} \mathrm{w} &= \frac{1}{2}\left[\begin{pmatrix} F_{\mathrm{op}} \\ -F_{\mathrm{env}} \end{pmatrix} + \begin{pmatrix} v_{\mathrm{op}} \\ v_{\mathrm{env}} \end{pmatrix}\right] \\ \mathrm{z} &= \frac{1}{2}\left[\begin{pmatrix} F_{\mathrm{op}} \\ -F_{\mathrm{env}} \end{pmatrix} - \begin{pmatrix} v_{\mathrm{op}} \\ v_{\mathrm{env}} \end{pmatrix}\right] \end{aligned} \tag{A.13}$$

with $F = \begin{pmatrix} F_{\mathrm{op}} \\ -F_{\mathrm{env}} \end{pmatrix}$ and $v = \begin{pmatrix} v_{\mathrm{op}} \\ v_{\mathrm{env}} \end{pmatrix}$ then,

$$\begin{bmatrix} \mathrm{w} \\ \mathrm{z} \end{bmatrix} = \frac{1}{2}\begin{pmatrix} I & I \\ I & -I \end{pmatrix}\begin{bmatrix} F \\ v \end{bmatrix} = G\begin{bmatrix} F \\ v \end{bmatrix} \tag{A.14a}$$

$$\begin{bmatrix} F \\ v \end{bmatrix} = G^{-1}\begin{bmatrix} \mathrm{w} \\ \mathrm{z} \end{bmatrix} \tag{A.14b}$$

Consider the quadratic supply function

$$S(F,v) = F^T v = F_{\text{op}} v_{\text{op}} - F_{\text{env}} v_{\text{env}} = \tag{A.15a}$$

$$= \begin{bmatrix} F \\ v \end{bmatrix}^T \begin{bmatrix} 0 & \frac{1}{2}I \\ \frac{1}{2}I & 0 \end{bmatrix} \begin{bmatrix} F \\ v \end{bmatrix} \tag{A.15b}$$

and using the change of variables defined in (A.13), the supply function becomes

$$\begin{aligned} S(F,v) &= \begin{bmatrix} F \\ v \end{bmatrix}^T \begin{bmatrix} 0 & \frac{1}{2}I \\ \frac{1}{2}I & 0 \end{bmatrix} \begin{bmatrix} F \\ v \end{bmatrix} \\ &= \begin{bmatrix} \mathrm{w} \\ \mathrm{z} \end{bmatrix}^T G^T \begin{bmatrix} 0 & \frac{1}{2}I \\ \frac{1}{2}I & 0 \end{bmatrix} G \begin{bmatrix} \mathrm{w} \\ \mathrm{z} \end{bmatrix} \\ &= \begin{bmatrix} \mathrm{w} \\ \mathrm{z} \end{bmatrix}^T \begin{bmatrix} I & 0 \\ 0 & -I \end{bmatrix} \begin{bmatrix} \mathrm{w} \\ \mathrm{z} \end{bmatrix} \\ &= \mathrm{w}^T\mathrm{w} - \mathrm{z}^T\mathrm{z} \end{aligned} \tag{A.16}$$

Thus, the supply function $S(F,v) = F_{\text{op}} v_{\text{op}} - F_{\text{env}} v_{\text{env}}$ is equivalent to $S(\mathrm{w},\mathrm{z}) = \mathrm{w}^T\mathrm{w} - \mathrm{z}^T\mathrm{z}$ considering w and z as defined in (A.13).

For T-periodic trajectories we may conclude that,

$$\int_{t_0}^{T} F^T(t)v(t) = \int_0^T \|\mathrm{w}\|^2 dt - \int_0^T \|\mathrm{z}\|^2 dt$$

and thus, passivity requires that,

$$\int_0^T \|\mathrm{w}\|^2 dt - \int_0^T \|\mathrm{z}\|^2 dt = 0$$

For L_2 trajectories we have that, with x(0)=0 and a stable system that $\forall\ F \in L_2,\ x \in L_2$ and hence $x(\infty)$=0. From (A.3) with $S(u,y) = F(t)^T v(t)dt$ we thus can conclude that,

$$\int_0^\infty F^T(t)v(t)dt = 0$$

for all L_2 trajectories of the system. Then, using the previous, it follows that,

$$\|\mathrm{w}\|_{L_2}^2 = \int_0^\infty \mathrm{w}^T\mathrm{w}dt = \int_0^\infty \mathrm{z}^T\mathrm{z}dt = \|\mathrm{z}\|_{L_2}^2$$

i.e., the system $\mathrm{w} \mapsto \mathrm{z}$ must be all-pass to be passive.

Stability Issues

Consider Σ

$$\Sigma : \begin{cases} \dot{x} = Ax + Bu \\ y = Cx + Du \end{cases} \tag{A.17}$$

and the change of variables:

$$\begin{cases} \mathrm{z} = \frac{u+y}{2} \\ \mathrm{w} = \frac{u-y}{2} \end{cases} \leftrightarrow \begin{cases} \mathrm{u} = \mathrm{z} + \mathrm{w} \\ \mathrm{y} = \mathrm{z} - \mathrm{w} \end{cases} \tag{A.18}$$

Q: State space representation of equivalent system Σ' mapping $\mathrm{w} \mapsto \mathrm{z}$.
A:

$$\begin{aligned} \mathrm{z} = \frac{u+y}{2} &= \frac{u}{2} + \frac{1}{2}(Cx + Du) = \frac{1}{2}(D+I)u + \frac{1}{2}Cx \\ &= \frac{1}{2}Cx + \frac{1}{2}(D+I)(\mathrm{z}+\mathrm{w}) \\ &= \frac{1}{2}Cx + \frac{1}{2}(D+I)\mathrm{z} + \frac{1}{2}(D+I)\mathrm{w} \end{aligned} \tag{A.19}$$

Hence:

$$\frac{1}{2}(I-D)\mathrm{z} = \frac{1}{2}Cx + \frac{1}{2}(D+I)\mathrm{w}$$

so that

$$\mathrm{z} = (I-D)^{-1}Cx + (I-D)^{-1}(I+D)\mathrm{w} \tag{A.20}$$

Similarly,

$$\begin{aligned} \dot{x} = Ax + Bu &= Ax + B(\mathrm{z}+\mathrm{w}) = \\ &= Ax + B[(I-D)^{-1}Cx + (I-D)^{-1}(I+D)\mathrm{w}] + B\mathrm{w} \\ &= [A + B(I-D)^{-1}C]x + [B(I + (I-D)^{-1}(I+D))]\mathrm{w} \\ &= [A + B(I-D)^{-1}C]x + 2B(I-D)^{-1}\mathrm{w} \end{aligned} \tag{A.21}$$

(Here we used that

$$(I-D)^{-1}(I+D)+I = (I-D)^{-1}(I+D)+(I-D)^{-1}(I-D) = (I-D)^{-1}[I+D+I-D] = 2(I-D)^{-1})$$

Hence:

$$\Sigma' : \begin{cases} \dot{x} = A + B(I-D)^{-1}Cx + 2B(I-D)^{-1}\mathrm{w} \\ \mathrm{z} = (I-D)^{-1}Cx + (I-D)^{-1}(I+D)\mathrm{w} \end{cases} \tag{A.22}$$

is the transformed system[2].

From this derivation we can conclude that, the stability of Σ does not guarantee that stability of Σ'. However, if Σ is dissipative, then Σ' is stable.

The above explained definitions were provided by Dr. Siep Weiland.

[2]This proof was provided by Dr. Siep Weiland

Example: Mass-Spring-Damper system

For the well-known dissipative mass-spring-damper system

$$F = m\ddot{x} + b\dot{x} + kx \tag{A.23}$$

where the system Σ is described in state-space representation as:

$$\Sigma \begin{cases} \begin{bmatrix} \dot{x} \\ \ddot{x} \end{bmatrix} = \begin{bmatrix} 0 & 1 \\ -k/m & -b/m \end{bmatrix} \begin{bmatrix} x \\ \dot{x} \end{bmatrix} + \begin{bmatrix} 0 \\ 1/m \end{bmatrix} F \\ y = \begin{bmatrix} 0 & 1 \end{bmatrix} \begin{bmatrix} x \\ \dot{x} \end{bmatrix} + \begin{bmatrix} 0 \end{bmatrix} F \end{cases} \tag{A.24}$$

it is sufficient to guarantee that $L(K) \leq 0$ for any symmetric $K \geq 0$. A suitable choice for a Lyapunov function for a mass-spring-damper system is the total energy of the system. That is,

$$V(x, \dot{x}) = \frac{1}{2}m\dot{x}^2 + \frac{1}{2}kx^2 \tag{A.25}$$

Note that the total energy is a quadratic positive definite function of the state of the system. In quadratic form, the total energy can be described as:

$$V(x) = x^T K x = \begin{bmatrix} x \\ \dot{x} \end{bmatrix}^T \underbrace{\begin{bmatrix} k/2 & 0 \\ 0 & m/2 \end{bmatrix}}_{K} \begin{bmatrix} x \\ \dot{x} \end{bmatrix} \tag{A.26}$$

where K is a symmetric semi-positive quadratic supply function for all m and for all b. Derivating (A.25)

$$\dot{V}(x) = \dot{x}^T(m\ddot{x} + Kx) = \dot{x}^T(F - b\dot{x}) \tag{A.27}$$

where it states that the rate of change of the total energy of the system is equal to the power input into the system minus the rate of energy dissipated in the system. In order to check dissipativity, we can calculate $L(K)$ and check if it is semi-negative definite. For the mass-spring-damper system this is,

$$L = \begin{bmatrix} 0 & 0 & 0 \\ 0 & -b & \frac{-1}{2} \\ 0 & \frac{-1}{2} & 0 \end{bmatrix} \tag{A.28}$$

where the damping is the only term is appearing in L. This result is expected due to the fact that the damper dissipates energy.

Appendix B

Conference Paper

This appendix contains the conference paper: "Haptic Feedback Designs in Teleoperation systems for Minimal Invasive Surgery" accepted in the IEEE International Conference on Systems, Man and Cybernetics (SMC04), The Hague, The Netherlands, 2004 (p. 2513-2518). The authors of this paper are Iciar Font, Siep Weiland, Martijn Franken, Maarten Steinbuch and Loy Rovers.

Haptic feedback designs in teleoperation systems for minimal invasive surgery*

Iciar Font[1], Siep Weiland[2], Martijn Franken[1], Maarten Steinbuch[1] and Loy Rovers[3]
[1]Eindhoven University of Technology, Department of Mechanical Engineering, Dynamics and Control Technology Group, Eindhoven, The Netherlands, Email: m.steinbuch@tue.nl.
[2]Eindhoven University of Technology, Department of Electrical Engineering, Email: s.weiland@tue.nl.
[3]Eindhoven University of Technology, Department of Industrial Design.

Abstract – *One of the major shortcomings of state-of-the-art robotic systems for minimal invasive surgery, is the lack of haptic feedback for the surgeon. In order to provide haptic information, sensors and actuators have to be added to the master and slave device. A control system should process the data and make a coupling between slave and master. Despite the significant amount of research on haptic devices, this control design problem is, largely, an open problem. This paper reports the results on three model-based control designs. Using the formalism of passivity, a robust controller has been designed, and is compared to a gain scheduled controller (LPV) which is adaptable for changes in the tissue characteristics.*

Keywords: Haptic feedback, H_∞ control, tele-operation systems, passivity.

1 Introduction

Robotic tele-surgery is becoming a popular technique for certain procedures since benefits of endoscopic techniques have become general knowledge. However, one of the major shortcomings of the present generation of tele-operated master-slave systems is the lack of haptic feedback; the surgeon that remotely controls the robot is not able to feel what is happening inside the patient.

In order to get a better insight into master-slave systems, in this paper we investigate the control design of a haptic device considering only kinesthetic sensing. To this end, we focus primarily on model-based control design within the framework of H_∞ optimization. Several controller architectures have been studied in simulations. Currently, implementations are performed and evaluated on a laboratory setup. It is a simple one degree-of-freedom setup, consisting of a master manipulator with force feedback and a slave manipulator actuated by an ordinary DC motor. Because of the relative low-bandwidth requirements (up to say 10 Hz), a relatively low sampling frequency can be used; this means that the forceps can be controlled with relatively simple hardware and existing communication protocols.

*0-7803-8566-7/04/$20.00 © 2004 IEEE.

In Section 2 we will give an overview of existing control design problem formulations as used in haptics literature, and the passivity based performance criterion will be introduced. In Section 3 the new optimization problems will be solved using model-based robust control design methodology, and simulation results will be shown. In Section 4 an application to the 1 dof master-slave system will be shown. Main results will be summarized in the form of conclusions in Section 5.

2 Problem formulation

Figure 1 depicts the general configuration of a controlled two-port teleoperation system. M, S and C denote components that are generally referred to as the *master*, the *slave* and the *controller* of the system. The master is a mechanical device that interacts with its environment by means of a human operator through the force F_{op} and the velocity v_{op}. Similarly, the slave interacts with its environment through the force F_{env} and the velocity v_{env}. It is assumed that M and S are given, while the controller C needs to be designed such that the two-port system that results from the interconnection has a desired behavior.

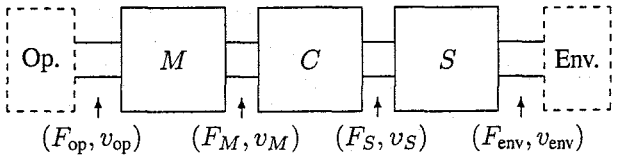

Figure 1: General two-port teleoperation system

2.1 Performance measures

Besides the fundamental requirement of *stability*, the ideal master-slave manipulator provides perfect *transparency*. That is, the human operator experiences the same forces as if he/she is touching the remote environment directly. Yokokohji and Yoshikawa defined transparency in terms of perfect tracking of both forces and positions [14]. Raju describes this goal in terms of impedances [9]. On either side of the

two-port the *impedance* and the *admittance* is defined by the relations

$$F_{\text{op}} = Z_{\text{op}}(v_{\text{op}}), \qquad F_{\text{env}} = Z_{\text{env}}(v_{\text{env}}) \tag{1}$$
$$v_{\text{op}} = G_{\text{op}}(F_{\text{op}}), \qquad v_{\text{env}} = G_{\text{env}}(F_{\text{env}}) \tag{2}$$

In robotic tele-surgery applications a basic requirement is good tracking in free space while the slave is in contact with a tissue. As a performance measure, [9] suggests that the impedance transmitted to the operator, Z_{op}, is the same as the environmental impedance Z_{env}. Another measure of transparency is given by Lawrence [8] who considered the ratio between the transmitted and the environmental impedance $T = \frac{Z_{\text{op}}}{Z_{\text{env}}}$ which needs to be kept close to one over a maximum bandwidth. However, in tele-surgery it is often more important to be able to detect variations in impedance, rather than perceive the exact impedance of the environment. Changes in impedance provide valuable information in two ways. First, the interaction between instruments and tissue can be sensed, for one can feel when a needle punctures or leaves a tissue. Second, structures hidden in the tissue, like blood vessels or tumors, can be detected by probing the tissue. An attempt to formalize this is given in Çavuşoğlu where a *fidelity criterion* is defined as

$$S_{\text{fid}} = \left\| W \frac{dZ_{\text{op}}}{dZ_{\text{env}}}|_{Z_{\text{env}}=\hat{Z}_{\text{env}}} \right\|_2 \tag{3}$$

Here, W is a frequency dependent weighting filter and $\hat{Z}_{\text{env}}$ is the nominal environment impedance, $\|\cdot\|_2$ denotes the H_2 norm and differentiation is understood in the sense that the impedance Z_{op} is viewed as function of the environmental impedance Z_{env}. The criterion therefore reflects variations in impedance. For kinesthetic feedback, a low-pass filter with a cutoff frequency of about 40 Hz is used for the weighting filter W. See [11], [12], [4].

H_∞ optimal performance

If Z_{op} and Z_{env} denote the transfer functions of the impedances, then the criterion to keep the transparency close to one for a specified bandwidth can be expressed in terms of the H_∞ norm. This amounts to finding a stabilizing controller C that minimizes the H_∞ norm

$$\|W(Z_{\text{op}} - Z_{\text{env}})\|_{H_\infty} \quad \text{or} \quad \|W(G_{\text{op}} - G_{\text{env}})\|_{H_\infty} \tag{4}$$

where W is a frequency weight reflecting the relevant bandwidth. Here,

$$\|Z\|_{H_\infty} := \sup_{\omega\in\mathbb{R}} \sigma_{\max}(Z(j\omega)) = \sup_{0<\|w\|_2<\infty} \frac{\|z\|_2}{\|w\|_2} \tag{5}$$

where $\sigma_{\max}(\cdot)$ denotes the maximum singular value, $z = Zw$ is the to-be-controlled output and $\|w\|_2$ denotes the usual two-norm $\|w\|_2^2 = \int_0^\infty |w(t)|^2 dt$.

Parameter varying performance

For applications in tele-surgery, the kinesthetic sensing of a tissue is a main objective. This means that the environment can be viewed as an uncertain dynamical system that represents the tissue. We will assume that the environment (the tissue) is described by

$$F_{\text{env}} = m_T\ddot{x}_T + b_T\dot{x}_T + k_T x_T, \quad v_{\text{env}} = \dot{x}_T \tag{6}$$

where x_T is the tissue displacement, and m_T, k_T and b_T represent the mass, the stiffness and the damping coefficient of the tissue. If the slave is in touch with the tissue the slave displacement x_S and the tissue displacement x_T coincide, i.e.,

$$x_T = x_S. \tag{7}$$

The parameter vector $p := \text{col}(k_T, b_T)$ is assumed to be an uncertain element in a polytopic subset $\mathcal{P}$ of $\mathbb{R}^2_+$. We will take this to be a box in that

$$p = \begin{pmatrix} k_T \\ b_T \end{pmatrix} \in \mathcal{P} := [k_T^-, k_T^+] \times [b_T^-, b_T^+] \tag{8}$$

where $k_T^- < k_T^+$ and $b_T^- < b_T^+$. In this way, the tele-operation system extended with the uncertain model (6),(7),(8) of the environment defines a *parameter varying* system. We consider the performance criterion

$$\gamma^*_{\text{LPV}}(\mathcal{P}) := \sup_{p\in\mathcal{P}} \inf_{C} \sup_{0<\|w\|_2<\infty} \frac{\|z\|_2}{\|w\|_2} \tag{9}$$

where w and z are the exogenous input and to-be-controlled output, respectively, and the infimum is taken over all LTI controllers C that stabilize the system for all $p \in \mathcal{P}$. Obviously, $\mathcal{P}' \subseteq \mathcal{P}''$ implies that $\gamma^*_{\text{LPV}}(\mathcal{P}') \leq \gamma^*_{\text{LPV}}(\mathcal{P}'')$. It is important to observe that this formulation implies that the resulting controller may depend on the parameter p. This problem can be solved explicitly using optimization techniques based on linear matrix inequalities (LMI's) [3] provided that the parameter p enters a state space representation of the to-be-controlled system in an *affine* way. In that case, the parameter p may, in principle, be time varying as long as it assumes values in the polytope $\mathcal{P}$.

Performance based on passivity

A drawback of the impedance based performance criteria is that they impose an input-output structure in the tele-operation system that does not necessarily correspond to the physical reality. Indeed, the two-port of Figure 1 has no 'natural' input and output structure. Passivity based performance criteria consider for each time t the power

$$p_{\text{op}}(t) = F_{\text{op}}(t)v_{\text{op}}(t), \quad p_{\text{env}}(t) = F_{\text{env}}(t)v_{\text{env}}(t) \tag{10}$$

on either side of the two-port[1]. The two port of Figure 1 is said to be *conservative* if there exists a nonnegative function

[1]The sign convention is that power is positive if energy is delivered to the system.

V such that

$$V(t_0) + \int_{t_0}^{t_1} (p_{\text{op}}(t) + p_{\text{env}}(t))\, dt = V(t_1) \qquad (11)$$

for all $t_0 \leq t_1$ and for all (F_M, F_S, v_M, v_S) that are compatible with the system. This expresses the existence of a *conservation law* where V, the internal energy, is preserved at all time and for all possible behavior of the system. Hence, passivity requires that the work done on the system, i.e., the energy that the operator (environment) supplies to the system in any time interval will be equal to the energy the system supplies to its environment (to the operator). Note that (11) implies that for *periodic* trajectories $(F_{\text{M}}, F_{\text{S}}, v_{\text{M}}, v_{\text{S}})$ the net-flow of energy into the system over each period is zero [5]. As a modification to the passivity concept, we will call the system *passive* if

$$\int_0^{\infty} (p_{\text{op}}(t) + p_{\text{env}}(t))\, dt = 0 \qquad (12)$$

for all (F_M, F_S, v_M, v_S) under the assumption that $V(0) = 0$. A conservative system is passive. However, a passive system may not be conservative [16].

2.2 Control structure

The general tele-operation system of Figure 1 may lead to many different control configurations. In turn, the performance of the controlled system will crucially depend on the bilateral control architecture [1]. In this paper we will consider the position error (PERR) control architecture depicted in Figure 2. The PERR architecture is the same as the open-loop impedance control in [4], the symmetric servo system in [7] and the force reflection in [2]. In this configuration, the forces F_M and F_S are generated by the controllers C_M and C_S, resp., that are fed by the position error $e = x_M - x_S$ between the master and the slave. Position and force tracking can only be obtained by using high controller gains, which are only possible at low bandwidths in order to prevent instabilities. Because the master and slave are coupled by a (stiff) controller, the human operator perceives inertia and damping of both the master and slave device on top of the environment impedance.

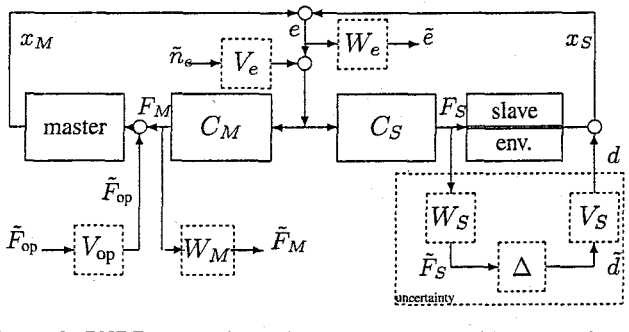

Figure 2: PERR control architecture (solid) and its extension for H_∞ control design (dashed)

3 Model-based control design

In this section we synthesize and compare three different controllers in the PERR controller architecture. The first one will be an H_∞ optimal and robust controller. The second will be a parameter varying controller that explicitly depends on (k_T, b_T). Finally, we synthesize a controller based on the passivity criterion (12).

3.1 Specifications

Both the master and the slave are represented by Newton's second law

$$m_M \ddot{x}_M = F_M - F_{\text{op}}, \quad m_S \ddot{x}_S = F_S - F_{\text{env}} \qquad (13)$$

where x_M and x_S denote the displacement of the master and the slave, respectively. For the H_∞ and LPV controller designs below, the environment is modeled as an uncertain mass-spring-damper system as given in (6)-(8). This setting leads to two relevant modes of operation: a 'free mode' in which the tissue is not connected to the slave and a 'contact mode' in which the slave touches the tissue. Here, we will exclusively consider the contact mode which is modelled by the equations (13),(6),(7),(8) where $m_M = 2 \times 10^{-4}$, $m_S = 8.5 \times 10^{-4}$, $m_T = 1 \times 10^{-2}$ [kg], $k_T^- = 0.1$, $k_T^+ = 0.9$ [Nm/rad], $b_T^- = 0.003$ and $b_T^+ = 0.1$ [Nms/rad]. Let $k_T^{\text{nom}} := \frac{k_T^+ + k_T^-}{2}$ and $b_T^{\text{nom}} := \frac{b_T^+ + b_T^-}{2}$ denote the *nominal values* of k_T and b_T. The force applied by the human operator is assumed to satisfy $|F_{\text{op}}(t)| < 10$ N. The bandwidth of the controlled system is based on human kinesthetic sensing and required to be at least 20π rad [13],[15]. Within the PERR controller structure the position error $e = x_M - x_S$ is required to be at most 0.01 rad when the maximal force is applied by the operator.

3.2 An H_∞ optimal design

The synthesis of an H_∞ optimal controller involves the partitioned plant

$$P_{\text{aug}} : \begin{pmatrix} w \\ u \end{pmatrix} \mapsto \begin{pmatrix} z \\ y \end{pmatrix} \qquad (14)$$

where the measurement $y = e = x_M - x_S$ and the control $u = \text{col}(F_M, F_S)$ are input and output of the controller C, respectively. The signals $w = \text{col}(\tilde{d}, \tilde{F}_{\text{op}}, \tilde{n}_e)$ and $z = \text{col}(\tilde{e}, \tilde{F}_M, \tilde{F}_S)$ denote exogenous inputs and outputs of the controlled system inferred from the extended PERR structure of Figure 2. Here, $\tilde{e} := W_e e$, $\tilde{F}_M = W_M F_M$, and $\tilde{F}_S = W_S F_S$ denote the weighted position error and the weighted control effort of the master and slave forces. Furthermore, the uncertainty inferred from the environment, restrictions on forces imposed by the human operator and prior knowledge on sensors is incorporated in the design by setting $d = V_d \tilde{d}$, $F_{\text{op}} = V_M \tilde{F}_{\text{op}}$ and $n_e = V_e \tilde{n}_e$ with appropriate weightings for V_d, V_M and V_e. The uncertainty of the environment is modelled as an additive uncertainty $S_{\text{nom}} + V_M \Delta W_S$ on the nominal slave transfer function

where $\|\Delta\|_{H_\infty} \leq 1$. See Figure 2. The controller is synthesized so as to achieve the performance

$$\gamma^* := \inf_C \sup_{0<\|w\|_2<\infty} \frac{\|z\|_2}{\|w\|_2} \tag{15}$$

With appropriate choices of the weighting filters, we find $\gamma^* = 3.25$ and the corresponding optimal controller C_{nom} is implemented in the PERR structure of Figure 2.

The Bode plot of the closed-loop transfer function mapping the operator force F_{op} to the position error $e = x_M - x_S$ is displayed in Figure 3. Figure 4 shows the step response of this closed loop transfer with a steady-state error of 0.013rad for a maximum torque specified in 3.1. The tracking specification is not fulfilled but is close to its desired value. The response, however, is rather slow. The system will be robustly stable against all uncertainties Δ with $\|\Delta\|_{H_\infty} \leq 1/\gamma^*$. Hence robust stability of the system is not guaranteed for the targeted set of uncertainties. The controlled system is not guaranteed stable for all parameters $p \in \mathcal{P}$, but it is if the box $\mathcal{P}$ is shrinked to about 42.7% of its area around the nominal value. Hence C_{nom} achieves robust (quadratic) stability for the parameter box

$$\mathcal{P}' = p_{\text{nom}} + \frac{43.7}{100}(\mathcal{P} - p_{\text{nom}}). \tag{16}$$

that lies inside $\mathcal{P}$. (Here, $p_{\text{nom}} = \text{col}(k_T^{\text{nom}}, b_T^{\text{nom}})$). The step

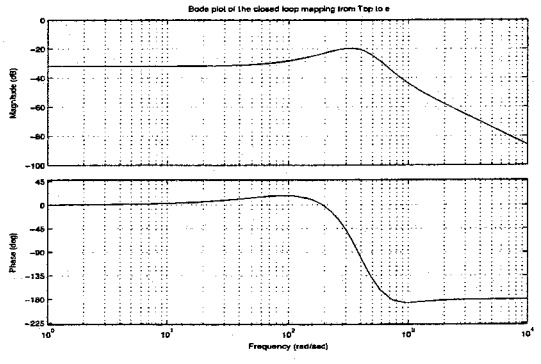

Figure 3: Bode plot from F_{op} to position error e

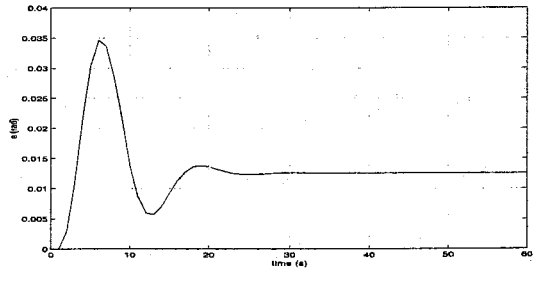

Figure 4: Closed-loop step response $F_{\text{op}} \mapsto e$ with C_{nom}

response of the master-slave system for *time-varying* tissue parameters $p(t)$ that vary in a spiral pattern in $\mathcal{P}$ is shown in Figure 5.a. Although no guarantee for (quadratic) stability

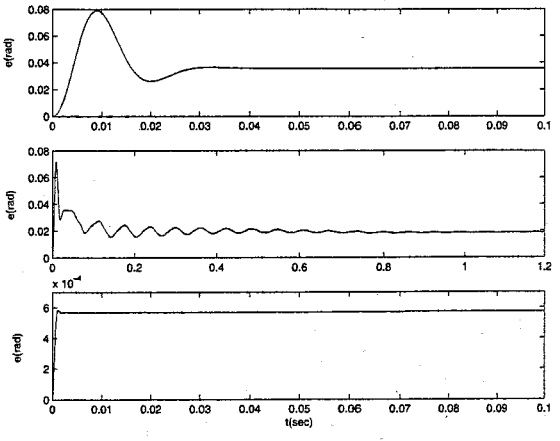

Figure 5: Step responses with time varying k_T and b_T with a) C_{nom}, b) C_{LPV} and c) C_{passive}.

can be given for this experiment, the response is still stable.

3.3 A linear parameter varying design

We consider the same system as in the previous subsection, but with the more explicit uncertainty description (8). The plant $P_{\text{aug}}(p)$ then becomes dependent of the parameter p and this dependence is, in fact, *affine* in the state space matrices of a suitable state space representation of the augmented system. This is necessary to apply LMI-based techniques for the synthesis of a parameter dependent controller that achieves the performance (9) with w and z as before. The resulting controller $C_{\text{LPV}}(p)$ explicitly depends on p and is implemented in the PERR structure of Figure 2. The achieved performance measures are $\gamma^*_{\text{LPV}}(\mathcal{P}) = 129.15$ and $\gamma^*_{\text{LPV}}(\mathcal{P}') = 16.31$. Hence, the performance is substantially better for the uncertainty box $\mathcal{P}'$ when compared with $\mathcal{P}$. Figure 5.b shows the step response when the parameter $p(t) = \text{col}(k_T(t), b_T(t))$ vary along a spiral in $\mathcal{P}$. Figure 6 shows the step response when the parameter p is captured randomly in $\mathcal{P}$. Robustness has been improved on the basis of the LPV plant and the corresponding LPV controller

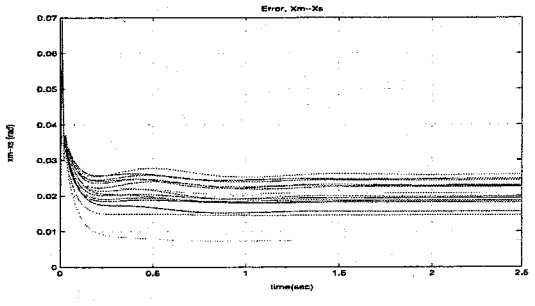

Figure 6: Step responses of the master-slave system for random k_T and b_T in $\mathcal{P}$

$C_{\text{LPV}}(p)$. The controller C_{nom} provides faster responses to time varying changes of k_T, b_T than C_{LPV} (Note the different scalings in Figure 5). However, the steady-state response of the system controlled by C_{LPV} is better than when controlled by C_{nom}.

3.4 A passive design

In this subsection we consider a passive design based on the passivity criterion (12). If we introduce a change of variables

$$w_1 = \frac{F_{\text{op}} + v_{\text{op}}}{2}, \qquad w_2 = \frac{F_{\text{env}} + v_{\text{env}}}{2} \tag{17a}$$

$$z_1 = \frac{F_{\text{op}} - v_{\text{op}}}{2}, \qquad z_2 = \frac{F_{\text{env}} - v_{\text{env}}}{2} \tag{17b}$$

and set $w = \text{col}(w_1, w_2)$ and $z = \text{col}(z_1, z_2)$ then one easily verifies that the total power $p_{\text{op}}(t) + p_{\text{env}}(t)$ defined in (10) satisfies

$$p_{\text{op}}(t) + p_{\text{env}}(t) = w^\top(t)w(t) - z^\top(t)z(t) \tag{18}$$

for all time t. Consequently, the passivity criterion (12) is equivalent to saying that

$$\begin{aligned} &\int_0^\infty \left(w^\top(t)w(t) - z^\top(t)z(t)\right) dt = \\ &= \|w\|_2^2 - \|z\|_2^2 = 0 \end{aligned} \tag{19}$$

for all possible (w, z) that satisfy the system equations. This means that the system will be passive if and only if the newly defined port variables w and z satisfy $\|w\|_2 = \|z\|_2$ for all possible square integrable trajectories. In the newly defined variables, w is taken as input and z as output so that the teleoperation system defines a hybrid representation $z = Hw$ in the frequency domain. Using Parseval, the system is then passive if and only if the singular values

$$\sigma(H(j\omega)) = 1 \tag{20}$$

for all frequencies $\omega \in \mathbb{R}$. To achieve this, we synthesized an H_∞ optimal controller C_{passive} for the augmented plant

$$H_{\text{aug}} : \begin{pmatrix} w \\ u \end{pmatrix} \mapsto \begin{pmatrix} z' \\ y \end{pmatrix} \tag{21}$$

where the control $u = \text{col}(F_M, F_S)$ and the measurement $y = e = x_M - x_S$ are as in the previous subsections and $z' = \text{col}(z, \tilde{e}, F_M, F_S)$ with $\tilde{e} = W_e e$ the weighted tracking error. The input-output relations in H_{aug} are defined by (13). Unlike the previous designs, the environment defined in (6) is now *not* part of the plant model. The passivity condition (20) is verified by inspecting the singular values of H in Figure 7. The closed-loop singular values $\sigma(H(j\omega))$ are 1.0007 and 0.9993 for all frequencies $0 \leq \omega \leq 40$ rad/s which shows that the system is 'approximately passive' for all trajectories in the relevant bandwitdh. For this controller, Figure 5.c shows a much faster and damped response to time varying parameter changes with a position error that is about a factor 10^2 smaller when compared to C_{nom} and C_{LPV}.

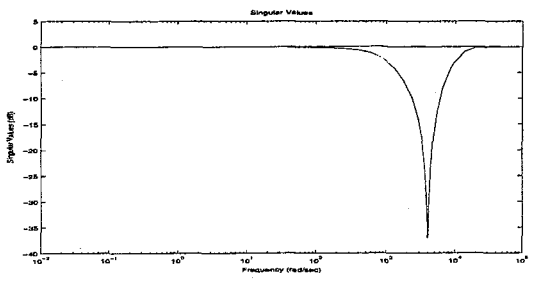

Figure 7: The singular values of the closed-loop transfer function from u to y

4 Experimental setup

4.1 Experimental setup

For the experimental setup it is chosen that both master and slave device must be able to perform a rotational motion. In this way a squeezing and pushing motion can be simulated. The specifications of both the devices consists of a maximum force level of 10 N at the tip and a bandwidth of at least 10 Hz. Assuming a distance of 60mm between the rotation point of the actuator and the force applied to the master/slave probe, a torque of 0.6 Nm is required. To satisfy these requirements, a special DC motor has been chosen as actuator for both master and slave. The Maxon RE-40 uses a special commutator design, that results in minimal torque ripple and a very small inertia. Because of the direct linking of probe and motor, the friction in the system is minimal.

The signals that are necessary for the control algorithms are the positions of the two devices and the force that is acting on the environment. For the position measurement, an encoder with 1000 counts per turn is used. For the force measurement, a load cell is used in the final design (Kyowa LM-2KA), because this is the only sensor that provides accurate force measurements. Figure 8 shows the resulting master and slave devices. Both systems have been build as a modular platform. This means that the tools connected to the motor can be replaced (e.g. the push-button interface for palpation that is connected to the master can be replaced by a forceps handle). Both DC motors are actuated by a current amplifier that is controlled by a computer using DAC interfaces.

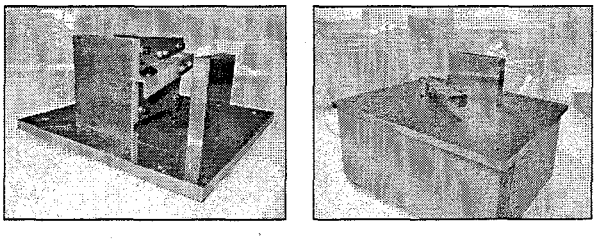

Figure 8: master (left) and slave (right)

4.2 Experiments

An initial experiment with a PERR control structure has been performed with a manually tuned controller. The master system is manipulated by a human operator, the slave is pushing against the environment. Time domain results are shown in Figure 9, with the position and force tracking.

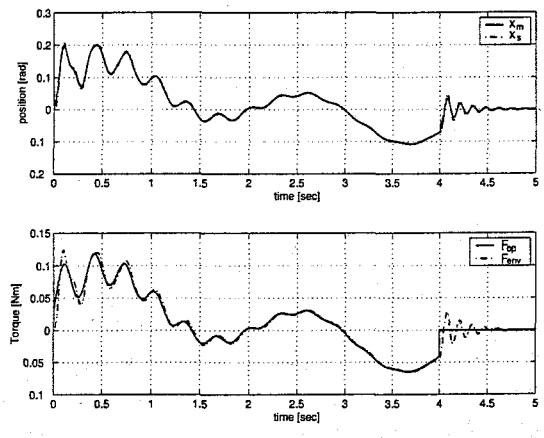

Figure 9: Time domain results of PERR structure

5 Conclusions

In this paper we have shown a model-based control design approach for haptic devices, comparing various methodologies. This includes a new method for inclusion of a passivity based criterion into an H_∞ controller design. The passivity based controller shows good tracking and robustness properties. Future research focusses on improving designs and experimentation for various tissues.

References

[1] P. Arcara, "Control of haptic and robotic telemanipulation systems," *Ph.D. Thesis, Universita degli Studi di Bologna - Facolta di Ingegneria -DEIS, 2002.*

[2] P. Arcara, C. Melchiorri, "Control scemes for teleoperation with time delay: a comparitive study," *Robotics and Autonomous Systems, Vol.38, No.1, Jan. 2002, p.49-64.*

[3] S. Boyd, L. El Ghaoui, E. Feron, and V. Balakrishnan, "Linear Matrix Inequalities in System and Control Theory," SIAM, 1994.

[4] R.C. Craig, R.C. Kevin, "Closed-loop force control for haptic simulation of virtual environments," *Haptics-e*, Vol. 1, No. 2, February 2000, (http://www.haptics-e.org).

[5] B. Hannaford, J.H. Ryu, "Time domain passivity control of haptic interfaces," *Proc. IEEE Conference on Robotics and Automation*, Seoul, p. 863-869, 2001.

[6] W.S. Kim, B. Hannaford, A.K. Bejczy, "Force-reflection and shared compliant control in operation telemanipulators with time delay," *IEEE Transactions on Robotics and Automation*, Vol. 8, No. 2, April 1992.

[7] S. Kudomi, H. Yamada, T. Muto. "Development of a hydraulic master-slave system for telerobotics," *Proc. of the 1st FPNI-PhD Symp.*, Hamburg 2000, p. 467-474.

[8] D.A. Lawrence, "Stability and transparency in Bilateral teleoperation," *IEEE Transactions on Robotics and Automation,* p. 624-637, October 1993.

[9] G. Raju, G. Verghese, and T. Sheridan, "Design issues in 2-port network models of bilateral remote manipulation," in *Proceedings of the IEEE International Conference on Robotics and Automation*, p. 1316-1321, 1989.

[10] A.F. Rovers, "Design of a robust master-slave controller for surgery applications with haptic feedback," Eindhoven University of Technology, DCT Report nr. 2003.54, June 2003.

[11] A. Sherman, M.C. Çavuşoğlu, F. Tendick, "Comparison of teleoperator control architectures for palpation task," in *Proceedings on IMECE'00, Symp. on Haptic Interfaces for Virtual Environments and Tele-operator Systems*, November 5-10, 2000, Orlando, Florida, U.S.A.

[12] M.C. Çavuşoğlu, A. Sherman, F. Tendick, "Bilateral controller design for telemanipulation in soft environments," in *Proceedings of the IEEE International Conference on Robotics and Automation (ICRA 2001),* Seoul, Korea, May 21-26, 2001.

[13] C.M. Smith, "Human Factors in Haptic Inter-faces," *ACM Crossroads Student Magazine, January 24, 2001* (www.acm.org/crossroads/xrds3-3/haptic.html).

[14] Y. Yokokohji and T. Yoshikawa, "Bilateral control of master-slave manipulators for ideal kinesthetic coupling-formulation and experiment," *IEEE Transactions on Robotics and Automation,* p. 605-620, October 1994.

[15] S.A. Wall, W. Harwin, "A high bandwith interface for haptic human computer interaction," Mechatronics 11 (2001) 371-387.

[16] J.C. Willems, "Dissipative Dynamical Systems, Part I: General Theory", Journal Arch. Rat. Mech. Anal., Vol. 45, p. 321-351, 1972.